CELL CYCLE REGULATION DURING DEVELOPMENT AND REGENERATION

Joy Hart Meserve

A dissertation submitted to the faculty at the University of North Carolina at Chapel Hill in partial fulfillment of the requirements for the degree of Doctor of Philosophy in the Genetics and Molecular Biology Curriculum in the School of Medicine.

Chapel Hill
2017

Approved by:

Robert J. Duronio

Victoria L. Bautch

Frank Conlon

Stephen S. Crews

Bob Goldstein

ABSTRACT

Joy H. Meserve: Cell cycle regulation during development and regeneration
(Under the direction of Robert J. Duronio)

During the development of multicellular organisms, proliferating, undifferentiated cells often transition into a differentiated and quiescent state. Programs coordinating cell cycle progression and differentiation are highly regulated to allow proper organismal growth and specification of a diverse array of cell types. Additionally, cell cycle activators are essential for regeneration following injury, while cell cycle inhibitors keep hyperplasia and tumor formation at bay. Although key cell cycle components have been studied for decades, significant points of cell cycle regulation remain uncertain. One open question is how proliferation and differentiation are coordinated during development *in vivo*. For my thesis work, I have utilized the developing *Drosophila melanogaster* retina as a model for cell cycle regulation during development and regeneration. My research has focused on two main questions: 1) what mechanisms drive quiescent cells to re-enter the cell cycle and proliferate in response to damage, and 2) how does prolonged arrest in G2 phase affect differentiation of a specific retinal lineage? Through a genetic RNAi screen, I have identified the transcription factor Scalloped as an essential regulator of compensatory proliferation following damage in the developing eye. Scalloped and its binding partner Yorkie are transcriptional regulators of the Hippo signaling pathway and promote proliferation by inducing expression of Cyclin E. My data suggest that Scalloped/Yorkie activation during eye regeneration is dependent on the Hippo pathway regulator Ajuba, which may be activated by increased cellular tension resulting from extrusion of apoptotic cells.

To further understand the relationship between cell cycle phase and cell fate, I also characterized the development of a population of G2-arrested cells in the *Drosophila* eye. I discovered these cells are selected as sensory organ precursors and undergo two divisions during pupal development to form mechanosensory bristle groups. These bristles are located at precise positions across the adult eye. Precocious mitotic entry of G2-arrested cells results in bristles that are misplaced and disorganized. These results support a model in which G2 arrest is required for proper selection of sensory organ precursors, which in turn affects bristle positioning. This suggests G2 arrest is a developmental mechanism that helps refine differentiation.

To all the women in science whose prior struggles and triumphs paved the way for my successful graduate career- thank you. I strive to one day be as inspiring.

ACKNOWLEDGEMENTS

I have been very fortunate to have a wonderful advisor while in graduate school. Bob is an exemplary graduate mentor: he offers a significant amount of independence to his students while remaining supportive, he is invested in maintaining a positive atmosphere within the lab, and he is very willing to discuss aspects of being a scientist outside of doing research. I joined Bob's lab under the condition that I wanted to start my own developmental cell cycle project, both because I wanted to ensure that I was truly invested in my project and because I believed starting a project from scratch would a valuable learning experience. While this approach turned out to be more challenging at times than I anticipated, discussing my progress and debating the broader questions of the field with Bob was essential for my project's success, both in terms of obtaining publications and shaping me as a scientist. I am privileged to have worked with an advisor who I admire greatly as a scientist, mentor, and person, and who I genuinely enjoy being around. Our discourse is effortless because we are usually on the same wavelength, and Bob doesn't let his ego get in the way of listening to my ideas, even if they challenge his own. I will certainly miss Bob as an advisor, and I hope he will continue to be my mentor and friend as I progress in my career.

I am also very thankful to numerous other individuals at UNC, including the faculty and peers who have given me feedback over the years and who I've had numerous conversations with about a variety of scientific issues. I am constantly amazed and encouraged by the global scientific community, whose passion, excitement, and generosity allow constant progress in the face of any challenge. Finally, I am forever indebted to my parents, who encouraged education, curiosity, and creativity, without which I would be lost, and my brother, who has been an excellent example and friend, both while growing up and even more so into adulthood.

TABLE OF CONTENTS

LIST OF FIGURES

LIST OF ABBREVIATIONS

Ac	Achaete
Ago	Archipelago
AiA	apoptosis-induced apoptosis
APC/C	anaphase-promoting complex/cyclosome
APF	after puparium formation
β-gal	β-galactosidase
ban	*bantam*
Bsk	Basket
BMP	Bone morphogenetic protein
BrdU	5-bromo-2′-deoxyuridine
CC3	Cleaved Caspase-3
Cdc25	Cell division cycle 25
Cdc42	Cell division control protein 42
CDK	cyclin-dependent kinase
Cdt1	Chromatin licensing and DNA replication factor 1
Ci	Cubitus interruptus
CKI	cyclin-dependent kinase inhibitor
CP	compensatory proliferation
CRE	cis-acting regulatory element
CycA	Cyclin A
CycB	Cyclin B
CycE	Cyclin E
Dap	Dacapo
DAPI	4',6-diamidino-2-phenylindole

Diap1	Death-associated inhibitor of apoptosis 1
Dlg	Discs large
dMSTn	*Drosophila* Mammalian Sterile20-like (Hippo); truncated
DN	dominant negative
DNA	deoxyribonucleic acid
Dp	Dimerization partner
Dpp	Decapentaplegic
Dronc	*Drosophila* Nedd2-like caspase
dsRNA	double-stranded RNA
E2f	E2-factor
EdU	5-ethynyl-2'-deoxyuridine
EGFR	Epidermal growth factor receptor
Elav	Embryonic lethal abnormal vision
Emc	Extramacrochaetae
Ex	Expanded
Ey	Eyeless
Fkh	Fork head
Flp	flippase
FRT	flippase recognition target
FUCCI	fluorescence ubiquitination cell cycle indicator
G	gap phase
GFP	green fluorescent protein
Gli	Glioblastoma
GMR	*glass multimer reporter*
GTP	Guanosine-5'-triphosphate
hESC	human embryonic stem cell

Hh	Hedgehog
Hid	Head involution defective
His2Av	Histone H2A variant
Hpo	Hippo
hrs	hours
hs	*heat shock*
Hth	Homothorax
JNK	Jun N-terminal kinase
Jub	Ajuba
Kni	Knirps
LGMR	*longGMR*
lacZ	*lac operon gene Z*
Lilli	Lilliputian
luc	*luciferase*
M	mitosis
Mef2	Myocyte enhancer factor-2
MF	morphogenetic furrow
mRNA	messenger RNA
NLS	nuclear localization signal
PBS	phosphate-buffered saline
PH3	Phospho-histone H3
Pros	Prospero
Puc	Puckered
Rbf	Retinoblastoma-family protein
RFP	red fluorescent protein
RNA	ribonucleic acid

Rok	Rho-kinase
Rux	Roughex
S	synthesis phase
Sc	Scute
SCF	Skp, Cullin, F-box containing
Sd	Scalloped
Sens	Senseless
Skp	S-phase kinase-associated protein
SMW	Second mitotic wave
SOP	sensory organ precursor
Ssrp	Structure specific recognition protein
Stg	String
Su(H)	Suppressor of Hairless
SWI/SNF	SWItch/Sucrose Non-Fermentable
TEA	Transcriptional enhancer activator
TEAD	TEA DNA binding domain
Tgi	Tondu-domain containing Growth Inhibitor
Tie	Tie-like receptor tyrosine kinase
Trl	Trithorax-like
TS	temperature sensitive
Tsh	Teashirt
UAS	Upstream Activation Sequence
Ubi	Ubiquitin
Wg	Wingless
Wnt	Wingless-related integration site
WT	Wild type

Wts	Warts
Yap	Yes-associated protein
Yki	Yorkie

CHAPTER 1: INTRODUCTION AND BACKGROUND

Regulation of the cell cycle is essential for the lives of all multicellular organisms and has been studied for decades, but there are still many open questions regarding cell cycle control. While a great deal of work using yeast and cell culture has elucidated the basic pathways controlling cell cycle progression and division, cell cycle regulation *in vivo* has additional layers of complexity that remain a challenge to uncover. There are a number of developmental inputs, both intrinsic and extrinsic, that influence a cell's decision to proliferate, arrest, or exit the cell cycle. Identifying the mechanisms underlying these decision points is critical for our knowledge of basic cell biology, proliferation control during regeneration, and mechanisms driving inappropriate proliferation in disease states like cancer. This review will give an overview of cell cycle regulation during development, with an emphasis on studies utilizing *Drosophila melanogaster* as an introduction to the results described in Chapters 2 and 3.

MASTER CELL CYCLE REGULATORS

To understand developmental control of the cell cycle, we must first identify the key cell cycle proteins that are regulated during development. Since Hartwell's studies in the 1970s investigating cell division in yeast (Hartwell et al., 1974), a number of genes he and others identified as critical cell cycle regulators have subsequently been found throughout the eukaryotic domain (Hunt, 1983; Lee and Nurse, 1987; Harashima et al., 2013). These genes include the cyclins and their associated cyclin-dependent kinases (CDKs). Cyclin/CDK complexes phosphorylate a host of cell cycle proteins and are essential for cell cycle progression. In *Drosophila*, the major complexes are Cyclin E/CDK2 (CycE/CDK), which promotes transition

from G1 into S phase, and Cyclin A/CDK1 (CycA/CDK) and Cyclin B/CDK1 (CycB/CDK), which promote transition from G2 into mitosis. Activity of cyclin/CDKs oscillate throughout the cell cycle due to interactions with inhibitory proteins, protein degradation, and transcriptional control (Lee and Orr-Weaver, 2003); these oscillations CDK activities result in changes in their target proteins' activities. The most well-characterized CycE/CDK targets are members of the tumor suppressor retinoblastoma family of proteins (Rbf in *Drosophila*) (Du et al., 1996; Du and Dyson, 1999). Rbf inhibits the transcription factor E2f (E2-factor), which is required for S phase entry (van den Heuvel and Dyson, 2008). CycE/CDK phosphorylation of Rb prevents its association with E2f, allowing E2f and its binding partner Dp (Dimerization partner) to activate transcriptional targets such *CycE* and other S phase genes (Duronio and O'Farrell, 1995). Similarly, there are a number of CycB/CDK substrates that regulate mitosis, such as KLP61F (Kinesin-like protein at 61F) (Sharp et al., 1999), a bipolar kinesin that regulates spindle assembly. Because of their numerous substrates, cyclin/CDK activity is essential to activate a cascade of molecular events that promote entry from G1 into S and G2 into M.

Once cyclin/CDKs initiate transition into S phase or mitosis, a robust network of cell cycle regulators ensures cell cycle progression continues to move forward; without this robust control, errors can occur, such as re-replication during S phase or mitotic errors during division. This cell cycle network includes transcription factors, like the aforementioned E2f, and ubiquitin ligase complexes, which target many cell cycle proteins for degradation once they have performed their function. For example, after entry into S phase, E2f and a number of S phase proteins, like the origin licensing factor Cdt1 (Chromatin Licensing And DNA Replication Factor 1), are targeted for degradation by $CRL4^{Cdt2}$ (Cullin ring E3 ligase 4 with the adapter Cdc10-dependent transcript 2) (Havens and Walter, 2009); this regulation ensures the DNA replication program is only initiated once per cell cycle. After a cell completes S phase, a host of factors determine whether a cell will progress from G2 into mitosis. Cyclin/CDK1 complexes are inactive at the beginning of G2 due to inhibitory phosphorylation by Wee1 on CDK1. Inhibitory phosphates are removed in G2 by a

phosphatase, Stg (String; *Drosophila* Cdc25 homolog), whose activity is highly regulated (see below) (Lee and Orr-Weaver, 2003). CycB/CDK activity subsequently initiates mitosis. Progression through mitosis is further regulated by another ubiquitin ligase complex, the APC/C (Anaphase promoting complex/cyclosome). The APC/C interacts with adaptor proteins that direct substrate specificity during different phases of mitosis and G1. One of the APC/C targets is CycB, which is degraded following ubiquitylation (Raff et al., 2002), ensuring mitosis occurs in a stepwise manner and ceases in G1. In addition to these well characterized cell cycle regulators, expression of a vast number of genes oscillate through the cell cycle in cell culture studies (Whitfield et al., 2002; Grant et al., 2013), suggesting there are more cell cycle genes to characterize that may be more important for specific tissues or at specific points in development.

DEVELOPMENTAL CONTROL OF PROLIFERATION

Proliferation is controlled during development by regulation of these key cell cycle proteins, which ensures tissues contain the appropriate cell number and variety of cell types. Signaling pathways that promote proliferation are generally considered mitogenic, while the ligands responsible are termed mitogens. These pathways can promote proliferation by inducing transcription of key cell cycle genes such as *CycE* and *stg*, which have complex cis-regulatory regions. *CycE* expression in the *Drosophila* embryo depends on activation of multiple tissue-specific cis-acting regulatory elements (CREs) (Jones et al., 2000), and *stg* expression in the developing *Drosophila* eye depends on a CRE that is unique from the multiple CREs driving *stg* expression in the embryo (Lehman et al., 1999; Lopes and Casares, 2015). Activation of these CREs is dependent on transcription factor binding, which is often the last step in a signaling pathway cascade. One such pathway is the Hedgehog pathway, which has well-defined ligands (Hh/Hedgehog in *Drosophila*) and transcriptional effectors (Gli family transcription factors) that promote growth. Secreted Hh activates a signaling cascade through the transmembrane receptors Smoothened and Patched (for review, see (Jiang and Hui, 2008)), resulting in activation of the

transcription factor Cubitus interruptus (Ci; *Drosophila* Gli homolog). Ci activates target genes such as *CycE* to promote proliferation (Duman-Scheel et al., 2002). In this pathway and other mitogenic pathways, proliferation is controlled by the cell's environment and whether surrounding cells secrete mitogenic ligands such as Hh.

Growth pathways can also be activated by developmental input outside of classical mitogenic ligands. The Hippo pathway is an excellent example; much of the input influencing whether the Hippo pathway is on or off is dependent upon cell-cell contacts, which relate to tissue size and mechanical input. In the developing *Drosophila* wing, when the tissue is small and contains relatively few cells, tension through E-cadherin interactions at cell-cell junctions is high; this high tension leads to inhibition of the Hippo pathway through α-catenin and other cytoskeletal components (Rauskolb et al., 2014). Inhibition of Hippo (Hpo) and other upstream effectors turns the Hippo pathway OFF, which leads to activation of the transcriptional effector Yorkie (Yki; *Drosophila* YAP homolog) (Halder and Johnson, 2011). Activated Yki is free to translocate into the nucleus and interact with transcription factors such as Scalloped (Sd; *Drosophila* TEAD-factor); the Yki/Sd complex subsequently activates cell cycle genes such as *CycE* (Goulev et al., 2008; Wu et al., 2008; Zhao et al., 2008). When the developing wing is fully grown and densely packed with cells, tension across the tissue is low, resulting in the Hippo pathway being turned ON; the activated Hippo pathway inhibits Yki, preventing expression of cell cycle genes. Regulation through the Hippo pathway and others allows proliferation control in a growing tissue without relying on a population of mitogen-secreting cells.

MECHANISMS REGULATING CELL CYCLE ARREST

While mitogenic pathways promote proliferation, other developmental pathways inhibit cell cycle progression and promote cell cycle arrest. While cell cycle arrest is often thought of as a state preceding cell cycle exit, arrest is also important during development to coordinate processes like morphogenetic movements and tissue patterning. During *Drosophila* embryogenesis, cells

arrest in G2 as they undergo movements throughout mesoderm invagination (Edgar and O'Farrell, 1989). Precocious entry into mitosis disrupts this morphogenetic process (Grosshans and Wieschaus, 2000; Mata et al., 2000; Seher and Leptin, 2000). In the developing *Drosophila* eye, proliferating precursor cells undergo G1 arrest as expression of patterning genes induces photoreceptor differentiation in a subset of precursor cells (Escudero and Freeman, 2007). In addition to pathways like the Hippo pathway that prevent transcriptional activation of cell cycle genes, a number of cell cycle inhibitors also promote cell cycle arrest. These proteins include CDK inhibitors (CKIs). The two characterized CKIs in *Drosophila* are Dacapo (Dap), a CycE/CDK inhibitor that is required for cell cycle arrest in the embryo and at later stages of development (de Nooij et al., 1996; Lane et al., 1996; Swanson et al., 2015), and Roughex (Rux), which is primarily required to regulate cell cycle arrest in the developing eye (Thomas et al., 1994). Rux suppresses CycA/CDK activity through binding to CycA, preventing its association with CDK1 (Foley et al., 1999). While CycA normally regulates mitosis in *Drosophila*, G1-stabilized CycA can drive S-phase re-entry in the absence of CycE (Jacobs et al., 2001). In the eye, developmentally induced G1-arrest is disrupted in a *rux* mutant due to accumulation of CycA (Thomas et al., 1994). Proteins other than CKIs also regulate cyclin/CDK activity; the F-box protein Archipelago (Ago), part of the SCF^{Ago} E3 ubiquitin ligase, interacts with CycE and targets it for destruction (Moberg et al., 2001). In addition to transcriptional regulation of cyclins and inhibition of cyclin/CDKs through protein interactions, translational control also regulates cyclin expression in certain contexts, such as during *Drosophila* meiosis when *CycA* translation is repressed by the RNA-binding protein Bruno (Sugimura and Lilly, 2006).

Just as expression and activity of CycE and Stg are highly regulated during development, levels of cell cycle inhibitors are developmentally controlled as well. The *dap* locus contains multiple CREs that are activated at various times and in various tissues during embryogenesis and later development to control expression (Meyer et al., 2002). Dap is also regulated at the protein level by the $CRL4^{Cdt2}$ ubiquitin ligase, which targets Dap for destruction during S phase

(Swanson et al., 2015). *ago* is transcriptionally activated in the developing *Drosophila* eye by the Notch transcription factor Su(H); Notch activity and subsequent *ago* expression are required for developmentally controlled G1-arrest (Nicholson et al., 2011). These examples and other uncharacterized mechanisms of regulation result in complex expression patterns of cell cycle inhibitors that ensure cell cycle progression and development are appropriately coordinated.

REGULATION OF EXIT FROM THE CELL CYCLE

Once a tissue has the proper number of cells and/or is the proper size, cells often transition from a proliferative state to a non-proliferating state preceding differentiation. Terminal differentiation is in part defined by a cell assuming a post-mitotic state (Reiner, 1983). It is important to note, however, that cells characterized as "post-mitotic" based on experiments where cells no longer divide *in vitro* are not necessarily permanently exited from the cell cycle *in vivo*. The concept of cellular senescence, where cells in culture permanently withdraw from the cell cycle in response to stress, is not very well defined *in vivo* and appears to relate to aging and disease states rather than normal developmental cell cycle exit (Sharpless and Sherr, 2015). Mechanisms controlling reversible cell cycle exit or quiescence *in vitro* may relate more closely to cell cycle exit *in vivo* (Buttitta and Edgar, 2007). Nonetheless, we should not be too dogmatic in our definitions of arrest, cell cycle exit, post-mitotic state, quiescence, senescence, terminal differentiation, or any other term designed to describe a specific cell cycle state as these terms are artificially defined and often vague; whether or not a cell *in vivo* will enter the cell cycle versus whether a cell can enter the cell cycle often depends on context. Additionally, there is a growing body of evidence that suggests that non-proliferation is an active process rather than a passive state of differentiation cells (Pajalunga et al., 2014).

Despite the complex semantics defining states of cell cycle exit, exit from the cell cycle *in vivo*, defined by cells ceasing to proliferate under normal developmental conditions without any evidence of cell cycle re-entry later in development, has been well studied. In the developing

Drosophila larval eye, cells transition from a G1-arrest, wherein some cells re-enter the cell cycle, to cell cycle exit, during which no cells undergo S phase or mitosis (Wolff and Ready, 1991). Shortly after this transition occurs, cells readily re-enter the cell cycle following heat-shocked induced expression of transgenic *CycE* (Richardson et al., 1995); this suggests cell cycle exit is relatively flexible at this stage in development. Ectopic *CycE* continues to induce cell cycle re-entry in developing eyes during early pupal development but is not sufficient to drive re-entry at later pupal stages (Buttitta et al., 2007). However, ectopic *CycE* will induce cell cycle re-entry at later pupal stages in the eye if combined with a mutation in *rbf*, which allows E2f activity (Buttitta et al., 2007). This suggests cells transition from a flexible cell cycle exit wherein cell cycle re-entry is readily induced to a more robust cell cycle exit that is dependent on suppression of CycE/CDK and E2f activities; this suppression is at least in part achieved by activity of Dap and APC/C (Buttitta et al., 2010). Rux also contributes to robust cell cycle exit in the developing eye (Ruggiero et al., 2012).

In addition to activation of pathways inhibiting cell cycle progression, chromatin changes that occur during differentiation ensure robust cell cycle exit. Cell cycle exit and differentiation are often correlated with increased chromatin condensation and formation of heterochromatic domains, which are typically transcriptionally inactive (Francastel et al., 2000). In the *Drosophila* eye, chromosomal movement becomes more constrained as cells differentiate, consistent with a more compact, less dynamic nuclear structure (Thakar and Csink, 2004). Because chromatin localization to the nuclear periphery is thought to be transcriptionally repressive (Ma et al., 2015), restricted chromosomal movement in differentiated cells may ensure cell cycle genes remain in transcriptionally inactive regions of the nucleus. Consistent with this hypothesis, work in *Drosophila* cell culture has indicated that SWI/SNF chromatin remodeling complexes are required to maintain open chromatin at the *stg* locus, which allows Stg expression during the G2/M transition (Moshkin et al., 2007). Experimental disruption of open chromatin at the *stg* locus by inhibition of SWI/SNF proteins results in cell cycle arrest (Moshkin et al., 2007).

Transition to more compact chromatin at the *stg* locus during differentiation may also prevent cell cycle entry by preventing binding of key transcription factors. Together with regulatory pathways that inhibit cell cycle activator proteins, chromatin changes that occur during differentiation ensure robust cell cycle exit.

COORDINATION OF THE CELL CYCLE AND DIFFERENTIATION

Because cell cycle exit often coincides with onset of differentiation, pathways that regulate the cell cycle and differentiation often overlap to ensure coordination between the two processes. In addition to exit and differentiation taking place concurrently, it is essential that these processes occur at the correct time during development. In the developing nervous system, time of cell cycle exit and fate are intimately correlated; progenitor cells that exit earlier in development become neurons while cells that exit later in development become glial cells. This is likely due in part to an intrinsic clock controlled by the accumulation of cell cycle inhibitors throughout multiple rounds of division (Ohnuma and Harris, 2003). Additionally, proteins that regulate cell fate also regulate cell cycle progression. For example, the *Drosophila* transcription factor Prospero (Pros) directs differentiation of neuronal cell fates by repressing neural stem cell gene expression and activating expression of differentiation genes (Choksi et al., 2006). At the same time, Pros activates *dap* expression (Colonques et al., 2011) and represses *CycE* and *stg* expression to promote cell cycle exit (Li and Vaessin, 2000). Molecular pathways that affect both cell cycle progression and differentiation ensure robust cell cycle exit at the onset of differentiation. Because these pathways often overlap, it is difficult to experimentally separate cell cycle exit from onset of differentiation and determine whether cell cycle exit is required for terminal differentiation *in vivo* (Buttitta and Edgar, 2007).

While developmental regulation ensures cells exit the cell cycle before terminally differentiating, it is also imperative cells don't exit the cell cycle prematurely. Precocious cell cycle exit reduces cell number of a tissue, which may result in defects in tissue function or organization

(de Nooij and Hariharan, 1995). Progression through the cell cycle is also essential for generating cell diversity. For example, cell fate determinants are often segregated asymmetrically during mitotic divisions; these asymmetric divisions are particularly important in the nervous system to generate the numerous neuronal cell types while retaining cycling neuroblasts (Sousa-Nunes and Somers, 2013; Paridaen and Huttner, 2014). Additionally, recent evidence suggests that progression through mitosis makes cells more amenable to nuclear reprograming as histone marks must be re-established following DNA replication, and chromatin is exposed to cytoplasmic components following nuclear envelope breakdown; this increased competency to reprogram cell fate is termed "mitotic advantage" (Halley-Stott et al., 2014). Similarly, some studies have suggested the process of DNA replication allows opening of chromatin, making cells in S phase more responsive to certain developmental signals (Remaud et al., 2008). Importantly, cells in S phase are not more amenable to factors inducing terminal differentiation. Experiments in human embryonic stem cells have demonstrated cells in G1 undergo spontaneous differentiation much more frequently than cells in S/G2 (Sela et al., 2012). These G1-cells are also more receptive to factors that induce differentiation of a number of cell types than cells in S phase or G2 (Pauklin and Vallier, 2013). This resistance to differentiation outside of G1 can be attributed in part to cell cycle regulators repressing differentiation factors. For example, in developing muscle precursor cells, CycE/CDK phosphorylation of the transcription factor MyoD, which promotes cell cycle exit and muscle cell differentiation, results in its degradation (Tintignac et al., 2000). Similarly, during *Drosophila* neural development, CycE inhibits the differentiation factor Pros, likely through CycE/CDK-mediated phosphorylation (Berger et al., 2010). The balance between pathways promoting proliferation and inhibiting differentiation and those pathways promoting cell cycle exit and terminal differentiation ensure development is properly coordinated.

PROLIFERATION CONTROL DURING REGENERATION

In addition to regulation of the cell cycle during normal development, cell cycle regulation is critical following injury. When a tissue loses cells following damage or injury, increased proliferation of the remaining cells in the tissue can compensate for this loss. Proliferation control during regeneration has been a hot topic in recent years, particularly as many problems associated with aging can be attributed in part to a loss of regenerative capabilities (Yun, 2015). In proliferative tissues, which are more prevalent during early development, increased mitogenic signaling drives compensatory proliferation following tissue damage. In the developing *Drosophila* wing, cells undergoing apoptosis following injury secrete the mitogens Hh and Dpp (Decapentaplegic, a *Drosophila* BMP homolog), which induces proliferation in surrounding cells (Huh et al., 2004; Ryoo et al., 2004; Perez-Garijo et al., 2005). Similar mitogenic signaling occurs following damage in other regenerative models (Ryoo and Bergmann, 2012).

Quiescent tissues face an additional hurdle to overcome during regeneration as cells must overcome cell cycle inhibition before re-entering the cell cycle. In some regenerating quiescent tissues, cells don't proliferate to increase cell number but will undergo cell growth, often coupled with endocycles (S phases without intervening mitoses), to replace lost tissue. Following tissue removal in the mammalian liver, hepatocytes undergo rounds of endocycles and increase in size to regenerate the liver mass (Miyaoka et al., 2012). Similarly, in the *Drosophila* ovary, following follicle cell loss, the remaining follicle cells undergo endocycles and cell growth (Tamori and Deng, 2013). In other regenerative quiescent tissues, cells do overcome cell cycle inhibition and re-enter proliferative cell cycles. Cell cycle re-entry in the injured mouse retina is achieved by downregulation of the cell cycle inhibitor p27 in quiescent glial cells; these cells subsequently re-enter the cell cycle and produce progeny that differentiate into neurons (Dyer and Cepko, 2000). In addition to level of CKIs, chromatin state likely plays a role in determining whether or not a cell is competent to re-enter the cell cycle in response to damage. During newt lens regeneration, epithelial cells in the eye re-enter the cell cycle and subsequently transdifferentiate into lens cells.

Prior to injury, these epithelial cell nuclei are small and have highly developed heterochromatic regions. Following injury and preceding cell cycle re-entry, the epithelial cell nucleus swells in size and more euchromatic, transcriptionally active regions appear; these newly active regions likely contain genes involved in proliferation (Maki et al., 2010). In the *Drosophila* intestine, the chromatin remodeling SWI/SNF protein Brahma is required for midgut cell proliferation following injury (Jin et al., 2013). Brahma is thought to promote regeneration by interacting with Sd/Yki complexes in the nucleus, where chromatin remodeling influences expression of Sd/Yki gene targets.

Although there are examples of quiescent tissues that undergo regeneration, there are many tissues that do not undergo regeneration, and it is not always clear what the differences between regenerative and non-regenerative tissues are. In some instances, regeneration can be induced in non-regenerative tissues by manipulation of cell cycle proteins. For example, ear punches in adult mice do not normally regenerate, but holes do close due to skin regeneration in a *p21* mutant mouse (Bedelbaeva et al., 2010). This suggests inhibition of CKIs may be sufficient to induce regeneration in some quiescent tissues. Other tissues are more resistant to cell cycle re-entry. Cortical neurons in the mammalian brain can be experimentally induced to re-enter the cell cycle but do not successfully undergo mitosis, leading to aneuploidy and apoptosis (Aranda-Anzaldo and Dent, 2016). Evidence of unsuccessful cell cycle re-entry is also observed under pathological conditions such as Alzheimer's disease (Zekanowski and Wojda, 2009), suggesting endogenous mechanisms may promote proliferation following injury. Researchers have demonstrated that the genome is densely packed in cortical neuron nuclei, and chromosomes are relatively rigid and not easily decatenated. Mitosis is likely unsuccessful in these cells due to this inflexible structure of the neuronal nucleus (Aranda-Anzaldo and Dent, 2016). Thus, cell cycle inhibition is not the only barrier that must be overcome to successfully regenerate damaged tissue.

DISSERTATION GOALS

The focus of my graduate work was to better understand the developmental mechanisms controlling cell cycle arrest and cell cycle re-entry, and the relationship between these processes of arrest and re-entry and the process of differentiation. I have investigated these questions using the developing *Drosophila* retina as an experimental model. The adult *Drosophila* compound eye is precisely patterned as a neurocrystalline lattice. This pristine organization begins to take shape in the developing larval eye imaginal disc, where developmental signaling directs cell cycle synchronization as well as stereotyped, stepwise differentiation (Kumar, 2012). Because cell cycle control and differentiation are intimately linked in the developing eye, this tissue is ideal for investigating the relationship between these two processes. My work has focused on two main areas: 1) investigating the mechanisms controlling cell cycle re-entry of undifferentiated, G1-arrested cells following tissue damage in the eye (Chapter 2), as well as the cell fates of these compensatory proliferating cells (Chapter 3); and 2) characterizing the fate of a population of G2-arrested cells in the developing eye and the requirement of G2 arrest for this fate (Chapter 3). Together, these results contribute to our comprehension of cell cycle regulation and its relationship with cell fate during development.

REFERENCES

Aranda-Anzaldo, A. and Dent, M. A. (2016). Why cortical neurons cannot divide, and why do they usually die in the attempt? J. Neurosci. Res. doi:10.1002/jnr.23765

Bedelbaeva, K., Snyder, A., Gourevitch, D., Clark, L., Zhang, X. M., Leferovich, J., Cheverud, J. M., Lieberman, P. and Heber-Katz, E. (2010). Lack of p21 expression links cell cycle control and appendage regeneration in mice. Proc. Natl. Acad. Sci. U. S. A. 107, 5845-5850.

Berger, C., Kannan, R., Myneni, S., Renner, S., Shashidhara, L. S. and Technau, G. M. (2010). Cell cycle independent role of Cyclin E during neural cell fate specification in Drosophila is mediated by its regulation of Prospero function. Dev. Biol. 337, 415-424.

Buttitta, L. A. and Edgar, B. A. (2007). Mechanisms controlling cell cycle exit upon terminal differentiation. Curr. Opin. Cell Biol. 19, 697-704.

Buttitta, L. A., Katzaroff, A. J. and Edgar, B. A. (2010). A robust cell cycle control mechanism limits E2F-induced proliferation of terminally differentiated cells in vivo. J. Cell Biol. 189, 981-996.

Buttitta, L. A., Katzaroff, A. J., Perez, C. L., de la Cruz, A. and Edgar, B. A. (2007). A double-assurance mechanism controls cell cycle exit upon terminal differentiation in Drosophila. Dev. Cell 12, 631-643.

Choksi, S. P., Southall, T. D., Bossing, T., Edoff, K., de Wit, E., Fischer, B. E., van Steensel, B., Micklem, G. and Brand, A. H. (2006). Prospero acts as a binary switch between self-renewal and differentiation in Drosophila neural stem cells. Dev. Cell 11, 775-789.

Colonques, J., Ceron, J., Reichert, H. and Tejedor, F. J. (2011). A transient expression of Prospero promotes cell cycle exit of Drosophila postembryonic neurons through the regulation of Dacapo. PLoS One 6, e19342.

de Nooij, J. C. and Hariharan, I. K. (1995). Uncoupling Cell Fate Determination from Patterned Cell-Division in the Drosophila Eye. Science 270, 983-985.

de Nooij, J. C., Letendre, M. A. and Hariharan, I. K. (1996). A cyclin-dependent kinase inhibitor, dacapo, is necessary for timely exit from the cell cycle during Drosophila embryogenesis. Cell 87, 1237-1247.

Du, W. and Dyson, N. (1999). The role of RBF in the introduction of G1 regulation during Drosophila embryogenesis. EMBO J 18, 916-925.

Du, W., Vidal, M., Xie, J. and Dyson, N. (1996). RBF, a novel RB-related gene that regulates E2f activity and interacts with cyclin E in Drosophila. Genes Dev. 10, 1206-1218.

Duman-Scheel, M., Weng, L., Xin, S. and Du, W. (2002). Hedgehog regulates cell growth and proliferation by inducing Cyclin D and Cyclin E. Nature 417, 299-304.

Duronio, R. J. and O'Farrell, P. H. (1995). Developmental control of the G1 to S transition in Drosophila: cyclin Eis a limiting downstream target of E2F. Genes Dev. 9, 1456-1468.

Dyer, M. A. and Cepko, C. L. (2000). Control of Muller glial cell proliferation and activation following retinal injury. Nat. Neurosci. 3, 873-880.

Edgar, B. A. and O'Farrell, P. H. (1989). Genetic control of cell division patterns in the Drosophila embryo. Cell 57, 177-187.

Escudero, L. M. and Freeman, M. (2007). Mechanism of G1 arrest in the Drosophila eye imaginal disc. BMC Dev. Biol. 7, 13.

Foley, E., O'Farrell, P. H. and Sprenger, F. (1999). Rux is a cyclin-dependent kinase inhibitor (CKI) specific for mitotic cyclin-CDK complexes. Curr. Biol. 9, 1392-1402.

Francastel, C., Schubeler, D., Martin, D. I. K. and Groudine, M. (2000). Nuclear compartmentalization and gene activity. Nat. Rev. Mol. Cell Biol. 1, 137-143.

Goulev, Y., Fauny, J. D., Gonzalez-Marti, B., Flagiello, D., Silber, J. and Zider, A. (2008). SCALLOPED interacts with YORKIE, the nuclear effector of the hippo tumor-suppressor pathway in Drosophila. Curr. Biol. 18, 435-441.

Grant, G. D., Brooks, L., 3rd, Zhang, X., Mahoney, J. M., Martyanov, V., Wood, T. A., Sherlock, G., Cheng, C. and Whitfield, M. L. (2013). Identification of cell cycle-regulated genes periodically expressed in U2OS cells and their regulation by FOXM1 and E2F transcription factors. Mol. Biol. Cell 24, 3634-3650.

Grosshans, J. and Wieschaus, E. (2000). A genetic link between morphogenesis and cell division during formation of the ventral furrow in Drosophila. Cell 101, 523-531.

Halder, G. and Johnson, R. L. (2011). Hippo signaling: growth control and beyond. Development 138, 9-22.

Halley-Stott, R. P., Jullien, J., Pasque, V. and Gurdon, J. (2014). Mitosis gives a brief window of opportunity for a change in gene transcription. PLoS Biol. 12, e1001914.

Harashima, H., Dissmeyer, N. and Schnittger, A. (2013). Cell cycle control across the eukaryotic kingdom. Trends Cell Biol. 23, 345-356.

Hartwell, L. H., Culotti, J., Pringle, J. R. and Reid, B. J. (1974). Genetic control of the cell division cycle in yeast. Science 183, 46-51.

Havens, C. G. and Walter, J. C. (2009). Docking of a specialized PIP Box onto chromatin-bound PCNA creates a degron for the ubiquitin ligase CRL4Cdt2. Mol. Cell 35, 93-104.

Huh, J. R., Guo, M. and Hay, B. A. (2004). Compensatory proliferation induced by cell death in the Drosophila wing disc requires activity of the apical cell death caspase Dronc in a nonapoptotic role. Curr. Biol. 14, 1262-1266.

Hunt, T. (1983). Cyclin: A protein specified by maternal mRNA in sea urchin eggs that is destroyed at each cleavage division. Cell 33, 389-396.

Jacobs, H. W., Keidel, E. and Lehner, C. F. (2001). A complex degradation signal in Cyclin A required for G1 arrest, and a C-terminal region for mitosis. EMBO J 20, 2376-2386.

Jiang, J. and Hui, C. C. (2008). Hedgehog signaling in development and cancer. Dev. Cell 15, 801-812.

Jin, Y. Y., Xu, J. J., Yin, M. X., Lu, Y., Hu, L. X., Li, P. X., Zhang, P., Yuan, Z. Q., Ho, M. S., Ji, H. B. et al. (2013). Brahma is essential for Drosophila intestinal stem cell proliferation and regulated by Hippo signaling. eLife 2.

Jones, L., Richardson, H. and Saint, R. (2000). Tissue-specific regulation of cyclin E transcription during Drosophila melanogaster embryogenesis. Development 127, 4619-4630.

Lane, M. E., Sauer, K., Wallace, K., Jan, Y. N., Lehner, C. F. and Vaessin, H. (1996). Dacapo, a cyclin-dependent kinase inhibitor, stops cell proliferation during Drosophila development. Cell 87, 1225-1235.

Lee, L. A. and Orr-Weaver, T. L. (2003). Regulation of cell cycles in Drosophila development: intrinsic and extrinsic cues. Annu. Rev. Genet. 37, 545-578.

Lee, M. G. and Nurse, P. (1987). Complementation used to clone a human homologue of the fission yeast cell cycle control gene cdc2. Nature 327, 31-35.

Lehman, D. A., Patterson, B., Johnston, L. A., Balzer, T., Britton, J. S., Saint, R. and Edgar, B. A. (1999). Cis-regulatory elements of the mitotic regulator, string/Cdc25. Development 126, 1793-1803.

Li, L. and Vaessin, H. (2000). Pan-neural Prospero terminates cell proliferation during Drosophila neurogenesis. Genes Dev. 14, 147-151.

Lopes, C. S. and Casares, F. (2015). Eye selector logic for a coordinated cell cycle exit. PLoS Genet 11, e1004981.

Ma, Y., Kanakousaki, K. and Buttitta, L. (2015). How the cell cycle impacts chromatin architecture and influences cell fate. Front Genet 6, 19.

Maki, N., Tsonis, P. A. and Agata, K. (2010). Changes in global histone modifications during dedifferentiation in newt lens regeneration. Mol. Vis. 16, 1893-1897.

Mata, J., Curado, S., Ephrussi, A. and Rorth, P. (2000). Tribbles coordinates mitosis and morphogenesis in Drosophila by regulating string/CDC25 proteolysis. Cell 101, 511-522.

Meyer, C. A., Kramer, I., Dittrich, R, Marzodko, S., Emmerich, J. and Lehner, C. F. (2002). Drosophila p27 Dacapo expression during embryogenesis is controlled by a complex regulatory region independent of cell cycle progresssion. Development 129, 319-328.

Miyaoka, Y., Ebato, K., Kato, H., Arakawa, S., Shimizu, S. and Miyajima, A. (2012). Hypertrophy and unconventional cell division of hepatocytes underlie liver regeneration. Curr. Biol. 22, 1166-1175.

Moberg, K. H., Bell, D. W., Wahrer, D. C. R., Haber, D. A. and Hariharan, I. K. (2001). Archipelago regulates Cyclin E levels in Drosophila and is mutated in human cancer cell lines. Nature 413, 311-316.

Moshkin, Y. M., Mohrmann, L., van Ijcken, W. F. and Verrijzer, C. P. (2007). Functional differentiation of SWI/SNF remodelers in transcription and cell cycle control. Mol. Cell. Biol. 27, 651-661.

Nicholson, S. C., Nicolay, B. N., Frolov, M. V. and Moberg, K. H. (2011). Notch-dependent expression of the archipelago ubiquitin ligase subunit in the Drosophila eye. Development 138, 251-260.

Ohnuma, S. and Harris, W. A. (2003). Neurogenesis and the cell cycle. Neuron 40, 199-208.

Pajalunga, Deborah, Mazzola, Alessia, Puggioni, Eleonora and Crescenzi, Marco (2014). Non-Proliferation as an Active State: Conceptual and Practical Implications. Cell Cycle 6, 1414-1417.

Paridaen, J. T. and Huttner, W. B. (2014). Neurogenesis during development of the vertebrate central nervous system. EMBO Rep. 15, 351-364.

Pauklin, S. and Vallier, L. (2013). The cell-cycle state of stem cells determines cell fate propensity. Cell 155, 135-147.

Perez-Garijo, A., Martin, F. A., Struhl, G. and Morata, G. (2005). Dpp signaling and the induction of neoplastic tumors by caspase-inhibited apoptotic cells in Drosophila. Proc. Natl. Acad. Sci. U. S. A. 102, 17664-17669.

Raff, J. W., Jeffers, K. and Huang, J. Y. (2002). The roles of Fzy/Cdc20 and Fzr/Cdh1 in regulating the destruction of cyclin B in space and time. J. Cell Biol. 157, 1139-1149.

Rauskolb, C., Sun, S., Sun, G., Pan, Y. and Irvine, K. D. (2014). Cytoskeletal tension inhibits Hippo signaling through an Ajuba-Warts complex. Cell 158, 143-156.

Reiner, J. M. (1983). Differentiation, ageing, and terminal differentiation: a semantic analysis. J. Theor. Biol. 105, 545-552.

Remaud, S., Audibert, A. and Gho, M. (2008). S-phase favours notch cell responsiveness in the Drosophila bristle lineage. PLoS One 3, e3646.

Richardson, H., Okeefe, L. V., Marty, T. and Saint, R. (1995). Ectopic Cyclin-E Expression induces premature entry into S phase and disrupts pattern-formation in the Drosophila eye imaginal disc. Development 121, 3371-3379.

Ruggiero, R., Kale, A., Thomas, B. and Baker, N. E. (2012). Mitosis in neurons: Roughex and APC/C maintain cell cycle exit to prevent cytokinetic and axonal defects in Drosophila photoreceptor neurons. PLoS Genet 8, e1003049.

Ryoo, H. D. and Bergmann, A. (2012). The role of apoptosis-induced proliferation for regeneration and cancer. Cold Spring Harb Perspect Biol 4, a008797.

Ryoo, H. D., Gorenc, T. and Steller, H. (2004). Apoptotic cells can induce compensatory cell proliferation through the JNK and the Wingless signaling pathways. Dev. Cell 7, 491-501.

Seher, T. C. and Leptin, M (2000). Tribbles, a cell-cycle brake that coordinates proliferation and morphogenesis during Drosophila gastrulation. Curr. Biol. 10.

Sela, Y., Molotski, N., Golan, S., Itskovitz-Eldor, J. and Soen, Y. (2012). Human embryonic stem cells exhibit increased propensity to differentiate during the G1 phase prior to phosphorylation of retinoblastoma protein. Stem Cells 30, 1097-1108.

Sharp, D. J., McDonald, K. L., Brown, H. M., Matthies, H. J., Walczak, C., Vale, R. D., Mitchison, T. J. and Scholey, J. M. (1999). The bipolar kinesin, KLP61F, cross-links microtubules within interpolar microtubule bundles of Drosophila embryonic mitotic spindles. J. Cell Biol. 144, 125-138.

Sharpless, N. E. and Sherr, C. J. (2015). Forging a signature of in vivo senescence. Nat. Rev. Cancer 15, 397-408.

Sousa-Nunes, R. and Somers, W. G. (2013). Mechanisms of asymmetric progenitor divisions in the Drosophila central nervous system. Adv. Exp. Med. Biol. 786, 79-102.

Sugimura, I. and Lilly, M. A. (2006). Bruno inhibits the expression of mitotic cyclins during the prophase I meiotic arrest of Drosophila oocytes. Dev. Cell 10, 127-135.

Swanson, C. I., Meserve, J. H., McCarter, P. C., Thieme, A., Mathew, T., Elston, T. C. and Duronio, R. J. (2015). Expression of an S phase-stabilized version of the CDK inhibitor Dacapo can alter endoreplication. Development 142, 4288-4298.

Tamori, Y. and Deng, W. M. (2013). Tissue repair through cell competition and compensatory cellular hypertrophy in postmitotic epithelia. Dev. Cell 25, 350-363.

Thakar, R. and Csink, A. K. (2004). Changing chromatin dynamics and nuclear organization during differentiation in Drosophila larval tissue. J. Cell Sci. 118, 951-960.

Thomas, B. J., Gunning, D. A., Cho, J. and Zipursky, L. (1994). Cell cycle progression in the developing Drosophila eye: roughex encodes a novel protein required for the establishment of G1. Cell 77, 1003-1014.

Tintignac, L. A., Leibovitch, M. P., Kitzmann, M., Fernandez, A., Ducommun, B., Meijer, L. and Leibovitch, S. A. (2000). Cyclin E-cdk2 phosphorylation promotes late G1-phase degradation of MyoD in muscle cells. Exp. Cell Res. 259, 300-307.

van den Heuvel, S. and Dyson, N. J. (2008). Conserved functions of the pRB and E2F families. Nat. Rev. Mol. Cell Biol. 9, 713-724.

Whitfield, M. L., Sherlock, G., Saldanha, A. J., Murray, J. I., Ball, C. A., Alexander, K. E., Matese, J. C., Perou, C. M., Hurt, M. M., Brown, P. O. et al. (2002). Identification of genes periodically expressed in the human cell cycle and their expression in tumors. Mol. Biol. Cell 13, 1977-2000.

Wolff, T. and Ready, D. F. (1991). The beginning of pattern formation in the Drosophila compound eye: the morphogenetic furrow and the second mitotic wave. Development 113, 841-850.

Wu, S., Liu, Y., Zheng, Y., Dong, J. and Pan, D. (2008). The TEAD/TEF family protein Scalloped mediates transcriptional output of the Hippo growth-regulatory pathway. Dev. Cell 14, 388-398.

Yun, M. H. (2015). Changes in Regenerative Capacity through Lifespan. Int J Mol Sci 16, 25392-25432.

Zekanowski C, Wojda U. (2009). Aneuploidy, chromosomal missegregation, and cell cycle re-entry in Alzheimer's disease. Acta Neurobiol. Exp. 69, 232–253.

Zhao, B., Ye, X., Yu, J., Li, L., Li, W., Li, S., Lin, J. D., Wang, C. Y., Chinnaiyan, A. M., Lai, Z. C. et al. (2008). TEAD mediates YAP-dependent gene induction and growth control. Genes Dev. 22, 1962-1971.

CHAPTER 2: SCALLOPED AND YORKIE ARE REQUIRED FOR CELL CYCLE RE-ENTRY OF QUIESCENT CELLS AFTER TISSUE DAMAGE[1]

SUMMARY

Regeneration of damaged tissues typically requires a population of proliferatively active stem cells. How damaged tissue is regenerated in quiescent tissues lacking a stem cell population is less well understood. We used a genetic screen in the developing *Drosophila melanogaster* eye to investigate the mechanisms that trigger quiescent cells to re-enter the cell cycle and proliferate in response to tissue damage. We discovered that Hippo signaling regulates compensatory proliferation after extensive cell death in the developing eye. Scalloped and Yorkie, transcriptional effectors of the Hippo pathway, drive expression of Cyclin E to induce cell cycle re-entry in cells that normally remain quiescent in the absence of damage. Ajuba, an upstream regulator of Hippo signaling that functions as a sensor of epithelial integrity, is also required for cell cycle re-entry. Thus, in addition to its well-established role in modulating proliferation during periods of tissue growth, Hippo signaling maintains homeostasis by regulating quiescent cell populations affected by tissue damage.

INTRODUCTION

Tissue regeneration has fascinated biologists for hundreds of years, but the molecular mechanisms underlying this process have only recently begun to be understood. Pioneering

[1]This chapter previously appeared as an article in Development, a journal of The Company of Biologists Ltd, and can be accessed here: http://dev.biologists.org/content/142/16/2740. The original citation is: "Scalloped and Yorkie are required for cell cycle re-entry of quiescent cells after tissue damage," Meserve, JH, Duronio, RJ. Development (2015) 142, 2740-2751.

experiments on regenerating hydra by the Abbe Trembley in the 1700's and on other organisms by researchers in the 1800's (Morgan, 1901) established that regeneration functions as a reparative process to replace tissues damaged by injury or disease and occurs as a restorative process to repair old and damaged tissues throughout the lifespan of an organism. Although early experiments on highly regenerative animals, such as hydra, are fundamental for our understanding of regeneration, the lack of facile genetic manipulation in these organisms made identifying molecular mechanisms difficult.

In the 1970's, *Drosophila melanogaster* emerged as a powerful and genetically tractable experimental system in which to study regeneration. Larval imaginal discs, which are epithelial tissues that proliferate during larval life and differentiate during pupation into adult structures, are able to regrow after substantial tissue loss due to irradiation or removal of fragments by surgery (Bryant, 1971; Haynie and Bryant, 1977; Worley et al., 2012). In these imaginal discs, a process called "compensatory proliferation (CP)" replaces cells lost by tissue damage. Research from several labs in the last decade has elucidated some of the mechanisms controlling CP. One important mechanism is the induction of proliferation by apoptotic cells. Caspases are required for robust regeneration in many organisms even though caspase activity and cell death contributes to initial tissue loss following damage. When apoptosis is blocked by the baculovirus effector-caspase inhibitor p35 in damaged *Drosophila* wing discs, "undead cells," which have initiated but not completed apoptosis induce hyperproliferation (Huh et al., 2004; Perez-Garijo et al., 2004). This hyperproliferation is dependent on the initiator caspase Dronc, suggesting that this caspase has a role in inducing proliferation independently of apoptosis (Huh et al., 2004). Proliferation induced by undead cells or genuine apoptotic cells may act in various contexts through multiple pathways, including the Wingless/Wnt, Dpp/BMP, Jun N-terminal kinase (JNK), and Hedgehog signaling pathways (Ryoo et al., 2004; Perez-Garijo et al., 2005; Fan and Bergmann, 2008). Apoptosis-induced proliferation involving mitogenic signaling is likely to be just one part of a larger pathway controlling CP (Mollereau et al., 2013).

The participation of apoptotic cells in regeneration is not unique to *Drosophila*. Studies in other organisms have revealed that caspase activity is required for regeneration in the *Xenopus laevis* tadpole tail (Tseng et al., 2007) and in the mammalian liver and skin (Li et al., 2010). Additionally, many of the pathways identified as being involved in CP regulation in *Drosophila* are also involved in vertebrate tissue repair. For example, both the Hedgehog (Cai et al., 2011) and JNK (Wuestefeld et al., 2013) pathways are required for mammalian liver regeneration, and Wnt signaling is required for limb regeneration in *Xenopus*, axolotl, and zebrafish (Kawakami et al., 2006). Thus, there are conserved mechanisms for regeneration between invertebrates and vertebrates.

How the cell cycle is regulated during regeneration to ensure proper levels of regrowth remains unclear. Tissue regrowth can be accomplished by increasing proliferation to restore cell number, as in *Drosophila* wing discs, or by cellular growth without cell division. During endoreplication, rounds of DNA synthesis occur without intervening mitoses, resulting in an increase in ploidy that is usually accompanied by an increase in cell size (Fox and Duronio, 2013). A strong proliferative response to damage occurs during planaria body regeneration (Wenemoser and Reddien, 2010), zebrafish heart regeneration (Poss et al., 2002), and *Xenopus* tail regeneration (Tseng et al., 2007), and endoreplication contributes to tissue repair in the mammalian liver (Sigal et al., 1999) and the *Drosophila* ovary (Tamori and Deng, 2013). In these tissues, a moderate increase in the number of proliferating or endoreplicating cells quickly replaces lost tissue.

In contrast, it is unclear how cell cycle exit in quiescent tissues could be overcome to allow proliferation following damage. Robust inhibition of cell cycle re-entry in quiescent tissues is necessary to maintain tissue homeostasis and prevent neoplasia and cancer. This inhibition of cell cycle re-entry thus presents a high hurdle to overcome before regeneration can take place. We investigated this issue using the *Drosophila* eye imaginal disc. The eye disc contains a population of cells that are normally quiescent but will undergo cell cycle re-entry after induction of massive

cell death (Fan and Bergmann, 2008). We used the developing eye as a model for CP and performed a genetic screen to identify regulators of this process. With this approach, we identified the transcription factor Scalloped (Sd) as a novel regulator of CP. We show that Sd and the Sd binding partner Yorkie (Yki) are required for cell cycle re-entry following damage in the eye imaginal disc. Yki is a transcriptional effector of the Hippo pathway and was previously identified as a regulator of CP in wing discs (Sun and Irvine, 2011; Grusche et al., 2011). We also found that CP in the eye disc requires the Hippo pathway regulator Ajuba (Jub), similar to recent results in the wing disc (Sun and Irvine, 2013). However, activation of Jub during CP is likely to be differentially regulated in these two tissues. Our study demonstrates that Hippo signaling is required for quiescent cells to re-enter the cell cycle following tissue damage and is likely to provide insight into a variety of regenerative systems, particularly those within non-proliferative tissues.

RESULTS

Quiescent cells re-enter the cell cycle after tissue damage in the developing eye

The developing *Drosophila* eye is ideal for studying regeneration in a quiescent cell population. Many genetic tools are available for manipulating cells in the eye imaginal disc, and even subtle defects in eye development caused by these manipulations are readily apparent in the highly organized adult eye (Dominguez and Casares, 2005; Gutierrez-Avino et al., 2009). The neurocrystalline lattice of the *Drosophila* eye takes shape by precise control of the cell cycle and differentiation during development (Fig. 1A,L). In early larval development, the eye disc grows as undifferentiated cells proliferate asynchronously to expand the population of precursor cells. During the third and last stage of larval development, a wave of differentiation associated with an apical constriction of the epithelial sheet called the morphogenetic furrow (MF) moves from posterior to anterior across the disc. Cells within the MF arrest in G1, and a subset begin to differentiate into photoreceptors. After the MF has passed, the remaining undifferentiated cells

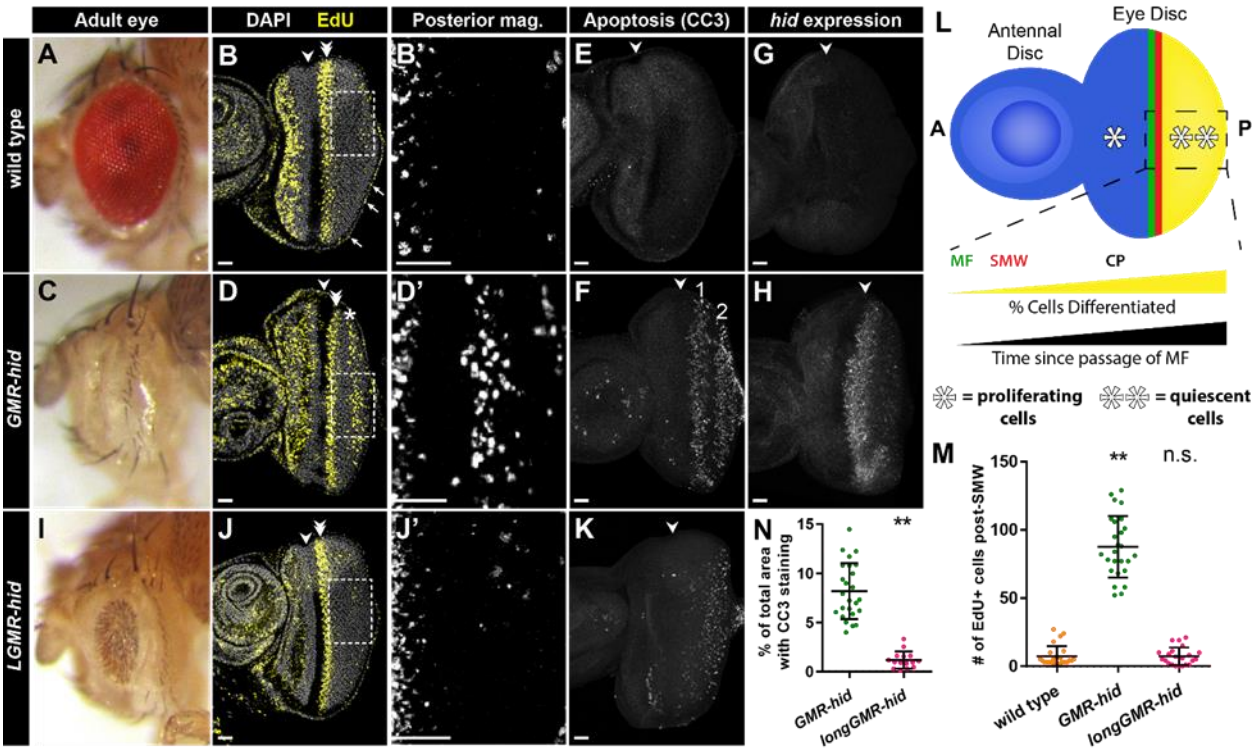

Fig. 1. Hid expression induces CP in the eye imaginal disc. (A,C,I) Adult eyes of the indicated genotypes. Wild-type (A) is Oregon R. (B,D,J) DAPI (DNA; single confocal slice in gray) and EdU (S phase; projection in yellow) staining of eye imaginal discs, indicating the MF (arrowheads) and the SMW (double arrowheads), respectively. Note that EdU+ cells in the row of cells around the disc (arrows in B) are margin cells and not part of the disc proper. Asterisk denotes CP (D). Boxes indicate areas of magnification shown in B′D′,J′. (E,F,K) Cleaved Caspase-3 (CC3) staining of apoptotic cells in discs of the indicated genotypes. The first (1) and second (2) apoptotic waves are indicated in (F). (G,H) In situ hybridization for hid mRNA in the indicated genotypes. (L) The eye disc, attached to the anterior (A) antennal disc, is composed of undifferentiated, proliferating cells (blue) anterior to the MF (green) and both undifferentiated and differentiated quiescent cells (yellow) posterior (P) to the SMW (red). Cells furthest from the MF (most posterior) are the most differentiated. (M) Quantification of CP in the indicated genotypes. All post-SMW, EdU+ eye disc cells were counted. Each circle represents the number of cells counted for a single disc, and bars represent mean and one standard deviation. For each genotype, n≥22 discs. **P=2.6×10−17. (N) Quantification of percentage of total disc area with CC3 staining. Each circle represents the percentage for a single disc, and bars represent mean and one standard deviation. n>15 discs. **P=2.4×10−14. n.s., not significant. Anterior is oriented to the left. Scale bars: 20 μm.

synchronously enter S-phase in what is termed the second mitotic wave (SMW) (Fig. 1B). After the SMW, these cells become quiescent and await cues to differentiate (Fig. 1L) (Firth and Baker, 2005). This population is considered to be quiescent as very few cells posterior to the SMW enter S-phase (Fig. 1B') or undergo mitosis (Baker and Yu, 2001). Cells remain quiescent by mechanisms that prevent cell cycle re-entry, including CDK inhibition by Dacapo and repression of E2f1-dependent transcription by Retinoblastoma/Rbf1 (Buttitta et al., 2007; Ruggiero et al.,

2012), as well as destruction of cell cycle regulators by the anaphase promoting complex (Buttitta et al., 2010; Bandura et al., 2013).

Although cells posterior to the SMW are normally quiescent, cell cycle re-entry is induced when the tissue responds to cell death (Fan and Bergmann, 2008). Expression of the pro-apoptotic gene *hid* with the *GMR* promoter, which is expressed throughout the eye disc posterior to the MF (Fig. S1A), induces extensive cell death (Fig. 1E,F). Dying, caspase-positive cells with pyknotic nuclei are extruded from the basal surface of the eye disc (Fig. S1B-C), as shown in previous studies of apoptosis in imaginal discs (Gibson and Perrimon, 2005; Shen and Dahmann, 2005). Interestingly, not all cells posterior to the SMW die, and some overcome the mechanisms keeping them quiescent and re-enter S-phase in a wave of proliferation (Fig. 1D,D'), as described previously (Fan and Bergmann, 2008). However, eyes are nearly absent in adult *GMR-hid* flies (Fig. 1C), indicating this increased proliferation cannot fully compensate for tissue loss, probably because *GMR-hid* continues to be expressed into pupal stages and induces extensive apoptosis after the potential to re-enter the cell cycle is lost. Thus, *GMR-hid* eye imaginal discs behave somewhat differently to previous CP models in the wing in which tissue regrowth is more complete (Mollereau et al., 2013). Nonetheless, cell cycle re-entry posterior to the MF in response to tissue damage in the eye disc provides a valuable model for studying CP in a quiescent cell population.

Because apoptotic cells play a crucial role during CP, we further characterized the relationship between dying and proliferating cells in the eye disc. Interestingly, rather than uniform apoptosis across *GMR-hid* discs, two distinct waves of cleaved Caspase-3 positive cells occur on either side of the CP wave (Fig. 1F, S1D-E). Because the CP wave overlaps substantially with the apoptosis-free zone between the two waves of cleaved Caspase-3 staining, it was previously suggested that proliferating cells might inhibit apoptosis (Fan and Bergmann, 2008). However, these two waves of apoptosis persist when CP is blocked (see below and Fig. 3B,C), suggesting that CP does not inhibit apoptosis. Rather, variations in Hid activity across the disc

may account for the observed pattern of apoptosis. Hid protein accumulation and activity varies posterior to the MF (Fan and Bergmann, 2014). In addition, we found that *hid* mRNA is not uniformly expressed across *GMR-hid* discs, with high levels immediately posterior to the MF and lower levels more posteriorly (Fig. 1G,H). *hid* mRNA can be regulated by the miRNA *bantam* (*ban*) (Brennecke et al., 2003), which protects cells from apoptosis in certain damaged tissues after being up-regulated by a Tie-like receptor tyrosine kinase (Tie)-dependent mechanism (Bilak et al., 2014). We did not detect *ban* induction in *GMR-hid* discs (Fig. S5C), and RNAi targeting of Tie does not affect the pattern of apoptosis (Fig. S2A). These results suggest that Tie-dependent induction of *bantam* is not responsible for decreased *hid* transcripts in the posterior eye disc.

Because *hid* transcripts are low in the posterior of the disc, we considered the possibility that dying cells in the first apoptotic wave promote apoptosis-induced apoptosis (AiA), resulting in the second apoptotic wave. AiA is mediated by JNK signaling (Perez-Garijo et al., 2013). However, expression of a dominant-negative version of the *Drosophila* JNK homolog Basket (Bsk) does not affect the pattern of apoptosis in *GMR-hid* discs (Fig. S2B). Interestingly, although JNK signaling is required for CP in the wing disc (Ryoo et al., 2004), CP is not decreased in *GMR-hid* eye discs when JNK signaling is suppressed by expression of Bsk^{DN} or Puckered (Puc), a negative regulator and downstream target of the JNK pathway (Fig. S2C,D,G). Additionally, although *puc* is induced after damage in the wing (Bergantinos et al., 2010), *puc-lacZ* is not induced in *GMR-hid* eye discs (Fig. S2E,F). We conclude from these data that regulation of Hid expression and activity, rather than S-phase entry, *bantam* induction, or AiA, determines the pattern of apoptosis in *GMR-hid* eye discs and that JNK signaling is not a major contributor to CP in response to apoptosis posterior to the MF.

Next, we explored contributions to the pattern of CP in *GMR-hid* discs. The region of CP occurs in a well-defined wave that does not typically extend to the posterior edge of the disc (Fig. 1D,D'). Previous work demonstrated that undifferentiated cells, and not photoreceptors, re-enter S-phase in *GMR-hid* discs (Fan and Bergmann, 2008). Because undifferentiated cells are present

at the posterior edge of the eye disc, we hypothesized that cells lose the competency to re-enter S-phase prior to differentiation, perhaps as a result of prolonged quiescence. To address this hypothesis, we shifted the wave of apoptosis towards the posterior edge of the disc by expressing *hid* under the control of *longGMR* (*LGMR*), a version of the *GMR* promoter that contains an additional transcriptional repressor element and is therefore only expressed in a subset of photoreceptors (Wernet et al., 2003; Fig. S1F). Although we were unable to obtain clear *hid* mRNA signal in this genotype, probably owing to lower levels of accumulation than in *GMR-hid* discs, we did observe a single wave of apoptosis in the posterior region of *LGMR-hid* larval eye discs (Fig. 1K). In addition, adult *LGMR* flies have a reduced eye phenotype similar to, but less severe than, *GMR-hid* flies (Fig. 1I). Unlike in *GMR-hid* discs, however, CP is not induced in *LGMR-hid* discs (Fig. 1J,J',M). This result is consistent with the idea that undifferentiated cells at the posterior of the disc have become refractory to cell cycle re-entry in response to tissue damage. Alternatively, a lower level of apoptosis in *LGMR-hid* discs compared to *GMR-hid* discs (Fig. 1N) may not be sufficient to induce a compensatory response.

An RNAi screen identifies genes required for compensatory proliferation

How do undifferentiated cells overcome quiescence to re-enter the cell cycle in response to tissue damage? The mechanisms that control CP in quiescent cells of the eye disc are distinct from those in proliferating cells of the wing disc (Fan and Bergmann, 2008). For example, JNK signaling is required for CP in the wing disc (Ryoo et al., 2004) whereas our data suggest that it is not required in the eye disc (Fig. S2). To identify pathways necessary for cell cycle re-entry in the regenerating eye, we designed a genetic screen based on adult eye phenotypes. We expressed hairpin RNAs targeting individual genes in *GMR-hid* eye discs using the GAL4/UAS system and assessed the effect on CP by scoring the adult eye phenotype. To drive expression of UAS-transgenes, we constructed a *GMR-hid, GMR-Gal4/+* (*GMR>hid, Gal4*) line (unless otherwise noted, genotypes written as *GMR>hid, transgene* are heterozygous for *GMR-hid, GMR-Gal4*,

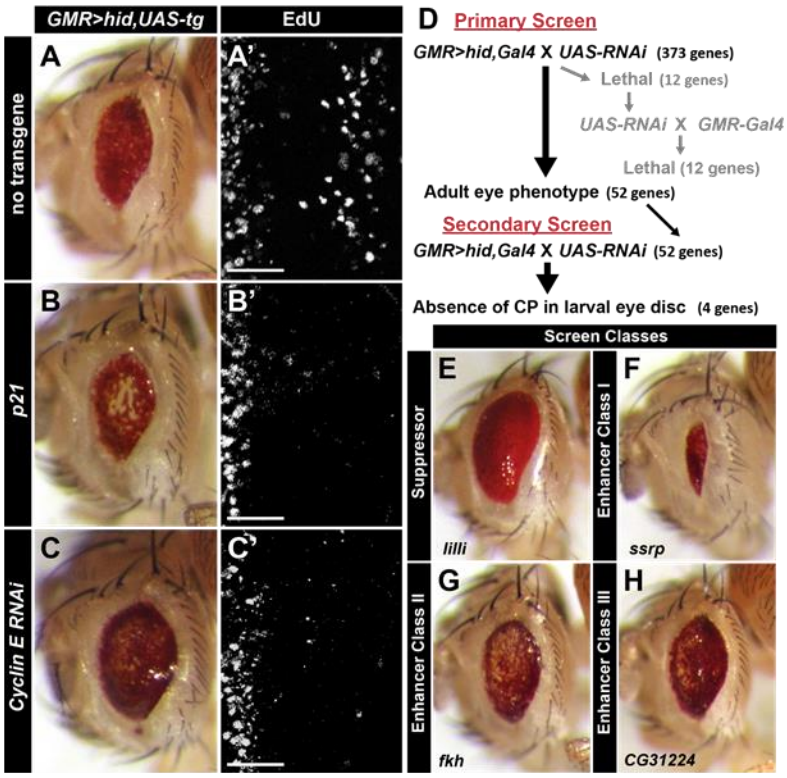

Fig. 2. Genetic screen for regulators of compensatory proliferation. (A-C′) Adult eyes (A-C) and high magnification view of posterior eye imaginal discs (A′-C′; as in Fig. 1B′) expressing the indicated UAS-transgenes in *GMR-hid, GMR-Gal4/+* individuals. (D) Schematic of the RNAi screen. (E-H) Representative examples of the four categories of adult eye phenotypes resulting from the RNAi screen. See also supplementary material Table S1 and Figs S3,S4. Anterior is oriented to the left. Scale bars: 20 μm.

and a UAS-transgene). Eyes in *GMR>hid, Gal4* flies are drastically reduced in size compared to wild type but larger than *GMR-hid* eyes (compare Figs. 1A,C and 2A). *GMR>hid, Gal4* larval eye discs exhibit a strong compensatory proliferative response (Fig. 2A') with similar numbers of cells re-entering S-phase compared to *GMR-hid* (p-value=0.39). We tested whether inhibiting CP would result in a detectable adult eye phenotype by expressing the mammalian CDK inhibitor p21 or dsRNA targeting *Cyclin E* in *GMR>hid, Gal4* eye discs. In these genotypes, CP is blocked and a reproducible adult eye phenotype results in which pigment is reduced (Fig. 2B-C'). Because pigment cells are one of the last cell types to differentiate, this result suggests that the undifferentiated, precursor pool size is reduced when CP is blocked and that cells that undergo CP contribute to the adult eye. Importantly, the SMW does not appear to be affected in *GMR-Gal4, GMR-hid/UAS-p21* discs (Fig. S3A,B), in contrast to *GMR-p21* flies in which the SMW is

ablated (Fig. S3C, (de Nooij and Hariharan, 1995)). These data suggest that the accumulation of Gal4 required to drive high UAS-transgene expression does not occur until posterior to the SMW, allowing us to assess phenotypes during CP without confounding defects in the SMW. In addition, these data indicate that we can detect loss of CP by monitoring adult eye phenotypes.

Using this approach, we screened a collection of UAS-RNAi lines targeting *Drosophila* transcription factors. Our rationale for this strategy is that many signaling pathways affecting cell cycle entry and CP have a transcriptional output. In addition, because multiple inputs can result in activation of the same transcription factor, we reasoned that knocking down the transcription factor itself would result in a stronger phenotype than knocking down one of the upstream components. Of the 544 transcription factors included in both the Fly Transcription Factor Database (Pfreundt et al., 2010) and the Animal Transcription Factor Database (Zhang et al., 2012), we tested the 373 genes for which there was an available RNAi line (Table S1). In our primary screen, candidate genes were identified based on suppression or enhancement of the *GMR>hid, Gal4* eye adult phenotype (Fig. 2D). *luciferase* (*luc*) RNAi was used as a negative control. Twelve UAS-RNAi lines caused lethality with *GMR>hid, Gal4* and were not examined further as they were also lethal with *GMR-Gal4* alone (Table S1).

Fifty two UAS-RNAi lines modified the *GMR>hid, Gal4* adult eye phenotype: three acted as suppressors, including *glass*, the transcription factor that binds to and activates *GMR* (Fig. 2E,S4); twelve displayed a small eye (Enhancer Category I; Fig. 2F,S4); seven displayed moderate pigment loss (Enhancer Category II; Fig. 2G,S4); twenty one displayed mild pigment loss (Enhancer Category III; Fig. 2H,S4); and two displayed other eye phenotypes (Other Category; Fig. S4). These 52 lines were also crossed to *GMR-Gal4* alone to determine if they disrupted eye development independently of *GMR-hid* (Fig. S4). Included in the lines identified in our unbiased screen were genes required for cell proliferation, such as *E2f1* and *Dp*, and genes required for eye development, such as *cut* and *prospero*, confirming the validity of our approach.

Because many of these UAS-RNAi lines caused a rough eye phenotype with *GMR-Gal4* alone and thus may disrupt eye development in a process separate from CP, we performed a secondary screen to assess CP within the larval eye discs (Fig. 2D). In many of the 52 RNAi lines tested, we observed normal or slightly disrupted CP in *GMR>hid, RNAi* eye discs (Fig. S4). We observed a striking loss of CP in four RNAi lines: *Dp*, *scalloped* (*sd*), *fork head*, and *knirps*. *Dp* is known to be required for entry into S-phase (Frolov et al., 2005) and thus was not characterized further. Of the remaining three genes, we focused our studies on Sd, a TEAD/TEF transcription factor that regulates growth and apoptosis in many developing tissues (Simmonds et al., 1998; Wu et al., 2008; Zhang et al., 2008).

Scalloped is required for compensatory proliferation

CP is substantially reduced in *GMR-hid* discs by *sd* knockdown with either of two independently derived RNAi lines (Fig. 3A,B,G). To verify this result, we tested whether a *sd* mutation would also block CP. Because *sd* null mutants are embryonic lethal (Deshpande et al., 1997), we generated *sd* mutant clones in *GMR-hid* eye discs using the *ey>Flp/FRT* system (Fig. 3C-C'''). Whereas wild type clones contain 5-ethynyl-2′-deoxyuridine (EdU)-positive cellsin the position of the CP wave, *sd* mutant clones do not (Fig. 3C'',C'''). Although apoptosis is slightly decreased in *GMR>hid, sd RNAi* discs compared to *GMR>hid, luc RNAi* (Fig. 3A,B,H), the decrease in CP is not due to a decrease in apoptosis because many *GMR>hid, sd RNAi* discs have the same extent of apoptosis as controls, whereas none have the same degree of CP as controls (Fig. 3H). Taken together these results indicate that Sd is a bona fide regulator of CP.

Recent results suggest that in certain contexts, Sd can act as a suppressor of genes controlling apoptosis and growth. This suppressor activity is dependent on the Tondu-domain-containing Growth Inhibitor (Tgi) cofactor (Koontz et al., 2013). We reasoned that the slight decrease in apoptosis in *GMR>hid, sd RNAi* discs could reflect this suppressor activity of Sd. However, the amount of apoptosis is unchanged in *GMR>hid, tgi RNAi* discs relative to control

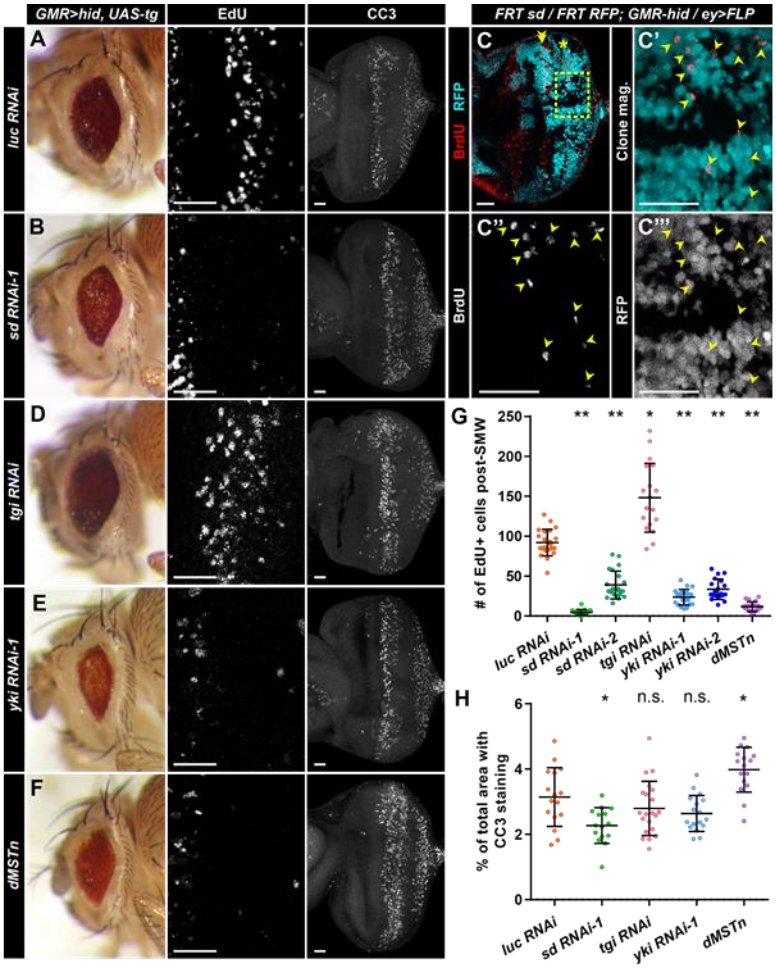

Fig. 3. *sd* and *yki* are required for compensatory proliferation. (A,B,D-F) Adult eyes (left panels), high magnification of posterior eye discs stained with EdU (middle panels), and apoptosis as detected by CC3 staining (right panels) in *GMR>hid, Gal4* discs expressing the indicated transgenes. *luciferase* (*luc*) RNAi is used as a control (A). (C-C‴) Clones of wild-type (RFP+, cyan) and *sd* mutant (RFP−) cells in the *GMR-hid* background. Boxed area in C indicates area of magnification shown in C′-C‴. Double arrowhead indicates SMW; asterisk indicates CP. Arrowheads indicate BrdU+ cells. (G) Quantification of CP in the *GMR>hid, Gal4* background for the indicated UAS-transgenes. Each circle represents the number of cells counted for a single disc, and bars represent mean and one standard deviation. For each genotype, n≥19 discs. (H) Quantification of percentage of total disc area with CC3 staining in the *GMR>hid, Gal4* background for the indicated UAS-transgenes. Each circle represents the percentage for a single disc, and bars represent mean and one standard deviation. For each genotype, n≥15 discs. *P≤3×10−3, **P≤3×10−13. n.s., not significant. Anterior is oriented to the left. Scale bars: 20 μm.

(Fig. 3D,H). Interestingly, CP increases in *GMR>hid, tgi RNAi* discs (Fig. 3D,G), possibly as a result of increased expression of growth genes (Fig. 3D). The opposing phenotypes of *sd* and *tgi* RNAi in the *GMR-hid* background make it unlikely that Sd is acting as a suppressor to induce CP.

Yorkie is required for compensatory proliferation

Sd activates expression of target genes in the eye disc as part of a complex with Yorkie (Yki), the transcriptional effector of the Hippo pathway (Goulev et al., 2008; Wu et al., 2008; Zhang et al., 2008). The Hippo pathway controls tissue growth by regulation of Yki, targets of which include cell cycle regulators, such as *Cyclin E* (Huang et al., 2005) and *E2f1* (Goulev et al., 2008) and anti-apoptotic genes such as *Diap1* (Huang et al., 2005*)* and *ban* (Thompson and Cohen, 2006). Flux through the Hippo pathway is governed by Hippo (Hpo) phosphorylation of Warts (Wts), which in turn phosphorylates Yki. Phosphorylated Yki cannot translocate to the nucleus (Oh and Irvine, 2008). Thus, increased Hippo signaling reduces transcription of Yki target genes. Unphosphorylated, nuclear Yki acts as a co-activator for transcription factors like Sd and the Homothorax (Hth)/Teashirt (Tsh) complex (Peng et al., 2009). Because Yki itself does not bind DNA, it was not included in our screen of transcription factor RNAi lines. Targeting *yki* with two independently derived UAS-RNAi transgenes reduced CP in the *GMR>hid, Gal4* background and resulted in an adult eye phenotype similar to that after *sd* RNAi (Fig. 3E,G). Levels of apoptosis in *GMR>hid, yki RNAi* discs were not significantly different from controls (Fig. 3H). We further probed the contribution of Yki to CP by over-expressing the Hpo kinase domain (dMSTn (Zhang et al., 2008)), which blocks Yki activity. Again, the adult eye phenotypes were similar to those elicited by *sd* or *yki* RNAi (Fig. 3F), and CP in the eye disc was significantly reduced compared to controls (Fig. 3F,G). We conclude that Yki is necessary to induce CP in eye discs, suggesting a shared role for Hippo signaling in regulating CP in eye and wing discs.

Cyclin E is induced by Sd/Yki during compensatory proliferation

Targets of Sd/Yki include *Cyclin E*, *Diap1*, *expanded* (*ex*), and *ban* (Wu et al., 2008; Zhang et al., 2008). As Cyclin E is required for CP (Fig. 2C), we compared Cyclin E levels in wild type and *GMR-hid* discs. In proliferating cells, like those anterior to the MF or within the SMW, Cyclin E levels rise during G1 to induce entry into S-phase (Fig. 4F, (Knoblich et al., 1994)), then fall

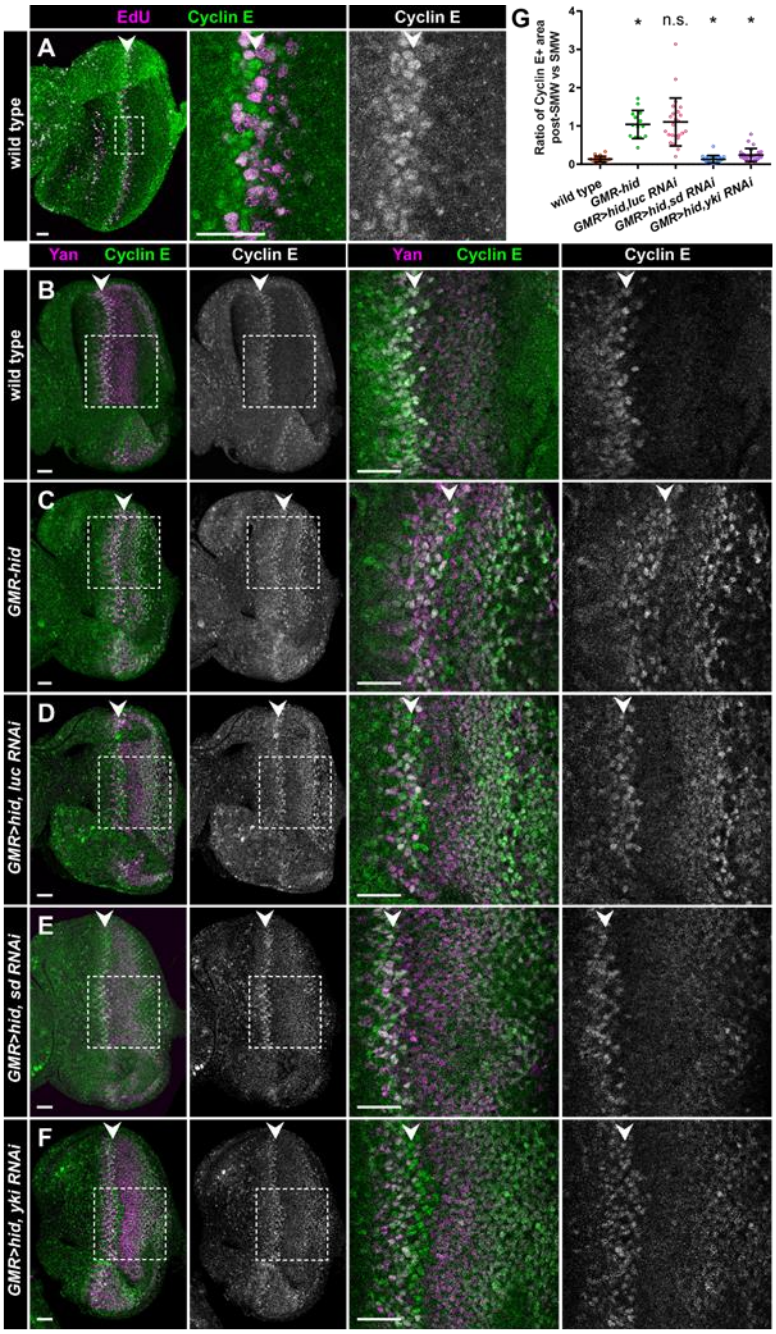

Fig. 4. Sd and Yki are required for elevated Cyclin E levels during CP. (A) Eye disc labeled with EdU (magenta) and anti-Cyclin E (green) antibodies. Cyclin E accumulates prior to and during S phase of the SMW (arrowhead). Box in left panel indicates area of magnification in middle and right panels. (B-F) Eye discs of the indicated genotypes stained with anti-Cyclin E (green) and anti-Yan (marker of undifferentiated cells; magenta) antibodies. Boxes indicate areas shown at higher magnification on the right. Arrowheads indicate SMW. (G) Quantification of Cyclin E staining in Yan+ cells of the indicated genotypes. The ratio of post-SMW Cyclin E staining versus SMW Cyclin E staining is displayed. Each circle represents the ratio calculated for a single disc, and bars represent mean and one standard deviation. For each genotype, n≥14 discs. *P≤1.8×10−7. Significance was calculated for wild type (w^{1118}) versus *GMR-hid, GMR-hid* versus *GMR>hid, luc RNAi, GMR>hid, luc RNAi* versus *GMR>hid, sd RNAi*, and *GMR>hid, luc RNAi* versus *GMR>hid, yki RNAi*. n.s., not significant. Anterior is oriented to the left. Scale bars: 20 μm.

during S-phase and mitosis as a result of transcriptional (Duronio and O'Farrell, 1995) and post-translational (Moberg et al., 2001) regulation. In wild type eye discs, Cyclin E levels are low in quiescent cells posterior to the SMW (Fig. 4B, (Richardson et al., 1995)). In contrast, Cyclin E expression is high posterior to the SMW in *GMR-hid* and *GMR>hid, luc RNAi* discs (Fig. 4C,D). This increase in Cyclin E accumulation occurred primarily in Yan+ undifferentiated cells rather than in photoreceptors (Fig. 4C,D). *sd* or *yki* RNAi prevents Cyclin E accumulation with expression more similar to control discs (Fig. 4E,F,G). These data suggest Sd/Yki induce Cyclin E expression in regenerating eye discs, thus allowing S-phase entry during CP.

We next examined expression of the Yki targets *ex* and *ban* in *GMR-hid* tissues. Whereas we observe CP (Fig. S5A) and apoptosis (Fig. S5B) in clones of *GMR-hid* expressing cells, we do not observe differences in expression of a transgene that detects *ban* activity (Brennecke et al., 2003) (Fig. S5C) or in *ex-lacZ* expression (Fig. S5D) between wild type and *GMR-hid* clones. Additionally, we do not observe an increase in *ban* sensor expression or *ex-lacZ* in *GMR-hid* discs compared to wild type (Fig. S5E,F).

Overexpression of Yki rescues GMR-hid phenotypes

Because overexpression of Yki induces *Cyclin E* expression and proliferation (Huang et al., 2005), we tested whether increased expression of Yki rescues *GMR-hid* phenotypes. We expressed wild type Yki and a version of Yki (Yki^{S168A}) that is hyperactive due to reduced phosphorylation by Wts (Oh and Irvine, 2008). In an otherwise wild type eye disc, *GMR-Gal4* driven expression of either Yki or Yki^{S168A} induces Cyclin E and ectopic S phase but not apoptosis posterior to the MF (Fig. S6B-D"). Yki^{S168A} expression induces a considerable number of cells to enter S phase, resulting in extensive overgrowth in both the larval imaginal disc (Fig. S6B") and the adult eye (Fig. S6A"). Similar results were obtained in the *GMR>hid, Gal4* background (Fig. 5). Both Yki and Yki^{S168A} expression result in high Cyclin E accumulation throughout the posterior of *GMR>hid, Gal4* discs (Fig. 5C-C"). Although the adult eye morphology, CP, and apoptosis

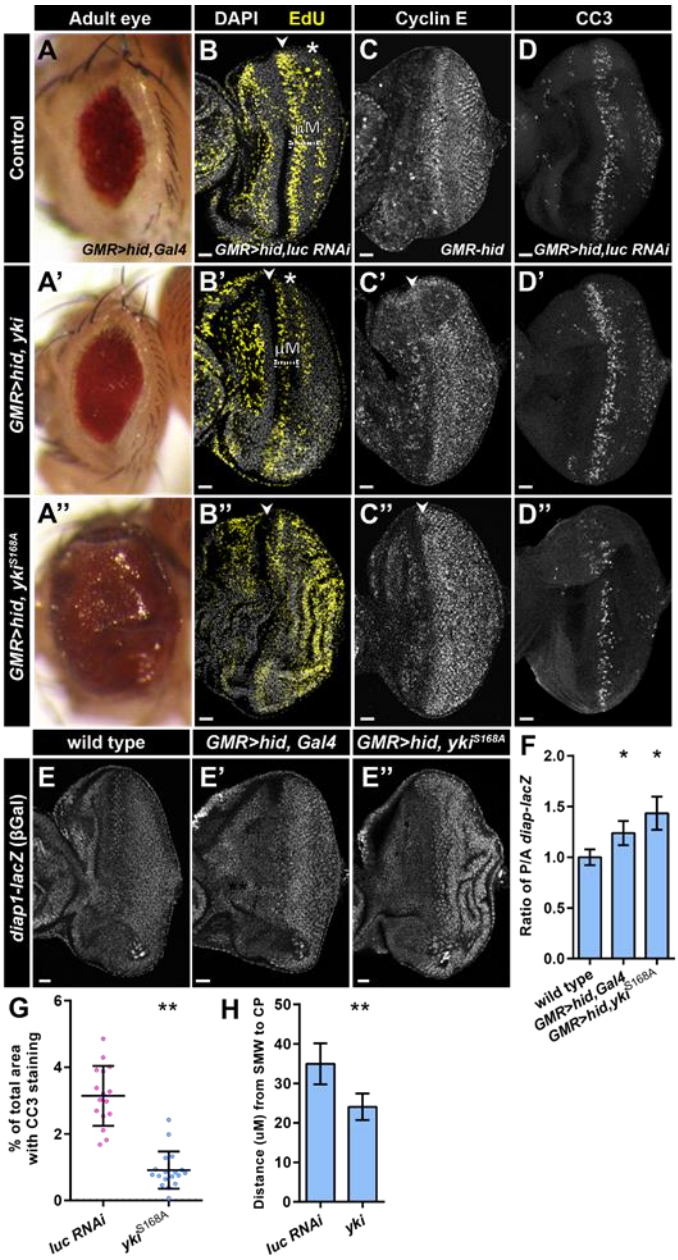

Fig. 5. Expression of transgenic *yki* modifies the *GMR-hid* phenotype. (A-A″) *GMR>hid, Gal4* adult eyes (control in A) after expression of *yki* (A′) or yki^{S168A} (A″). (B-B″) EdU staining (yellow) in eye discs of the indicated genotypes. Arrowheads indicate SMW. The white bar (B,B′) indicates the distance measured between the SMW and CP (asterisk) (data shown in H). (C-C″) Cyclin E staining of the indicated genotypes. (D-D″) CC3 staining of the indicated genotypes. (E-E″) β-Gal staining of the indicated genotypes detects *Diap1-lacZ* expression. (F) Quantification of *Diap1-lacZ* expression by β-Gal staining [ratio of posterior to anterior (P/A) eye disc, normalized to w^{1118} control] in the indicated genotypes. Error bars represent one standard deviation. *P≤6×10−4, n≥11 discs. (G) Quantification of percentage of total disc area with post-furrow CC3 staining in *GMR>hid, Gal4* eye discs expressing *luc* RNAi (n=16) or yki^{S168A} (n=18). Each circle represents the percentage calculated for a single disc, and bars represent mean and one standard deviation. **P=3.64×10−6. (H) Quantification of the distance between the SMW and CP wave in *GMR>hid, Gal4* eye discs expressing *luc* RNAi (n=25) or *yki* RNAi (n=22). **P=8.47×10−11. Error bars represent one standard deviation. Anterior is oriented to the left. Scale bars: 20 μm.

appear similar in control and *GMR>hid, yki* discs (Fig. 5A',B',D'), there is an increase of cells in S-phase in *GMR>hid, yki*^{S168A} discs (Fig. 5B"), and overgrowth occurs in both the disc and adult eye (Fig. 5A",B"). Therefore, overexpression of Yki^{S168A} rescues the small eye phenotype caused by *GMR-hid*, indicating that activation of Yki is sufficient to overcome cell loss after Hid induction.

Although suppression of the *GMR>hid, Gal4* eye phenotype by Yki^{S168A} expression is likely to be due primarily to extensive over-proliferation, we also measured apoptosis in this genotype. Apoptosis is significantly decreased in *GMR>hid, yki*^{S168A} discs, particularly in the second wave of apoptosis (Fig. 5D",G). As *Diap1* is a Yki target and suppressor of apoptosis, we measured *Diap-lacZ* levels after Hid and Yki^{S168A} expression. *Diap-lacZ* levels posterior to the furrow increase after Hid expression and increase further with Hid and Yki^{S168A} expression (Fig. 5E,F). Thus, Yki-driven induction of *Diap1* may play a role in limiting cell death after induction of *hid*. Although apoptosis is not increased in *GMR>hid, yki RNAi* discs, we observed an increase in apoptosis in *GMR>hid, dMSTn* discs (Fig. 3F,H). *GMR>hpo* discs also display moderate apoptosis, independently of Hid expression (Verghese et al., 2012). These data suggest that in addition to its role in CP, modulation of Yki activity by Hippo signaling can regulate apoptosis during tissue damage.

Our data suggest that Yki activation is a key regulatory step in the initiation of CP. We therefore hypothesized that Yki activity is limiting for entry into S phase during CP. If true, an increase in Yki posterior to the MF would sensitize cells to CP signals, resulting in more rapid S phase entry that would be manifested by an anterior shift in position of the CP. Indeed, we observe a decrease in the distance between the anterior border of the SMW and the anterior border of the compensatory wave in *GMR>hid, yki* discs when compared to *GMR>hid, luc RNAi* (Fig. 5B,H). Because distance across the anteroposterior axis of the eye disc is a proxy for time, these data indicate that cells re-enter S-phase sooner in *GMR-hid* discs expressing additional Yki compared to those without. These data suggest that levels of Yki are important for controlling the timing of CP and that active Yki may be the limiting factor for inducing cell cycle re-entry.

Ajuba, an inhibitor of Hippo signaling, is required for compensatory proliferation

How is Hippo signaling inhibited to allow Yki activation during tissue regeneration? Flux through the Hippo pathway is modulated by events at the cell cortex that monitor epithelial integrity and cell-cell interaction (Yu and Guan, 2013). One mechanism for inhibiting Hippo signaling is through the LIM domain protein Ajuba (Jub). Jub antagonizes Hippo signaling and is essential for eye development (Das Thakur et al., 2010). Activated Jub is thought to inhibit Hippo signaling by binding Wts, thereby Wts from phosphorylating Yki (Rauskolb et al., 2014). *jub* RNAi enhances the *GMR>hid, Gal4* adult eye phenotype and reduces CP (Fig. 6A,B,L). This observation is consistent with observations in the wing disc, where regeneration is inhibited in genotypes with reduced Jub (Sun and Irvine, 2013). Jub localizes with DE-cadherin at apical adherens junctions in larval eye discs (Fig. 6C), as it does in pupal eye discs and wing discs (Das Thakur et al., 2010; Sun and Irvine, 2013). This localization is most apparent at the apical surface of photoreceptors (Fig. 6D). We did not observe obvious accumulation or re-localization of Jub in *GMR-hid* clones (Fig. 6E), suggesting that increased activation rather than re-localization of Jub may be required to inhibit Hippo signaling during CP.

Jub can be activated in wing discs by JNK signaling (Sun and Irvine, 2013) or by an increase in cellular tension (Rauskolb et al., 2014). Because our data suggest JNK signaling does not play a significant role in CP in the eye disc (Fig. S2B-G), we investigated whether increased cellular tension modulates CP. We induced an increase in cellular tension by expressing the catalytic domain of Rho-kinase (RokCAT), which phosphorylates myosin and leads to increases in myosin contractility (Winter et al., 2001). In *GMR>hid, RokCAT* discs, CP increases by twofold, whereas the adult eye phenotype is not noticeably altered (Fig. 6F,L). Conversely, *Rok* RNAi results in a mild but statistically significant decrease in CP (Fig. 6L). Rok is activated by the Rho1 GTPase (Warner et al. 2010), which is inhibited in the pupal retina by Cdc42 (Warner and Longmore, 2010). Cdc42 also inhibits CP in irradiated wing discs (Warner et al., 2010). We observed an increase in CP in *GMR-hid* discs with expression of a dominant-negative form of

Cdc42 ($Cdc42^{DN}$) (Fig. 6I,L). These results suggest that regulation of cellular tension through Cdc42/Rho/Rok plays a role in CP, presumably through Jub regulation.

We predicted that increases in cellular tension in the absence of Hid expression would also activate Jub and induce cell cycle re-entry. Indeed, we observed ectopic S phases in the posterior of the disc when RokCAT was expressed with *GMR-Gal4* in the absence of Hid (Fig. 6G,L). We also observed a low level of apoptosis in *GMR>rokCAT* eye discs (Fig. 6G), similar to previous results in wing discs (Warner et al., 2010). Surprisingly, apoptosis was induced both posterior to the furrow where RokCAT was expressed and anterior to the furrow where RokCAT was not expressed. To determine whether the increase in proliferation we observed in the posterior of *GMR>rokCAT* discs was due solely to the presence of apoptotic cells, we labeled *GMR>rokCAT, p35* eye discs with EdU and anti-CC3 antibodies. p35 blocks RokCAT-induced apoptosis, which we confirmed by the lack of basally extruded cells and pyknotic nuclei, but does not block CC3 staining due to non-cleaved-caspase epitopes of the anti-CC3 antibodies, as shown previously (Fan and Bergmann, 2010). While CC3 staining persists in undead cells posterior to the furrow in *GMR>rokCAT, p35* discs, CC3 staining anterior to the furrow, where p35 is not expressed, is largely lost (Fig. 6H). This result suggests that the anterior induction of apoptosis in *GMR>rokCAT* discs is dependent on apoptosis posterior to the furrow, similar to AiA, though the mechanism is unclear. Nevertheless, while apoptosis is suppressed posterior to the furrow in *GMR>rokCAT, p35* discs, we still observed ectopic EdU-positive cells posterior to the SMW (Fig. 6H,L). This result is similar to results in wing discs where co-expression of RokCAT and p35 induces hyperproliferation (Warner et al., 2010). These increases in proliferation in wing imaginal discs could be attributed to the formation of undead cells rather than increases in tension directly inducing proliferation. However, as p35 expression blocks CP in post-furrow eye discs and does not induce mitogenic undead cells (Fan and Bergmann, 2008), our results suggest that modulation of cellular tension through RokCAT directly induces cell cycle re-entry. We also observed cell cycle re-entry in *GMR>cdc42^{DN}* discs, even when p35 was co-expressed (Fig. 6J-L).

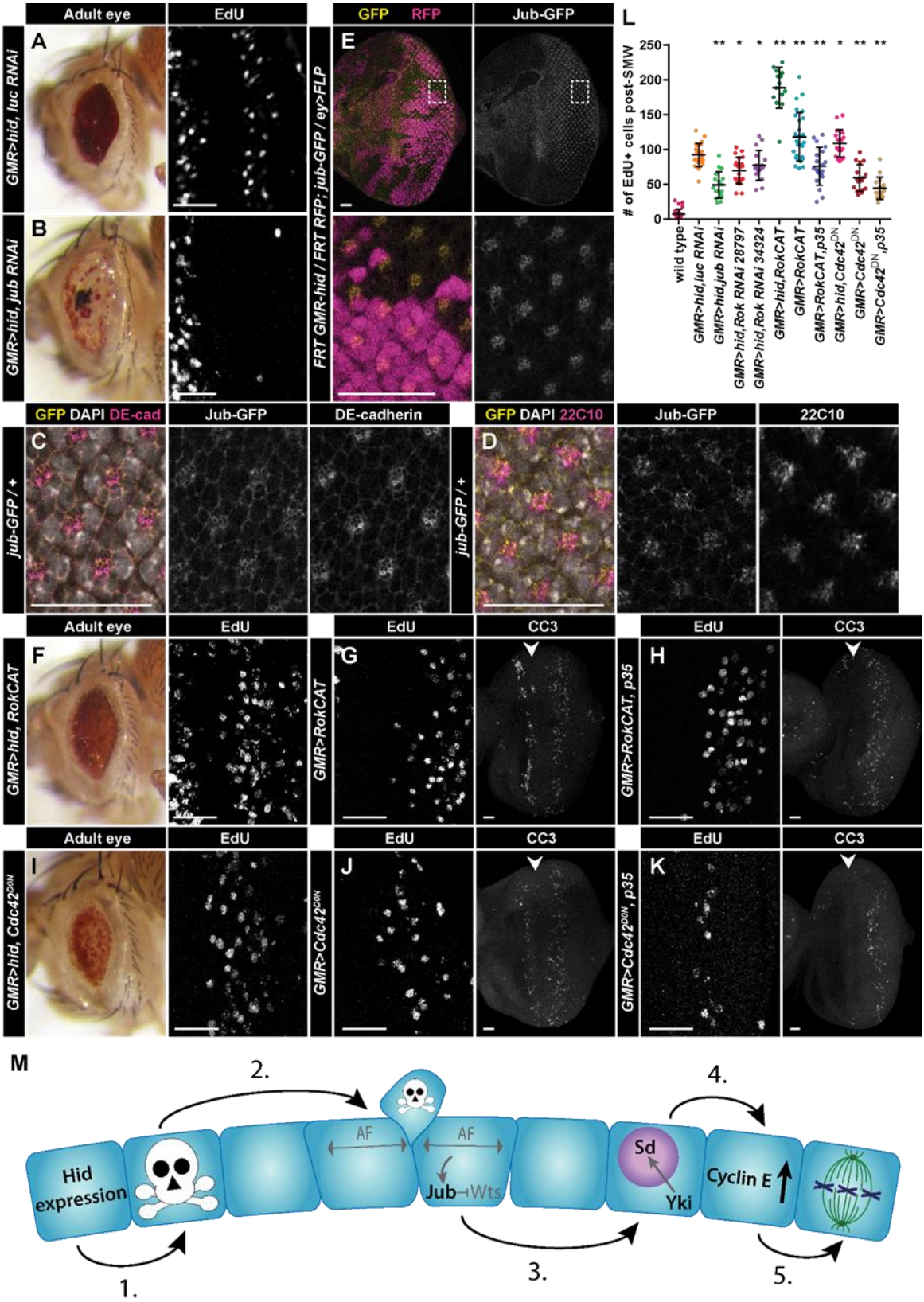

Fig. 6. See next page for legend.

Fig. 6. Jub and cellular tension regulate compensatory proliferation. (A,B,F,I) Adult eyes (left panels) and high magnification of post-furrow EdU staining (right panels) of the indicated genotypes. (C,D) Jub-GFP (yellow) colocalizes with DE-cadherin (magenta; C) and Futsch/22C10, a marker of neuronal membranes (magenta; D), at the apical surface of post-furrow eye discs. (E) Clones of *GMR-hid* (no marker) and wild-type (RFP+, magenta) cells expressing Jub-GFP (yellow). Boxes in top panels indicate area of magnification shown in bottom panels. (G,H,J,K) High magnification of postfurrow EdU staining (left panels) and CC3 staining (right panels) of the indicated genotypes. Arrowheads mark the MF. *GMR>RokCAT* (G) and *GMR>Cdc42^{DN}* (J) induce CC3-positive apoptotic cells posterior to the MF. Interestingly, apoptotic cells are also observed anterior to the furrow in these discs. The mechanism triggering this apoptosis is unknown, but its absence in *GMR>RokCAT, p35* (H) or *GMR>Cdc42^{DN}, p35* (K) discs suggests the anterior induction of apoptosis in *GMR>RokCAT* and *GMR>Cdc42^{DN}* discs is dependent on apoptosis posterior to the furrow. CC3 staining persists posterior to the furrow after p35 expression (H,K) because undead cells express noncleaved-caspase epitopes of the anti-CC3 antibodies (Fan and Bergmann, 2010). (L) Quantification of CP in the indicated genotypes. *GMR>hid, Gal4* genotypes were compared with *GMR>hid, luc RNAi*, whereas *GMR>Gal4* genotypes were compared with wild type (*w^{1118}*). Each circle represents the number of cells counted for a single disc, and bars represent mean and one standard deviation. For each genotype, n≥14 discs. *P≤0.02, **P≤1×10−7. (M) Model for induction of CP in a quiescent epithelium. Text in gray indicates proposed possibilities that have not formally been observed in this study. (1) Hid expression/tissue damage induces apoptosis in a subset of cells. (2) Basal extrusion of apoptotic cells induces apoptotic force (AF), which activates Jub, leading to Wts inhibition. (3) Wts inhibition results in Yki translocating to the nucleus and acting as a transcriptional co-activator for Sd. (4) Sd/Yki induce high levels of Cyclin E, which induces cell cycle re-entry (5). Anterior is oriented to the left. Scale bars: 20 μm.

DISCUSSION

To maintain tissue homeostasis and prevent inappropriate cell divisions, the threshold for S-phase entry is higher in quiescent cells than in cycling cells. Consequently, to undergo regeneration efficiently, quiescent tissues must overcome robust controls that restrain cell cycle entry. The mechanisms that drive cell cycle re-entry and regeneration in a quiescent cell population are largely unknown, in part because many studies of regeneration have been performed in proliferative tissues or tissues with an active stem cell population. Here we report the results from a genetic screen identifying regulators of tissue damage-induced cell cycle reentry of a quiescent cell population in *Drosophila*.

Scalloped and Yorkie regulate compensatory proliferation in eye imaginal discs

We found that Sd and Yki are required for quiescent cells in the eye imaginal disc to enter the cell cycle in response to tissue damage caused by extensive apoptosis. Sd and Yki are required

for Cyclin E accumulation following damage, suggesting that Sd and Yki cooperate to activate *Cyclin E* transcription. The interaction between Sd and Yki is complex. Initial experiments suggested Yki and Sd act together to drive gene transcription, as Sd is required for the overgrowth and target gene induction that occurs following Yki over-expression in the eye disc (Wu et al., 2008; Zhang et al., 2008). However, their roles during eye development are clearly distinct as *yki* mutant clones grow very poorly in the eye disc (Huang et al., 2005) whereas *sd* mutant clones grow normally (Zhang et al., 2008). In addition, Yki and Sd have both overlapping and unique binding sites throughout the genome, many of which are tissue-dependent (Slattery et al., 2013). Curiously, growth defects in *yki* mutant clones can be rescued by mutation of *sd*, suggesting that Yki acts by relieving Sd-mediated gene repression (Koontz et al., 2013). Additional factors, like Tgi, probably function as co-factors for Sd suppressor function (Koontz et al., 2013). Conversely, Sd/Yki may act synergistically with E2f1 (Nicolay et al., 2011) and GAGA factor/Trl (Bayarmagnai et al., 2012; Oh et al., 2013) to drive gene expression. Although our data suggests Sd activates gene transcription during CP, it will be important to determine how abundance of Sd/Yki co-factors are regulated during development and how this regulation might change to allow robust Sd/Yki target gene expression following tissue damage.

Cyclin/Cdk regulation is a conserved mechanism for inducing regeneration

Cyclin/Cdk regulation is essential for regeneration in a variety of model organisms. For example, in post-mitotic *Caenorhabditis elegans* muscle cells, ectopic expression of cyclins drives DNA replication and cell division (Korzelius et al., 2011). Manipulation of Cyclin/Cdk regulation also confers regenerative capabilities on otherwise non-regenerative tissue. Mice mutant for the CDK inhibitor p21 robustly regenerate lost skin in the ear while wild type mice have limited abilities to repair lost ear tissue (Bedelbaeva et al., 2010). This phenotype is attributed to a lack of a p21-dependent G1 checkpoint which normally causes arrest and blocks proliferation.

Our model posits that Sd/Yki activate gene expression to induce CP in the *Drosophila* eye imaginal discs, consistent with previous studies showing that high levels of cell cycle regulators are required drive cell cycle re-entry in post-mitotic cells (Buttitta et al., 2007). Regulation of the G1-S transition is driven by a positive feedback loop between E2f1 and Cyclin E where E2f1 induces transcription of *Cyclin E*, and Cyclin E inhibits Rbf1, the E2f1 inhibitor. In post-mitotic, differentiated photoreceptors, high levels of Rbf1 and Dacapo keep both E2f1 and Cyclin E in check, and activation of both is necessary to overcome cell cycle arrest after cell cycle exit (Buttitta et al., 2007). In contrast, high levels of ectopic Cyclin E are sufficient to overcome cell cycle arrest and drive S-phase in quiescent, undifferentiated cells of the developing eye disc (Richardson et al., 1995). These undifferentiated cells may be poised to respond to damage-induced Cyclin E expression.

Although our results suggest Sd/Yki induce Cyclin E accumulation during CP, there are likely to be other inputs that drive cell cycle re-entry. The Hedgehog pathway transcription factor Ci, which is required for CP in the post-furrow eye (Fan and Bergmann, 2008), can directly activate *Cyclin E* transcription in the eye disc (Duman-Scheel et al., 2002). Furthermore, both Yki and Ci have cell cycle targets other than *Cyclin E*: Yki can activate *E2f1* transcription in the wing disc (Goulev et al., 2008) and Ci activates expression of *Cyclin D* in the eye disc (Duman-Scheel et al., 2002). We postulate that a combination of Ci and Sd/Yki activity drives a *Cyclin E*-containing gene expression program that induces cell cycle entry and contributes to the induction of CP.

Apoptotic force may link cell death to Yki activation

In the wing imaginal disc, Yki activity during CP is driven by Jub-dependent inhibition of Hippo signaling (Sun and Irvine, 2013). Our data indicate that Jub is also required for CP in the eye, suggesting a shared mechanism for Yki regulation between tissues. However, although Jub-dependent inhibition of Hippo signaling in the wing disc requires JNK signaling, we did not find

a requirement for JNK signaling for CP in the eye disc. Recent data suggests that increased cellular tension within an imaginal disc epithelium activates Jub through α-catenin and provides a mechanism for inhibition of Hippo signaling independent of the JNK pathway (Rauskolb et al., 2014). Interestingly, mechanical force has also been shown to regulate the activity of the mammalian Yorkie homolog Yes-associated protein (YAP) (Aragona et al., 2013) and induce cell proliferation in culture (Streichan et al., 2014). Because we show that expression of active Rok or dominant-negative Cdc42, which can increase cellular tension, increases CP in *GMR-hid* discs, we propose that cellular tension in the eye disc epithelium modulates CP.

One possible source of increased cellular tension in *GMR-hid* discs is from "apoptotic force" generated by the extrusion of dying cells. The phenomenon of apoptotic force has been described in *Drosophila* embryos, in which actin/myosin-driven constriction of dying amnioserosa cells exerts force on overlying epithelial cells to drive dorsal closure (Toyama et al., 2008). Apoptotic force in *GMR-hid* discs may increase cellular tension and drive Jub activation. Several pieces of data are consistent with a model that physical extrusion of apoptotic cells is required to generate the force necessary to induce CP. First, we found that *LGMR-hid*, which induces less apoptosis than does *GMR-hid* and presumably less apoptotic force, does not induce CP. Additionally, expression of the apoptotic-inhibitor p35, which blocks basal extrusion of apoptotic cells, inhibits CP in the eye disc posterior to the MF (Fan and Bergmann, 2008). Finally, clones of *GMR-hid* only induce S-phase entry in cells within and immediately bordering the clone (Fig. S5, (Fan and Bergmann, 2008)). This observation suggests CP could result from local changes in tension rather than a long range signal.

Conclusions

The Hippo pathway is a well-conserved regulator of tissue growth and is modulated in processes such as regeneration and tumor growth. The mammalian Yki homolog Yes-associated protein (YAP) is required for intestinal regeneration in mice (Cai et al., 2010) and confers

regenerative ability in normally non-regenerative mouse hearts (Xin et al., 2013). Importantly, tight control of the Hippo pathway is crucial for tissue homeostasis, as YAP hyperactivity or inhibition of the Hippo pathway promotes cancer in many contexts (for review, see (Johnson and Halder, 2014)). Therefore, knowledge gained from studies of CP in *Drosophila* imaginal discs will contribute to an understanding of the role of Hippo signaling in mammalian regeneration and cancer.

EXPERIMENTAL PROCEDURES

Mutants and Transgenes

Fly stocks used in this studied were obtained from the Bloomington Stock Center or from colleagues (see Supplemental Experimental Procedures for more details), with the exception of *LGMR-hid* (construction described in the Supplemental Experimental Procedures). All lines used for the RNAi screen were generated by the Transgenic RNAi Project (TRiP) at Harvard Medical School, with details provided in Table S1.

Immunostaining

Eye discs were dissected from wandering third instar larvae. Discs were incubated with 100 μg/ml 5-ethynyl-2′-deoxyuridine (EdU) or 1 mg/ml 5-bromo-2′-deoxyuridine (BrdU) for 60 min and fixed for 20 min with 4% formaldehyde. EdU detection was performed with the Click-iT EdU Alexa Fluor 555 kit (Molecular Probes) according to the manufacturer's protocol. Antibodies used are as follows: rabbit anti-cleaved Caspase-3 (1:200; 9661, Cell Signaling), rat anti-Elav [1:100; 7E8A10, Developmental Studies Hybridoma Bank (DSHB)], mouse anti-βGal (1:1000; 40-1a, DSHB), mouse anti-Cyclin E (1:200; 8B10, a gift from H. Richardson, The Peter MacCallum Cancer Centre, Melbourne, Australia), mouse anti-Yan (1:500; 8B12H9, DSHB), rat anti-DE-cadherin (1:1000; DCAD2, DSHB), mouse anti-Futsch/22C10 (1:1000; DSHB), mouse anti-BrdU (1:200; B44, BD Biosciences), Alexa 488-conjugated goat anti-rabbit (1:500; 111-545-144,

Jackson ImmunoResearch), Cy5-conjugated donkey anti-rat (1:500; 712- 175-153, Jackson ImmunoResearch). For CC3 staining, discs were incubated with primary antibodies for 48 h at 4°C in PBS and a 2 h PBS-0.1%Triton X-100; 5% normal goat serum block was performed prior to applying secondary antibodies. Fluorescence in situ hybridizations were performed as previously described (Tomancak et al., 2002) with the following modifications: RNA probe was generated by T7 polymerase in vitro transcription in the presence of digoxigenin-11-UTP (Roche) from linearized hid cDNA (clone AT13267, BDGP). Detection was performed with peroxidase-conjugated anti-DIG (1:100; Roche) and Cy5-conjugated tyramide reagent (1:50; Perkin Elmer). See supplementary Methods for details on image quantification.

SUPPLEMENTARY FIGURES

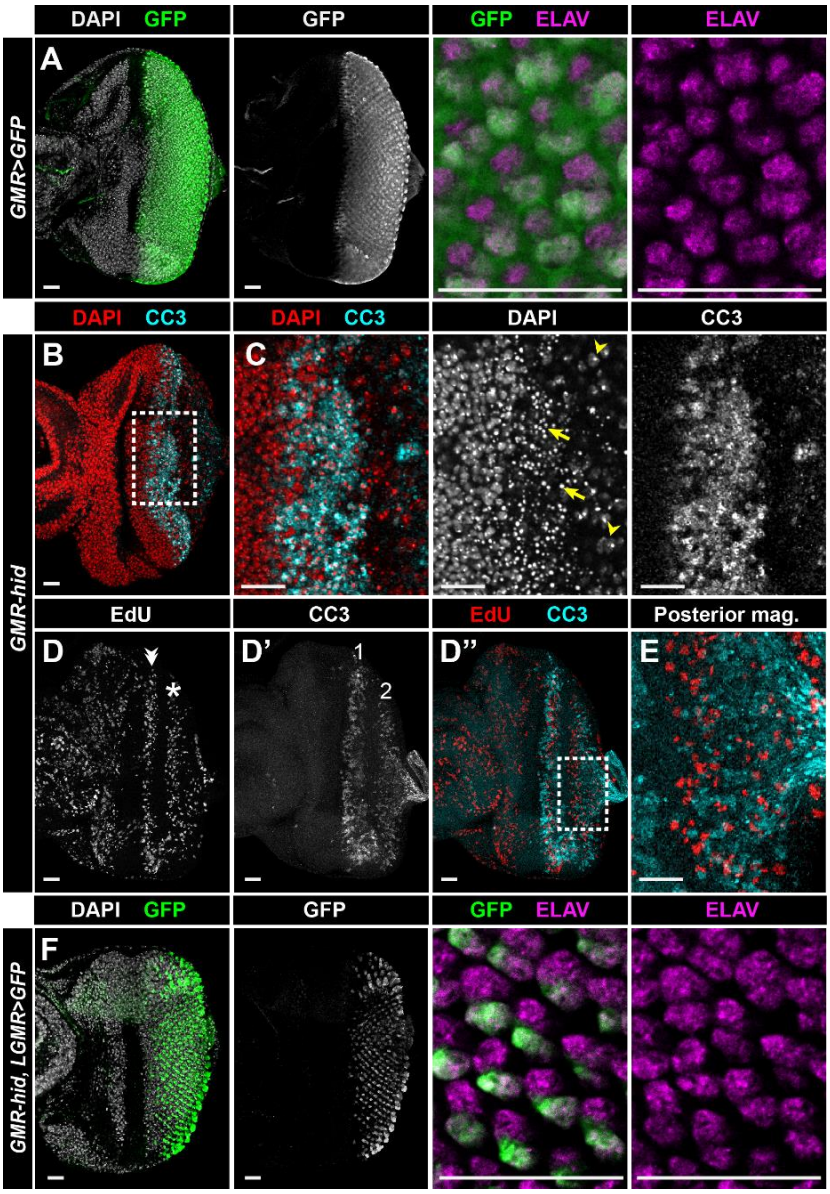

Fig. S1 (related to Fig. 1). Characterization of *GMR-Gal4*, *longGMR-Gal4*, and *GMR-hid* transgenes.
A,F) Expression of GFP (green) driven by *GMR-Gal4* (A) or *longGMR-Gal4* (*LGMR-Gal4*, (F)). Higher magnification of posterior cells in the right two panels indicates photoreceptors stained with ELAV (purple). GFP is expressed in all photoreceptors with *GMR-Gal4* (A) and in a subset of photoreceptors with *LGMR-Gal4* (F).
B-C) DAPI staining of nuclei (red) and staining of apoptotic cells with anti-CC3 antibodies (cyan) on the basal surface of a *GMR-hid* disc. Box in (B) indicates area of magnification in (C). Pyknotic nuclei (arrows) and glial cell nuclei (arrowheads) are present on the basal surface of the disc.
D-E) EdU staining of cells in S-phase (red in D") in *GMR-hid* discs marks the SMW (double arrowhead) and CP (*). CC3 staining (cyan in D") marks the two waves of apoptosis (1 and 2). Box in D" indicates area of magnification in E.
Anterior is oriented to the left. Scale bars: 20 μM.

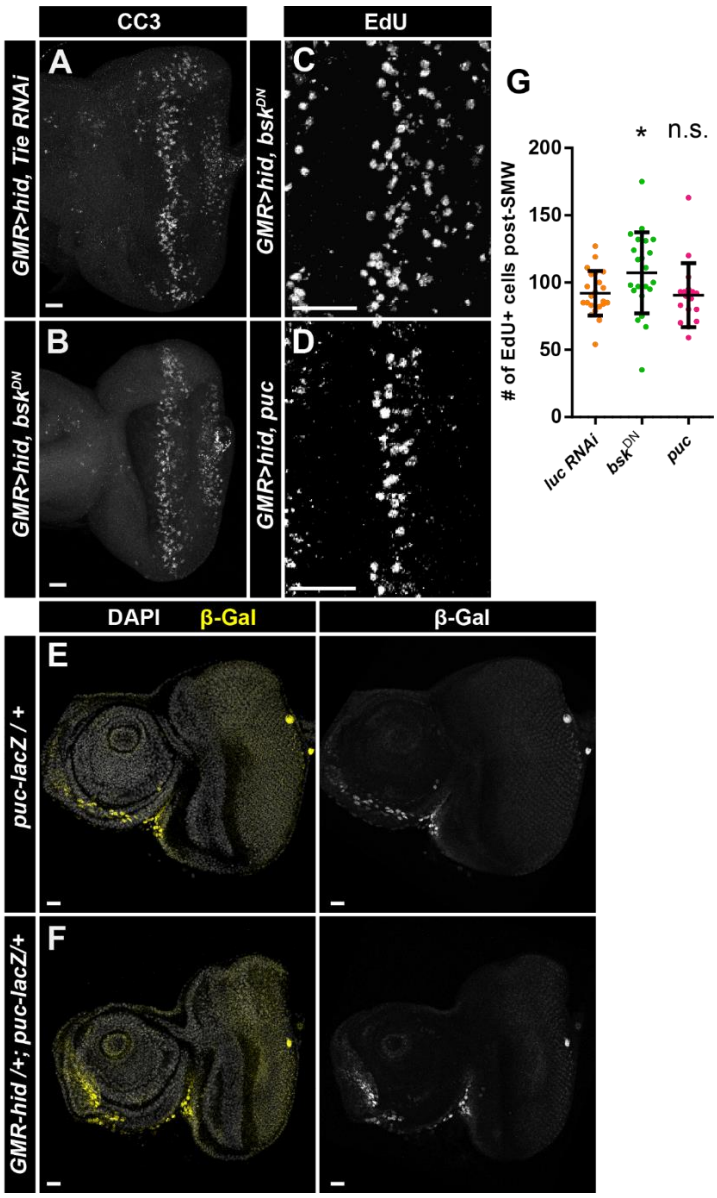

Fig. S2 (related to Fig. 1). Inhibition of signaling through JNK or Tie does not modify the *GMR-hid* phenotype.

A,B) Apoptotic cells stained with anti-CC3 antibodies in the indicated genotypes.

C,D) EdU incorporation in the posterior of eye discs of the indicated genotypes.

E,F) *puc-lacZ* expression, marked by βGal in yellow, is similar in wild type (E) and *GMR-hid* (F) tissues.

G) Quantification of compensatory proliferating cells in the *GMR>hid,Gal4* background for the indicated UAS-transgenes. All post-SMW, EdU^{+} eye disc cells were counted. Each circle on the graph represents the number of cells counted for a single disc. For each genotype, $n \geq 17$ discs. Bars represent mean and one standard deviation. n.s., not significant. While *GMR>hid, bsk^{DN}* CP is significantly increased compared to *GMR>hid, luc RNAi* (*P=0.047), it is not significantly different from another control (*GMR>hid, Gal4/CyO*; P=0.43). Therefore, we are wary about drawing conclusions about the biological significance of an increase in CP in *GMR>hid, bsk^{DN}* discs.

Anterior is oriented to the left. Scale bars: 20 μM.

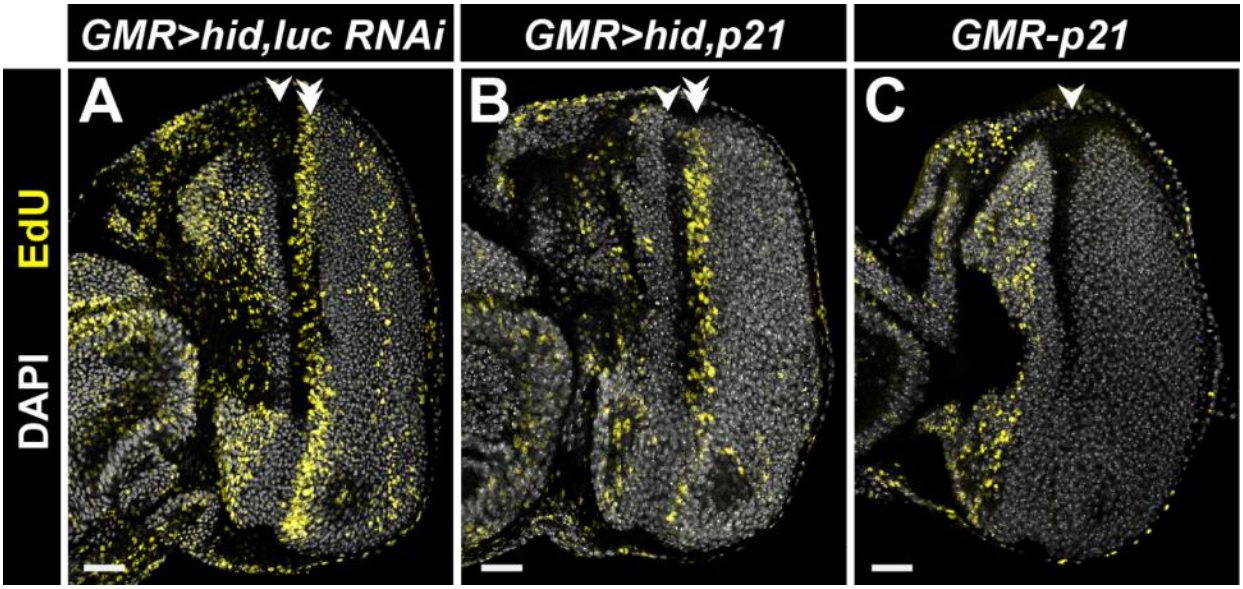

Fig S3 (related to Fig. 2). Transgenes expressed using *GMR-Gal4* do not affect the second mitotic wave.
A) *GMR>hid, luc RNAi* eye discs stained with DAPI (grey) and EdU (yellow) to indicate MF (arrowhead) and SMW (double arrowhead), respectively.
B) The SMW appears normal when *p21* is expressed with *GMR-Gal4* in the *GMR-hid* background.
C) Expressing p21 via *GMR-p21* results in ablation of the SMW.
Anterior is oriented to the left. Scale bars: 20 μM.

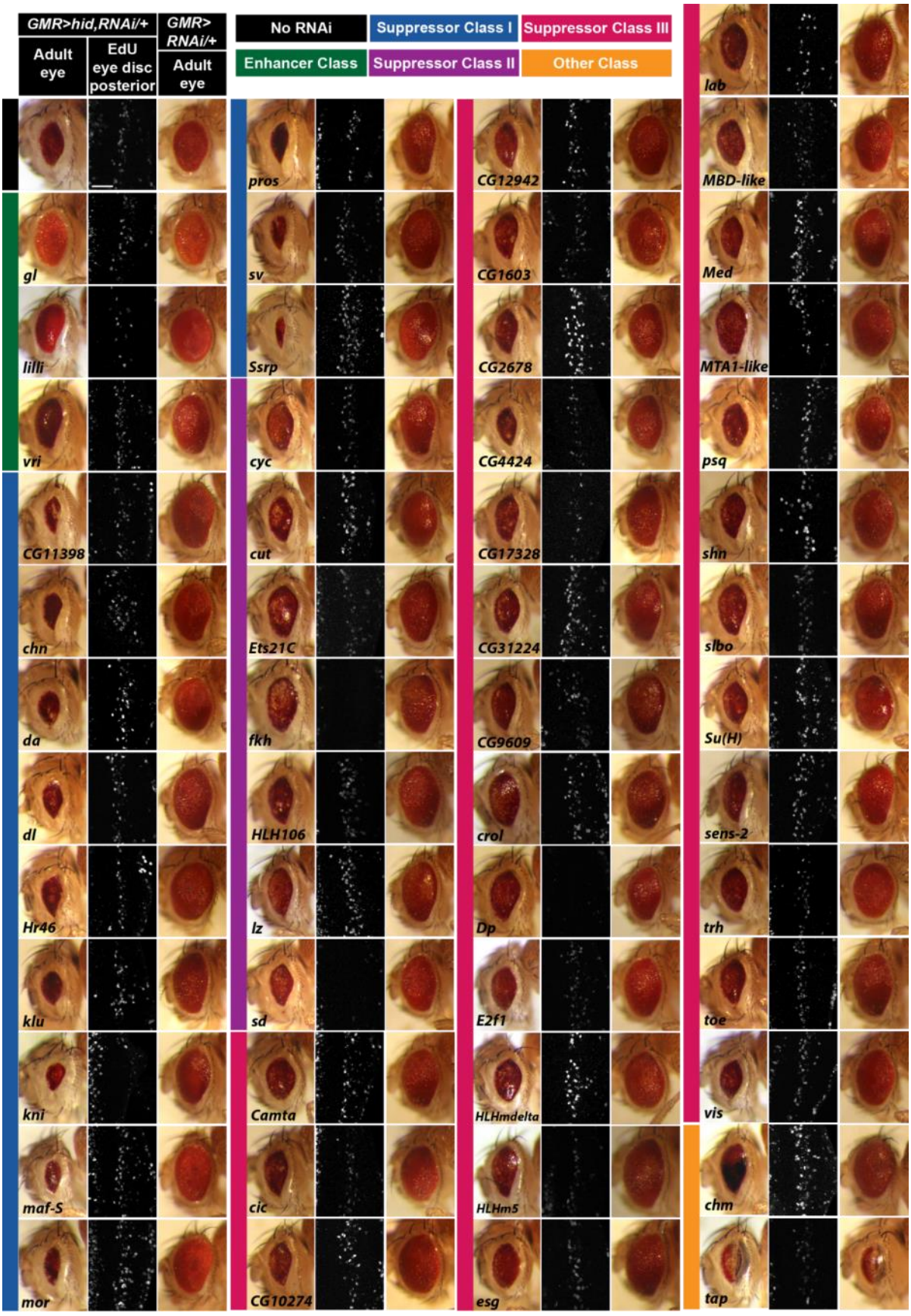
GMR>hid,RNAi/+
Adult eye
EdU eye disc posterior
GMR> RNAi/+
Adult eye
No RNAi
Suppressor Class I
Suppressor Class III
Enhancer Class
Suppressor Class II
Other Class
gl
lilli
vri
CG11398
chn
da
dl
Hr46
klu
kni
maf-S
mor
pros
sv
Ssrp
cyc
cut
Ets21C
fkh
HLH106
lz
sd
Camta
cic
CG10274
CG12942
CG1603
CG2678
CG4424
CG17328
CG31224
CG9609
crol
Dp
E2f1
HLHmdelta
HLHm5
esg
lab
MBD-like
Med
MTA1-like
psq
shn
slbo
Su(H)
sens-2
trh
toe
vis
chm
tap

Fig. S4 (related to Fig. 2). 52 RNAi lines caused a change in the *GMR-hid* adult eye phenotype.
Each UAS-RNAi line was crossed to *GMR>hid, Gal4*. For each line, the adult eye phenotype is displayed in the left column, while the EdU staining of the posterior eye disc is displayed in the right column (centered on the compensatory wave; scale bar: 20 μM and magnification is the same throughout; anterior is oriented to the left). Each line was also crossed to *GMR-Gal4* alone (adult eye phenotype in third column). See Table S1 for full gene names and all RNAi lines tested. First row of images represents the "No RNAi" control. Phenotype classes (see text for explanation): Suppressors=green, Enhancer Class I=blue, Enhancer Class II=purple, Enhancer Class III=pink, Other=orange

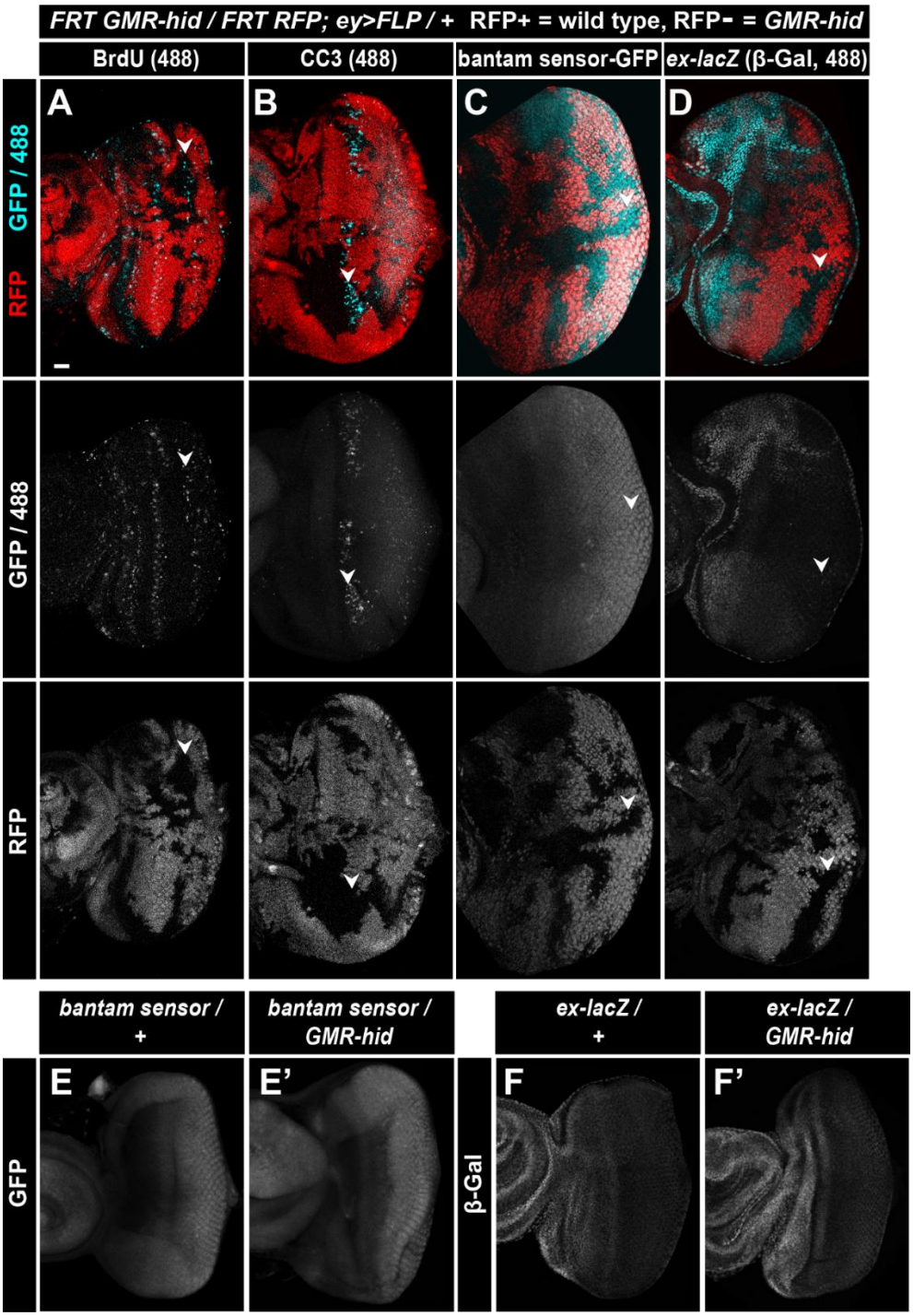

Fig. S5 (related to Fig. 4). A *bantam* sensor and *ex-lacZ* are not induced by *hid* expression in the eye disc.
A-D) *GMR-hid* clones (RFP negative, arrowheads) exhibit CP, marked by EdU (cyan, A), and apoptosis, marked by anti-CC3 staining (cyan, B). *bantam*, measured by the *bantam* sensor-GFP (cyan, C), and *ex-lacZ*, marked by β-Gal (cyan, D), are not induced in *GMR-hid* clones.
E) *bantam* sensor-GFP expression in control (E) and *GMR-hid* (E') eye discs.
F) *ex-lacZ* induction, marked by β-Gal, in control (F) and *GMR-hid* (F') eye discs.
Anterior is oriented to the left. Scale bars: 20 μM.

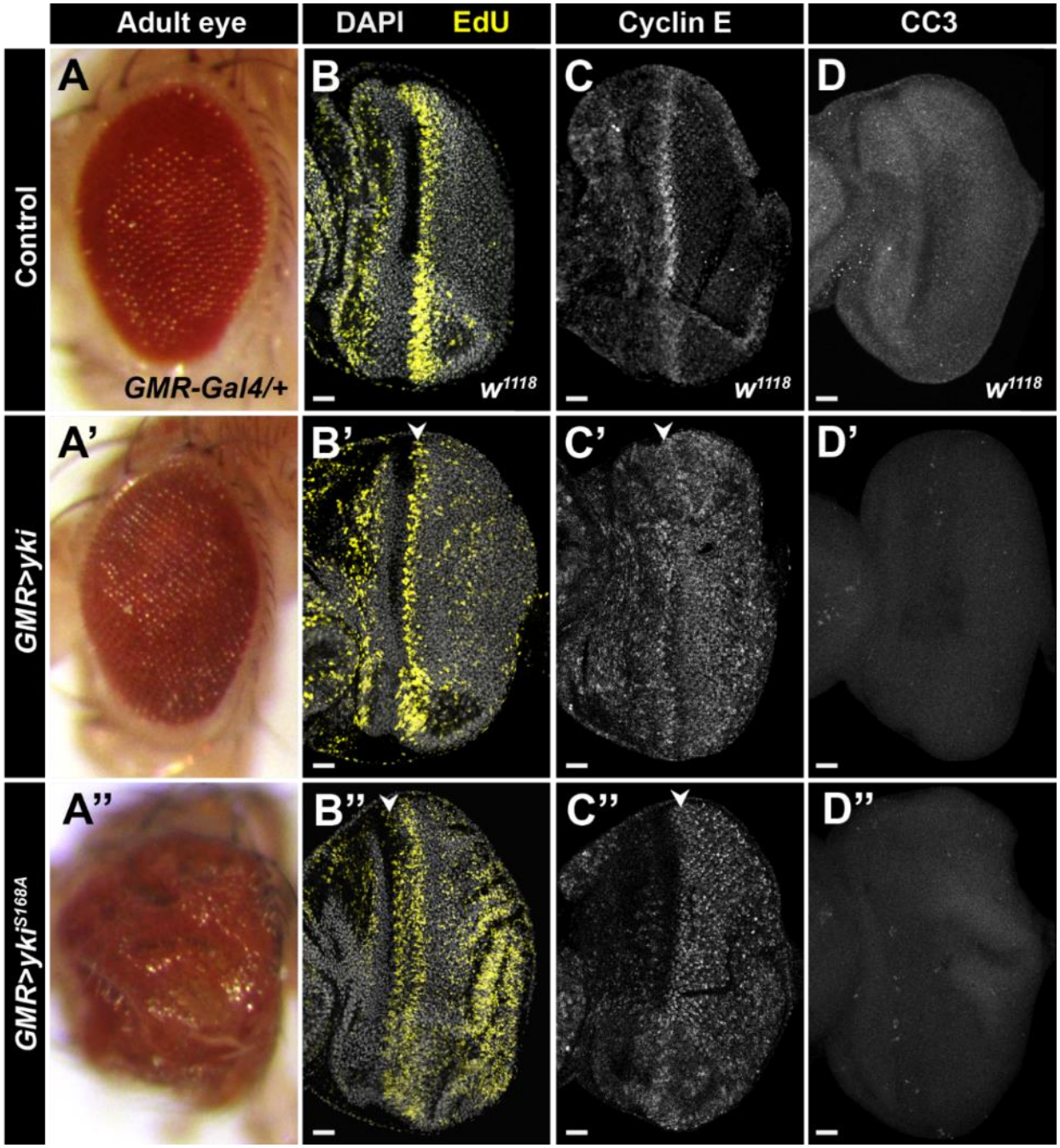

Fig. S6 (related to Fig. 5). Expression of Yki or Yki^{S168A} induces larval and adult eye phenotypes.

A) Adult eyes with *GMR-Gal4* alone (A), with *UAS-Yki* (A'), or with *UAS-Yki^{S168A}* (A").

B) DAPI staining of nuclei (grey) and EdU staining of S phase cells (yellow) in the indicated genotypes.

C) Staining with anti-Cyclin E antibodies in the indicated genotypes.

D) Staining of apoptotic cells with anti-CC3 antibodies in the indicated genotypes

Anterior is oriented to the left. Scale bars: 20 μM.

SUPPLEMENTARY EXPERIMENTAL PROCEDURES

Fly stocks

RNAi lines used in the screen are listed in supplementary material Table S1. Additional fly stocks used are as follows, with full genotype and Bloomington Stock Center number or providing lab listed in parentheses: ***GMR-hid*** (*P{w[+mC]=GMR-hid}G1*, #5771), ***Tie RNAi*** (*y^1 v^1; P{TRiP.HMJ21428}attP40*, #54005), ***UAS-bsk^{DN}*** (made by K. Matsumoto, obtained from J. Poulton), ***UAS-puc*** (made by A. Martinez Arias, obtained from J. Poulton), ***puc-lacZ*** (*puc-lacZ^{E69}*, made by A. Martinez Arias, obtained from J. Poulton), ***luciferase (luc) RNAi*** (*y^1 v^1; P{TRiP.JF01355}attP2*, #31603), ***Cyclin E RNAi*** (*y^1 v^1; P{TRiP.JF02473}attP2*, #29314), ***UAS-p21*** (I. Hariharan), ***GMR-p21*** (*y^1 w^{1118}; P{GMR-p21.Ex}3/TM3, Sb^1 Ser^1*, #8414), ***sd RNAi-1*** (*y^1 v^1; P{TRiP.JF02514}attP2*, #29352), ***sd RNAi-2*** (*sd (N+C) RNAi*, J. Jiang), ***FRT sd*** (*FRT19A sd^{47m}*, D. Pan), ***FRT RFP*** (*P{Ubi-mRFP.nls}1, w^{1118}, P{neoFRT}19A*, #31416), **FRT GMR-hid; *ey>FLP*** (*P{GMR-hid}SS1, y^1 w* P{neoFRT}19A; P{GAL4-ey.H}SS5, P{UAS-FLP.D}JD2*, #5248), ***Tgi RNAi*** (*y^1 sc* v^1; P{TRiP.HMS00981}attP2*, #34394), ***yki RNAi-1*** (*y^1 v^1; P{TRiP.HMS00041}attP2*, #34067), ***yki RNAi-2*** (*y^1 v^1; P{TRiP.JF03119}attP2*, #31965), ***UAS-dMSTn*** (J. Jiang), ***bantam sensor*** (made by S. Cohen, obtained from T.T. Su), ***ex-lacZ*** (*w*; ex^{e1} P{neoFRT}40A/CyO*, #44249), ***Diap1-lacZ*** (*y^1 w*; P{lacW}Diap1^{j5C8}/TM3, Sb^1*, #12093), ***UAS-yki*** (*y^1 w^*; P{UAS-yki.GFP}4-12-1*, #28815), ***UAS-yki^{S168A}*** (*w*; P{UAS-yki.S168A.V5}attP2*, #28818), ***jub RNAi*** (*y^1 sc* v^1; P{TRiP.HMS00714}attP2*, #32923), ***jub-GFP*** (*w^*; P{jub$^{+t.T:Avic\GFP}$}18A/TM2*, #56806), ***UAS-RokCAT*** (*y^1 w*; P{UAS-Rok.CAT}3.1*, #6669), ***UAS-Cdc42^{DN}*** (*w^*; P{UAS-Cdc42.N17}3*, #6288).

Genotypes for clones are as follows:

sd clones: *FRT19A sd^{47m}/FRT19A Ubi-mRFP.NLS; GMR-hid/+; ey-Gal4, UAS-FLP/+*

GMR-hid clones: *FRT19A GMR-hid/FRT19A Ubi-mRFP.NLS; ey-Gal4, UAS-FLP/+*

GMR-hid clones with *bantam* sensor: *FRT19A GMR-hid/FRT19A Ubi-mRFP.NLS; bantam sensor GFP/+; ey-Gal4, UAS-FLP/+*

GMR-hid clones with *ex-lacZ*: *FRT19A GMR-hid/FRT19A Ubi-mRFP.NLS; ex-lacZ/+; ey-Gal4, UAS-FLP/+*

jub-GFP clones: FRT19A GMR-hid/FRT19A Ubi-mRFP.NLS; jub-GFP/ey-Gal4, UAS-FLP

longGMR-hid transgene construction

To make *longGMR-hid* transgenic flies, the *longGMR* (*LGMR*) enhancer and *hid* ORF were cloned into pMINTGATE, a kind gift from J. Pearson. *LGMR-Gal4* transgene was obtained by PCR amplification from *LGMR-Gal4* flies (Bloomington #8121) with primers white 2161 (forward, GTGTCGCTCGTTGCAGAATA) and Gal4R (reverse, GCCTTGATTCCACTTCTGTCA). The *longGMR* enhancer was then PCR'ed from this fragment with primers LGMRpE F (forward, CACCCAAGCTTTCGCGAGCTCG) and LGMRpE R (reverse, TTTCGCCGGATCTCGACAATAG) and cloned into pENTR/D-TOPO (Invitrogen); pENTR LGMR was then recombined into pMINTGATE using the Gateway LR cloning system (Invitrogen), resulting in pMG LGMR. The *hid* ORF (sequence from BDGP clone AT13267) was synthesized by GenScript with AgeI and SpeI sites for cloning into pMG LGMR, which replaced the *GFP*, but retained the plasmid's SV40 3'UTR. The resulting construct (pMG LGMR hid) was injected by BestGene Inc into the attP40 site to make transgenic flies.

Image quantification

ImageJ (NIH) was used for all quantification. For all statistical measurements, p-values were calculated using the T-test function in Microsoft Excel with two-tailed distribution and two-sample unequal variance.

Measurement of SMW to CP distance

Z-projections were made in ImageJ of EdU staining in control (*GMR>hid, luc RNAi*) or experimental (*GMR>hid, yki*) eye discs. From these images, the physical distance from the

anterior edge of the SMW to the anterior edge of the CP wave was measured. To mitigate confounding effects from preparation artifacts at the dorsal and ventral edges of the disc (e.g. curling over), the distance between the SMW and CP was measured at the approximate midpoint (determined qualitatively) along the D-V axis. In all cases, the farthest distance was measured. Since the CP wave is not entirely synchronous, single EdU^+ cells considerably anterior to other cells in the wave (>10 μM away) were considered anomalies and were not considered in our determination of the anterior CP edge.

Cleaved-Caspase 3 staining

For cleaved Caspase-3 staining quantification, projections of images with anti-CC3 antibody staining were used to calculate total disc area in ImageJ (Huang thresholding to capture entire disc, followed by measurement of total area of particles >100 pixels, which in all cases was one particle, ie the whole disc) and area of CC3 posterior to the furrow (RenyiEntropy thresholding to capture CC3 staining, followed by measurement of total area of particles >3 pixels, which were all cells with CC3 staining). Thresholding was set manually to account for differences in background and signal between samples. Area was used as a measurement rather than total number of $CC3^+$ cells as fragmented cells with pyknotic nuclei could not be unambiguously counted as one or multiple cells. The total area of the disc was used to normalize the area of CC3 staining so that the measurement of CC3 staining is displayed as a percent of total disc area.

Diap-lacZ / β-Gal staining

β-Gal staining from discs with *Diap-lacZ* expression was quantified by calculating the ratio of average intensity of staining posterior and anterior to the furrow. For posterior measurements, a selection containing at least 50 undifferentiated cells (identified by their location apical to the glial cells) in a single slice was made posterior to the furrow. This selection specifically did not include any glial, peripodial, margin, or pre-furrow nuclei, which could

confound our measurements. DAPI staining was used to create a ROI containing nuclei. β-Gal fluorescence intensity was then measured in this nuclear ROI. A similar measurement was made with cells anterior to the furrow to normalize differences in staining between samples. The ratios of average nuclear β-Gal intensity in posterior versus anterior disc cells were used to compare genotypes.

Cyclin E staining

Because staining with anti-Cyclin E antibodies is variable throughout the posterior of eye discs, presumably due to differences in Cyclin E protein accumulation, in each disc we measured the average Cyclin E staining intensity for undifferentiated cells, where differences between genotypes appeared greatest. Since fluorescence from glial, peripodial, or photoreceptor cells could confound our measurements, we gated for undifferentiated cells by applying a mask of Yan staining to Z-stacks of Cyclin E staining. A maximum projection was generated from each gated Cyclin E Z-stack. The resulting image of Cyclin E staining in undifferentiated cells was thresholded using cells with high Cyclin E levels in the SMW as a reference point for Cyclin E positive cells. Since nuclei could not be separated in Z-projected images, area was used as a proxy for cell number. The area of Cyclin E positive cells posterior to the SMW was normalized to the area of Cyclin E positive cells within the SMW. The measurements displayed in Figure 4 and used for quantification are a ratio of post-SMW versus SMW Cyclin E staining area. We considered that the SMW Cyclin E area itself might be different between genotypes, especially considering that Hid expression disrupts the SMW. Therefore, we also measured the area of Cyclin E positive cells posterior to the SMW as a percentage of the total posterior area, based on projections of Yan staining. Statistical comparisons of percent of total posterior disc area with Cyclin E staining for each genotype gave similar significant P-values as our post-SMW versus SMW ratios. We chose to display the post-SMW versus SMW ratios in our results as we feel these measurements better account for differences in staining efficiency than post-SMW area alone.

REFERENCES

Aragona, M., Panciera, T., Manfrin, A., Giulitti, S., Michielin, F., Elvassore, N., Dupont, S. and Piccolo, S. (2013). A mechanical checkpoint controls multicellular growth through YAP/TAZ regulation by actin-processing factors. Cell 154, 1047-1059.

Baker, N. E. and Yu, S.-Y. (2001). The EGF receptor defines domains of cell cycle progression and survival to regulate cell number in the developing Drosophila eye. Cell 104, 699-708.

Bandura, J. L., Jiang, H., Nickerson, D. W. and Edgar, B. A. (2013). The molecular chaperone Hsp90 is required for cell cycle exit in Drosophila melanogaster. PLoS Genet. 9, e1003835.

Bayarmagnai, B., Nicolay, B. N., Islam, A. B. M. M. K., Lopez-Bigas, N. and Frolov, M. V. (2012). Drosophila GAGA factor is required for full activation of the dE2f1-Yki/Sd transcriptional program. Cell Cycle 11, 4191-4202.

Bedelbaeva, K., Snyder, A., Gourevitch, D., Clark, L., Zhang, X.-M., Leferovich, J., Cheverud, J. M., Lieberman, P. and Heber-Katz, E. (2010). Lack of p21 expression links cell cycle control and appendage regeneration in mice. Proc. Natl. Acad. Sci. USA 107, 5845-5850.

Bergantinos, C., Corominas, M. and Serras, F. (2010). Cell death-induced regeneration in wing imaginal discs requires JNK signalling. Development 137, 1169-1179.

Bilak, A., Uyetake, L. and Su, T. T. (2014). Dying cells protect survivors from radiation-induced cell death in Drosophila. PLoS Genet. 10, e1004220.

Brennecke, J., Hipfner, D. R., Stark, A., Russell, R. B. and Cohen, S. M. (2003). bantam encodes a developmentally regulated microRNA that controls cell proliferation and regulates the proapoptotic gene hid in Drosophila. Cell 113, 25-36.

Bryant, P. J. (1971). Regeneration and duplication following operations in situ on the imaginal discs of Drosophila melanogaster. Dev. Biol. 26, 637-651.

Buttitta, L. A., Katzaroff, A. J., Perez, C. L., de la Cruz, A. and Edgar, B. A. (2007). A double-assurance mechanism controls cell cycle exit upon terminal differentiation in Drosophila. Dev. Cell 12, 631-643.

Buttitta, L. A., Katzaroff, A. J. and Edgar, B. A. (2010). A robust cell cycle control mechanism limits E2F-induced proliferation of terminally differentiated cells in vivo. J. Cell Biol. 189, 981-996.

Cai, J., Zhang, N., Zheng, Y., de Wilde, R. F., Maitra, A. and Pan, D. (2010). The Hippo signaling pathway restricts the oncogenic potential of an intestinal regeneration program. Genes Dev. 24, 2383-2388.

Cai, Y., Zheng, H., Gong, W., Che, Y. and Jiang, B. (2011). The role of hedgehog signaling pathway in liver regeneration. Hepatogastroenterology 58, 2071-2076.

Das Thakur, M., Feng, Y., Jagannathan, R., Seppa, M. J., Skeath, J. B. and Longmore, G. D. (2010). Ajuba LIM proteins are negative regulators of the Hippo signaling pathway. Curr. Biol. 20, 657-662.

de Nooij, J. C. and Hariharan, I. K. (1995). Uncoupling cell fate determination from patterned cell division in the Drosophila eye. Science 270, 983-985.

Deshpande, N., Chopra, A., Rangarajan, A., Shashidhara, L. S., Rodrigues, V. and Krishna, S. (1997). The human transcription enhancer factor-1, TEF-1, can substitute for Drosophila scalloped during wingblade development. J. Biol. Chem. 272, 10664-10668.

Dominguez, M. and Casares, F. (2005). Organ specification-growth control connection: new in-sights from the Drosophila eye-antennal disc. Dev. Dyn. 232, 673-684.

Duman-Scheel, M., Weng, L., Xin, S. and Du, W. (2002). Hedgehog regulates cell growth and proliferation by inducing cyclin D and cyclin E. Nature 417, 299-304.

Duronio, R. J. and O'Farrell, P. H. (1995). Developmental control of the G1 to S transition in Drosophila: cyclin Eis a limiting downstream target of E2F. Genes Dev. 9, 1456-1468.

Fan, Y. and Bergmann, A. (2008). Distinct mechanisms of apoptosis-induced compensatory proliferation in proliferating and differentiating tissues in the Drosophila eye. Dev. Cell 14, 399-410.

Fan, Y. and Bergmann, A. (2010). The cleaved-Caspase-3 antibody is a marker of Caspase-9-like DRONC activity in Drosophila. Cell Death Differ. 17, 534-539.

Fan, Y. and Bergmann, A. (2014). Multiple mechanisms modulate distinct cellular susceptibilities toward apoptosis in the developing Drosophila eye. Dev. Cell 30, 48-60.

Firth, L. C. and Baker, N. E. (2005). Extracellular signals responsible for spatially regulated proliferation in the differentiating Drosophila eye. Dev. Cell 8, 541-551.

Fox, D. T. and Duronio, R. J. (2013). Endoreplication and polyploidy: insights into development and disease. Development 140, 3-12.

Frolov, M. V., Moon, N.-S. and Dyson, N. J. (2005). dDP is needed for normal cell proliferation. Mol. Cell. Biol. 25, 3027-3039.

Gibson, M. C. and Perrimon, N. (2005). Extrusion and death of DPP/BMP compromised epithelial cells in the developing Drosophila wing. Science 307, 1785-1789.

Goulev, Y., Fauny, J. D., Gonzalez-Marti, B., Flagiello, D., Silber, J. and Zider, A. (2008). SCALLOPED interacts with YORKIE, the nuclear effector of the hippo tumor-suppressor pathway in Drosophila. Curr. Biol. 18, 435-441.

Grusche, F. A., Degoutin, J. L., Richardson, H. E. and Harvey, K. F. (2011). The Salvador/Warts/Hippo pathway controls regenerative tissue growth in Drosophila melanogaster. Dev. Biol. 350, 255-266.

Gutierrez-Avino, F. J., Ferres-Marco, D. and Dominguez, M. (2009). The position and function of the Notch-mediated eye growth organizer: the roles of JAK/STAT and four-jointed. EMBO Rep. 10, 1051-1058.

Haynie, J. L. and Bryant, P. J. (1977). The effects of X-rays on the proliferation dynamics of cells in the wing disc of Drosophila melanogaster. Dev. Genes Evol. 183, 85-100.

Huang, J., Wu, S., Barrera, J., Matthews, K. and Pan, D. (2005). The Hippo signaling pathway coordinately regulates cell proliferation and apoptosis by inactivating Yorkie, the Drosophila Homolog of YAP. Cell 122, 421-434.

Huh, J. R., Guo, M. and Hay, B. A. (2004). Compensatory proliferation induced by cell death in the Drosophila wing disc requires activity of the apical cell death caspase Dronc in a nonapoptotic role. Curr. Biol. 14, 1262-1266.

Johnson, R. and Halder, G. (2014). The two faces of Hippo: targeting the Hippo pathway for regenerative medicine and cancer treatment. Nat. Rev. Drug Discov. 13, 63-79.

Kawakami, Y., Rodriguez Esteban, C., Raya, M., Kawakami, H., Marti, M., Dubova, I. and Izpisua Belmonte, J. C. (2006). Wnt/beta-catenin signaling regulates vertebrate limb regeneration. Genes Dev. 20, 3232-3237.

Knoblich, J. A., Sauer, K., Jones, L., Richardson, H., Saint, R. and Lehner, C. F. (1994). Cyclin E controls S phase progression and its down-regulation during Drosophila embryogenesis is required for the arrest of cell proliferation. Cell 77, 107-120.

Koontz, L. M., Liu-Chittenden, Y., Yin, F., Zheng, Y., Yu, J., Huang, B., Chen, Q., Wu, S. and Pan, D. (2013). The Hippo effector Yorkie controls normal tissue growth by antagonizing scalloped-mediated default repression. Dev. Cell 25, 388-401.

Korzelius, J., The, I., Ruijtenberg, S., Prinsen, M. B. W., Portegijs, V., Middelkoop, T. C., Groot Koerkamp, M. J., Holstege, F. C. P., Boxem, M. and van den Heuvel, S. (2011). Caenorhabditis elegans cyclin D/CDK4 and cyclin E/CDK2 induce distinct cell cycle re-entry programs in differentiated muscle cells. PLoS Genet. 7, e1002362.

Li, F., Huang, Q., Chen, J., Peng, Y., Roop, D. R., Bedford, J. S. and Li, C. Y. (2010). Apoptotic cells activate the “phoenix rising” pathway to promote wound healing and tissue regeneration. Sci. Signal. 3, ra13.

Moberg, K. H., Bell, D. W., Wahrer, D. C. R., Haber, D. A. and Hariharan, I. K. (2001). Archipelago regulates Cyclin E levels in Drosophila and is mutated in human cancer cell lines. Nature 413, 311-316.

Mollereau, B., Perez-Garijo, A., Bergmann, A., Miura, M., Gerlitz, O., Ryoo, H. D., Steller, H. and Morata, G. (2013). Compensatory proliferation and apoptosis induced proliferation: a need for clarification. Cell Death Differ. 20, 181.

Morgan, T. H. (1901). Regeneration, Vol. VII. Norwood, MA: Norwood Press.

Nicolay, B. N., Bayarmagnai, B., Islam, A. B. M. M. K., Lopez-Bigas, N. and Frolov, M. V. (2011). Cooperation between dE2F1 and Yki/Sd defines a distinct transcriptional program necessary to bypass cell cycle exit. Genes Dev. 25, 323-335.

Oh, H. and Irvine, K. D. (2008). In vivo regulation of Yorkie phosphorylation and localization. Development 135, 1081-1088.

Oh, H., Slattery, M., Ma, L., Crofts, A., White, K. P., Mann, R. S. and Irvine, K. D. (2013). Genome-wide association of Yorkie with chromatin and chromatin remodeling complexes. Cell Rep. 3, 309-318.

Peng, H.W., Slattery, M. and Mann, R. S. (2009). Transcription factor choice in the Hippo signaling pathway: homothorax and yorkie regulation of the microRNA bantam in the progenitor domain of the Drosophila eye imaginal disc. Genes Dev. 23, 2307-2319.

Perez-Garijo, A., Martin, F. A. and Morata, G. (2004). Caspase inhibition during apoptosis causes abnormal signalling and developmental aberrations in Drosophila. Development 131, 5591-5598.

Perez-Garijo, A., Martin, F. A., Struhl, G. and Morata, G. (2005). Dpp signaling and the induction of neoplastic tumors by caspase-inhibited apoptotic cells in Drosophila. Proc. Natl. Acad. Sci. USA 102, 17664-17669.

Perez-Garijo, A., Fuchs, Y. and Steller, H. (2013). Apoptotic cells can induce nonautonomous apoptosis through the TNF pathway. Elife 2, e01004.

Pfreundt, U., James, D. P., Tweedie, S., Wilson, D., Teichmann, S. A. and Adryan, B. (2010). FlyTF: improved annotation and enhanced functionality of the Drosophila transcription factor database. Nucleic Acids Res. 38, D443-D447.

Poss, K. D., Wilson, L. G. and Keating, M. T. (2002). Heart regeneration in zebrafish. Science 298, 2188-2190.

Rauskolb, C., Sun, S., Sun, G., Pan, Y. and Irvine, K. D. (2014). Cytoskeletal tension inhibits Hippo signaling through an Ajuba-Warts complex. Cell 158, 143-156.

Richardson, H., Okeefe, L. V., Marty, T. and Saint, R. (1995). Ectopic cyclin E expression induces premature entry into S phase and disrupts pattern formation in the Drosophila eye imaginal disc. Development 121, 3371-3379.

Ruggiero, R., Kale, A., Thomas, B. and Baker, N. E. (2012). Mitosis in neurons: Roughex and APC/C maintain cell cycle exit to prevent cytokinetic and axonal defects in Drosophila photoreceptor neurons. PLoS Genet. 8, e1003049.

Ryoo, H. D., Gorenc, T. and Steller, H. (2004). Apoptotic cells can induce compensatory cell proliferation through the JNK and the Wingless signaling pathways. Dev. Cell 7, 491-501.

Shen, J. and Dahmann, C. (2005). Extrusion of cells with inappropriate Dpp signaling from Drosophila wing disc epithelia. Science 307, 1789-1790.

Sigal, S. H., Rajvanshi, P., Gorla, G. R., Sokhi, R. P., Saxena, R., Gebhard, D. R., Jr, Reid, L. M. and Gupta, S. (1999). Partial hepatectomy-induced polyploidy attenuates hepatocyte replication and activates cell aging events. Am. J. Physiol. 276, G1260-G1272.

Simmonds, A. J., Liu, X., Soanes, K. H., Krause, H. M., Irvine, K. D. and Bell, J. B. (1998). Molecular interactions between Vestigial and Scalloped promote wing formation in Drosophila. Genes Dev. 12, 3815-3820.

Slattery, M., Voutev, R., Ma, L., Ne`gre, N., White, K. P. and Mann, R. S. (2013). Divergent transcriptional regulatory logic at the intersection of tissue growth and developmental patterning. PLoS Genet. 9, e1003753.

Streichan, S. J., Hoerner, C. R., Schneidt, T., Holzer, D. and Hufnagel, L. (2014). Spatial constraints control cell proliferation in tissues. Proc. Natl. Acad. Sci. US 111, 5586-5591.

Sun, G. and Irvine, K. D. (2011). Regulation of Hippo signaling by Jun kinase signaling during compensatory cell proliferation and regeneration, and in neoplastic tumors. Dev. Biol. 350, 139-151.

Sun, G. and Irvine, K. D. (2013). Ajuba family proteins link JNK to Hippo signaling. Sci. Signal. 6, ra81.

Tamori, Y. and Deng, W.-M. (2013). Tissue repair through cell competition and compensatory cellular hypertrophy in postmitotic epithelia. Dev. Cell 25, 350-363.

Thompson, B. J. and Cohen, S. M. (2006). The Hippo pathway regulates the bantam microRNA to control cell proliferation and apoptosis in Drosophila. Cell 126, 767-774.

Tomancak, P., Beaton, A., Weiszmann, R., Kwan, E., Shu, S., Lewis, S. E., Richards, S., Ashburner, M., Hartenstein, V., Celniker, S. E. et al. (2002). Systematic determination of patterns of gene expression during Drosophila embryogenesis. Genome Biol. 3, research0088.14.

Toyama, Y., Peralta, X. G.,Wells, A. R., Kiehart, D. P. and Edwards, G. S. (2008). Apoptotic force and tissue dynamics during Drosophila embryogenesis. Science 321, 1683-1686.

Tseng, A.-S., Adams, D. S., Qiu, D., Koustubhan, P. and Levin, M. (2007). Apoptosis is required during early stages of tail regeneration in Xenopus laevis. Dev. Biol. 301, 62-69.

Verghese, S., Bedi, S. and Kango-Singh, M. (2012). Hippo signalling controls Dronc activity to regulate organ size in Drosophila. Cell Death Differ. 19, 1664-1676.

Warner, S. J. and Longmore, G. D. (2009). Cdc42 antagonizes Rho1 activity at adherens junctions to limit epithelial cell apical tension. J. Cell. Biol. 187, 119-133.

Warner, S. J., Yashiro, H. and Longmore, G. D. (2010). The Cdc42/Par6/aPK polarity complex regulates apoptosis-induced compensatory proliferation in epithelia. Curr. Biol. 20, 677-686.

Wenemoser, D. and Reddien, P. W. (2010). Planarian regeneration involves distinct stem cell responses to wounds and tissue absence. Dev. Biol. 344, 979-991.

Wernet, M. F., Labhart, T., Baumann, F., Mazzoni, E. O., Pichaud, F. and Desplan, C. (2003). Homothorax switches function of Drosophila photoreceptors from color to polarized light sensors. Cell 115, 267-279.

Winter, C. G., Wang, B., Ballew, A., Royou, A., Karess, R., Axelrod, J. D. and Luo, L. (2001). Drosophila Rho-associated kinase (Drok) links Frizzled-mediated planar cell polarity signaling to the actin cytoskeleton. Cell 105, 81-91.

Worley, M. I., Setiawan, L. and Hariharan, I. K. (2012). Regeneration and transdetermination in Drosophila imaginal discs. Annu. Rev. Genet. 46, 289-310.

Wu, S., Liu, Y., Zheng, Y., Dong, J. and Pan, D. (2008). The TEAD/TEF family protein Scalloped mediates transcriptional output of the Hippo growth-regulatory pathway. Dev. Cell 14, 388-398.

Wuestefeld, T., Pesic, M., Rudalska, R., Dauch, D., Longerich, T., Kang, T.-W., Yevsa, T., Heinzmann, F., Hoenicke, L., Hohmeyer, A. et al. (2013). A direct in vivo RNAi screen identifies MKK4 as a key regulator of liver regeneration. Cell 153, 389-401.

Xin, M., Kim, Y., Sutherland, L. B., Murakami, M., Qi, X., McAnally, J., Porrello, E. R., Mahmoud, A. I., Tan, W., Shelton, J. M. et al. (2013). Hippo pathway effector Yap promotes cardiac regeneration. Proc. Natl. Acad. Sci. USA 110, 13839-13844.

Yu, F.-X. and Guan, K.-L. (2013). The Hippo pathway: regulators and regulations. Genes Dev. 27, 355-371.

Zhang, L., Ren, F., Zhang, Q., Chen, Y.,Wang, B. and Jiang, J. (2008). The TEAD/TEF family of transcription factor Scalloped mediates Hippo signaling in organ size control. Dev. Cell 14, 377-387.

Zhang, H.-M., Chen, H., Liu, W., Liu, H., Gong, J., Wang, H. and Guo, A.-Y. (2012). AnimalTFDB: a comprehensive animal transcription factor database. Nucleic Acids Res. 40, D144-D149.

CHAPTER 3: A POPULATION OF G2-ARRESTED CELLS ARE SELECTED AS SENSORY ORGAN PRECURSORS FOR THE INTEROMMATIDIAL BRISTLES IN THE *DROSOPHILA* RETINA

SUMMARY

Cell cycle progression and differentiation are highly coordinated during the development of multicellular organisms. The mechanisms by which these processes are coordinated and how their coordination contributes to normal development are not fully understood. Here, we investigate the developmental fate of two populations of cells with unique cell cycle properties in the developing *Drosophila melanogaster* retina. We demonstrate that retinal precursor cells that arrest in G2 during larval development are selected as sensory organ precursors (SOPs) during pupal development and undergo two cell divisions to generate the four-cell interommatidial mechanosensory bristles. While G2 arrest is not required for bristle development, preventing G2 arrest results in incorrect bristle positioning in the adult eye. We conclude that G2-arrested cells provide a positional cue during development to ensure proper spacing of bristles in the eye. We further investigated a population of G1-arrested cells in the developing larval eye that can re-enter the cell cycle following tissue damage. Lineage tracing revealed that these cells are competent to differentiate into all accessory cell types in the retina but do not differentiate into photoreceptors, likely because cell cycle re-entry occurs after photoreceptor differentiation has completed. We conclude that the ability to re-enter the cell cycle in response to tissue damage is not restricted to precursors of a specific retinal

lineage and that cell cycle re-entry following damage to the eye disc does not disrupt developmental programs that control differentiation. Taken together, our results suggest the control of cell cycle progression refines cell fate decisions but the relationship between these two processes is not deterministic.

INTRODUCTION

Proliferation and differentiation are two important processes driving development of multicellular organisms. As such, these processes are highly regulated and fine-tuned through numerous overlapping genetic networks. Furthermore, cell cycle progression and differentiation are highly coordinated, as prior to terminally differentiating most cells permanently exit the cell cycle (Ruijtenberg and van den Heuvel, 2016). In fact, terminal differentiation is defined historically in part by a cell having exited the cell cycle (Reiner, 1983), and cell cycle exit is often viewed as a precursor to the final differentiated state of a cell.

There are a number of ways cell cycle regulators and regulators of differentiation interact to coordinate developmental processes, both at the level of transcriptional control and protein activity. Activating cell cycle regulators can suppress differentiation programs to keep proliferating precursor cells in an undifferentiated state. For example, in proliferating myoblasts, Cyclin/CDK complexes phosphorylate and inactivate MyoD and Mef2, two transcription factors that drive formation of myotubes (Tintignac et al., 2000; Di Giorgio et al., 2015). Similarly, cell cycle inhibitors can promote differentiation. pRb regulates the cell cycle by binding and inhibiting E2f transcription factors that drive cell cycle progression, but pRb can also bind and activate transcription factors that promote

differentiation, like the osteoblast-specific transcription factor CBFA1 (Thomas et al., 2001).

More recent studies have suggested that although cell cycle exit and differentiation occur concurrently, cell cycle exit is not necessarily required prior to the completion of cell differentiation, as defined by cell functionality and expression of differentiation markers. Under normal development, hepatocytes in the mammalian liver undergo rounds of S phase followed by mitoses, which may or may not be followed by cytokinesis, resulting in a heterogeneous population of diploid and polyploid cells (Anatskaya et al., 1994). Furthermore, some hepatocytes re-enter the cell cycle and proliferate or undergo endocycles during liver regeneration (Gentric et al., 2012). Experimentally, cell cycle exit can be blocked by genetically manipulating cell cycle regulators, which doesn't necessarily prevent differentiation. For example, neurons in the developing *Drosophila* wing with ectopic E2f/Cyclin-CDK activity continue to proliferate while still displaying markers of differentiated neurons (Buttitta et al., 2007). Similarly, muscle cells in *C. elegans* with ectopic Cyclin/CDK expression display markers of mitosis while still contracting as normal, functioning myocytes (Korzelius et al., 2011). These experiments and others suggest that rather than cell cycle progression and differentiation being completely incompatible, there is likely a great deal of flexibility depending on the tissue and cell type.

In addition to proliferation versus cell cycle exit, position in the cell cycle can also affect a cell's receptiveness to differentiation signals. Recently, elegant experiments using human embryonic stem cells (hESCs) that were isolated according to cell cycle phase by flow cytometry demonstrated that cells in G1 adopt a differentiated state more frequently than cells in other phases of the cell cycle (Pauklin and Vallier, 2013). Interestingly, cells in early G1 readily differentiate into endoderm or mesoderm but not neuroectoderm,

while cells in late G1 differentiate into neuroectoderm but not endoderm or mesoderm. These results suggest cell cycle regulators present in early versus late G1 may bias cells to adopt different lineages. Differences in chromatin accessibility during cell cycle phases may also influence a cell's responsiveness to developmental signals (Ma et al., 2015), as suggested by experiments in *Drosophila* wherein genetic manipulation of a chromatin regulator modulates the receptiveness of bristle cells in the notum to Notch signaling during S phase (Remaud et al., 2008; Ma et al., 2015). However, whether cell cycle phase directly influences cell fate and differentiation *in vivo* or is merely correlated with these processes during development is not clear.

An excellent model for studying relationships between cell cycle regulation and differentiation is the developing *Drosophila* eye. The larval eye imaginal disc, an epithelial sheet of cells that metamorphoses into the adult eye during pupation, undergoes a precise pattern of cell cycle progression and differentiation (Fig. 1A). During the first two larval stages, cells in the primordial eye disc undergo asynchronous cell divisions that increase the pool of precursor cells. During the third and final larval stage, a wave of differentiation sweeps across the disc epithelium from posterior to anterior. This wave is associated with an apical restriction resulting in an indentation in the disc called the morphogenetic furrow (MF) (Fig. 1A). Cells just anterior to the MF arrest in G1 phase and remain arrested in G1 within the furrow at which time a subset begin to differentiate into five of the eight photoreceptors that make up an ommatidium, the photoreception unit of the compound eye (Kumar, 2012). Immediately posterior to the MF, the remaining undifferentiated cells synchronously re-enter the cell cycle. Although for historical reasons this cell cycle is referred to as the Second *Mitotic* Wave (SMW)

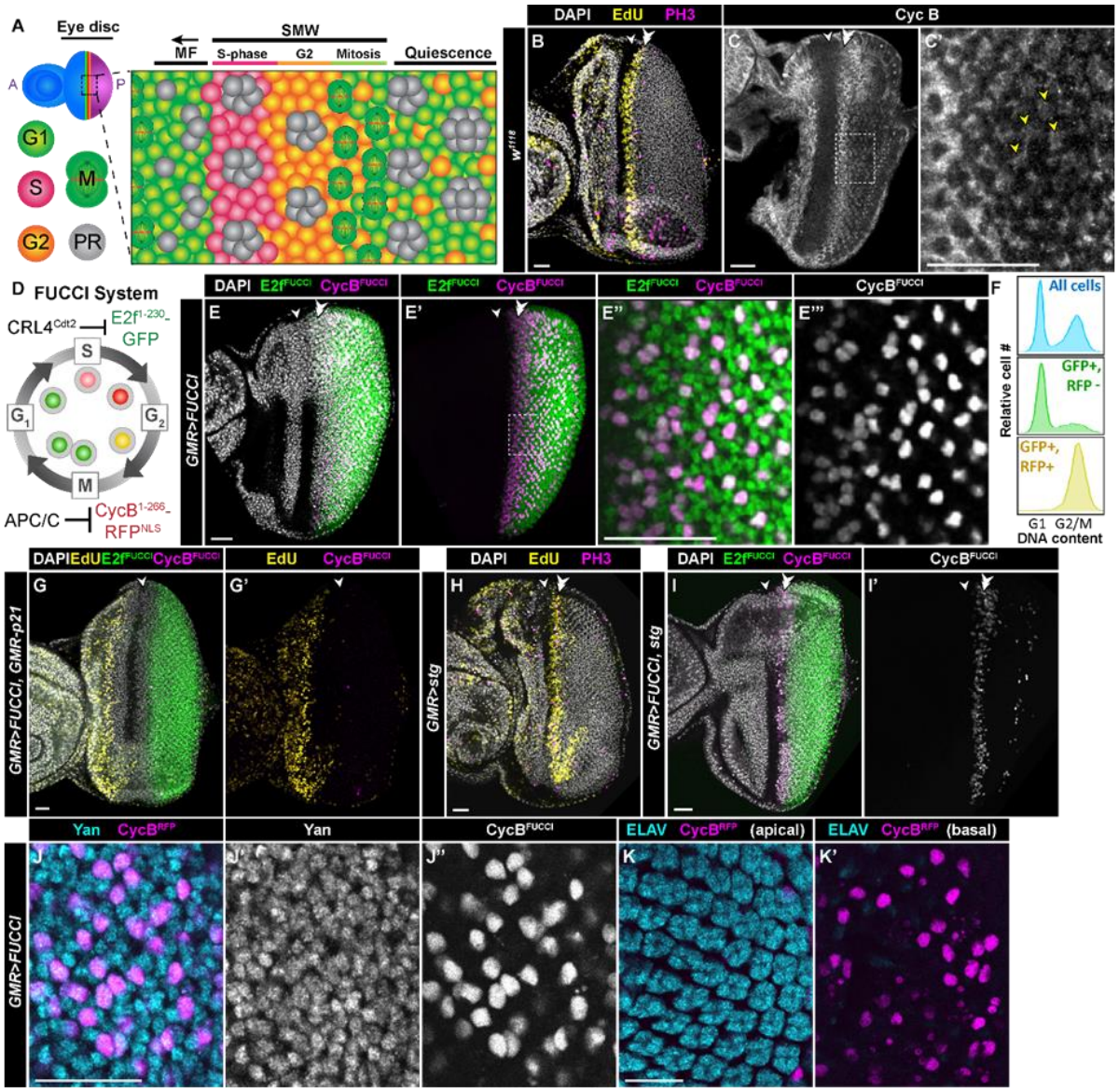

Fig. 1. A subset of cells arrest in G2 after S phase of the Second Mitotic Wave in eye discs. (A) Diagram of the onset of cell differentiation during *Drosophila* eye development. Cell differentiation during eye development begins during the third larval instar stage and occurs as a wave across the eye disc represented by the morphogenetic furrow (MF), which initiates at the posterior (P) and moves towards the anterior (A). Cells anterior to the furrow proliferate asynchronously (blue in full disc). Cells within the MF arrest in G1 (green cells), and a subset of these differentiate into the first five photoreceptors (PR; gray) while the remaining undifferentiated cells synchronously enter S-phase (red cells) of the second mitotic wave (SMW). The majority of these cells then enter mitosis (M), after which they sequentially differentiate and get recruited into developing ommatidia. Some cells (orange) posterior to the MF remain in G2. Relative area of each region is not to scale. (B-C') w^{1118} control larval eye disc stained with DAPI (DNA, gray), EdU (S-phase, yellow), and anti-phospho histone H3 antibodies (PH3, mitosis, magenta). In this and subsequent panels the white arrowhead indicates the MF and the double arrowhead indicates the SMW. (C,C') w^{1118} control larval eye disc stained with anti-Cyclin B antibodies (CycB, G2/mitosis, gray; dotted box indicates area of magnification in C'). Post-SMW cells with high levels of CycB are indicated with yellow arrowheads. (D) Diagram of the FUCCI *(cont next page)*

(*cont)* system. GFP-E2f$^{1-230}$ (E2f^{FUCCI}) is targeted for degradation by CRL4^{Cdt2} during S phase, and RFP-NLS-CycB$^{1-266}$ (CycB^{FUCCI}) is degraded by APC/C during mitosis and G1. (E-E"") *GMR-Gal4; UAS-FUCCI* (*GMR>FUCCI*) larval eye discs express both E2f^{FUCCI} (green) and CycB^{FUCCI} (E,E', magenta; E", grey) posterior to the MF; DAPI staining in gray (E'), dotted box indicates area of magnification in E",E"". (F) Flow cytometry histograms of relative cell number versus DNA content for dissociated *GMR>FUCCI* eye discs. Cell cycle phase peaks (G1 and G2/M) are based on measurements from all cells (top panel, blue). Cells expressing only E2f^{FUCCI} have G1 DNA content (middle panel, green) while cells expressing both E2f^{FUCCI} and CycB^{FUCCI} have G2 DNA content (bottom panel, yellow). (G,G') *GMR>FUCCI, GMR-p21* larval eye disc expressing E2f^{FUCCI} (green) and CycB^{FUCCI} (magenta) and stained with DAPI (G, gray) and EdU (yellow). No SMW is present, and all cells posterior to the MF express E2f^{FUCCI} but do not express CycB^{RFP}. (H) *GMR-Gal4, UAS-stg* (*GMR>stg*) eye disc stained with DAPI (gray), EdU (yellow), and anti-PH3 (magenta). (I,I') *GMR>FUCCI, stg* eye disc expressing E2f^{FUCCI} (green) and CycB^{FUCCI} (I, magenta; I', gray). Very few G2 cells (CycB^{FUCCI}+) are present posterior to the MF. (J,J') *GMR>FUCCI* eye disc stained with antibodies recognizing Yan (J, cyan; J', gray), a marker of undifferentiated cells. Yan positive cells expressing CycB^{FUCCI} (magenta) are in G2. (K,K') *GMR>FUCCI* eye disc stained with antibodies recognizing ELAV (cyan), a marker of differentiated photoreceptors. CycB^{FUCCI} cells (magenta) do not express ELAV. Both apical (K) and basal (K') sections are shown, as photoreceptors and undifferentiated cells reside in different focal plans. All eye discs are from third instar larvae and are oriented with the posterior to the right. Scale bars = 20mM.

(Wolff and Ready, 1991), this term is often used to refer to the resulting synchronous wave of S-phase readily visualized by EdU labeling (Fig. 1B). However, as described in this paper, not all of these cells undergo mitosis during eye imaginal development. Thus, here we use "SMW" specifically to describe the synchronous round of S-phase immediately posterior to the MF. Following this S-phase, cells enter G2 and the majority subsequently undergo mitosis and then become quiescent in G1 phase. As a result, posterior to the SMW no S-phases or mitoses occur within the larval disc (Fig. 1B). These undifferentiated cells will eventually differentiate into the remaining photoreceptors or retinal accessory cells or will be cleared from the retina by apoptosis during pupation, as there are more undifferentiated precursor cells in the disc than needed to assemble all ~800 ommatidia (Cagan and Ready, 1989). This precise and stereotyped program of cell cycle progression and differentiation results in the highly organized and latticed appearance of the adult eye. Consequently, defects in regulation of cell cycle progression or differentiation are

readily apparent as disruptions to the precisely patterned adult eye.

While numerous studies have investigated cell cycle arrest and differentiation in the developing *Drosophila* eye, less attention has been paid to how cell cycle phase might affect differentiation. We were particularly interested in this question as a previous study described a G2-arrested cell population posterior to the MF in the developing eye imaginal disc that remains uncharacterized. As part of their studies investigating G2→M progression following the SMW, Baker and Yu found that a small subset of undifferentiated cells posterior to the MF did not undergo mitosis and instead accumulated Cyclin B (CycB), a marker of cells in G2 (Fig. 1C,C') (Baker and Yu, 2001). However, the fate of these cells, particularly whether they contribute to a specific cell type in the adult eye, is not known. Here we hypothesize that an arrest in G2 might predispose these cells to adopt a certain lineage, or perhaps prevent them from prematurely adopting an inappropriate cell fate. Using newly developed transgenic cell cycle markers and flow cytometry we confirmed the presence of this G2-arrested cell population posterior to the MF. Additionally, we provide evidence that these G2-arrested cells re-enter the cell cycle during pupal development and become interommatidial mechanosensory bristles, which are evenly spaced throughout the adult eye. We propose a model in which G2 arrest predisposes cells to be selected as a sensory organ precursor cell and thus ensures efficient and precise bristle development.

RESULTS

A subset of eye disc cells that undergo S-phase of the SMW remain arrested in G2 throughout larval development.

The eye disc cells posterior to the MF described by Baker and Yu (2001) behaved

like G2-arrested cells because they rapidly entered mitosis upon expression of String, a CDC25-like phosphatase that activates mitotic CDK1 kinases (Edgar and O'Farrell, 1990). We first sought to confirm the presence of G2-arrested cells posterior to the MF in the developing eye disc using flow cytometry. We took advantage of the newly developed Fluorescent Ubiquitylation Cell Cycle Indicators (FUCCI) (Zielke et al., 2014) to identify cells in different phases of the cell cycle. The FUCCI system is composed of two parts: 1) a transgene expressing a fragment of CycB fused to RFP that is functionally inert but targeted for destruction during mitosis and G1 by the Anaphase-Promoting Complex (APC/C); and 2) a transgene expressing a fragment of E2f1 fused to GFP that is also inert but targeted for destruction during S phase by $CRL4^{Cdt2}$. The co-expression of these two fluorescent indicators ($E2f^{FUCCI}$ and $CycB^{FUCCI}$) allows cytological visualization of cell cycle position (Fig. 1D). Cells expressing both transgenes are presumed to be in G2. When we express *UAS-FUCCI* transgenes using *GMR-Gal4* (*GMR>FUCCI*), which drives expression posterior to the MF in the eye disc (Hay et al., 1994), we observe a number of $E2f^{FUCCI}$ and $CycB^{FUCCI}$ double-positive cells in the posterior of the disc (Fig. 1E-E'''). These cells, which are presumably the same CycB-accumulating cells observed by Baker and Yu (2001), persist to the posterior edge of the disc, suggesting they do not undergo mitosis during larval development. To determine whether these $E2f^{FUCCI}$ and $CycB^{FUCCI}$ double-positive cells are indeed in G2, we performed flow cytometry on trypsin-dissociated *GMR>FUCCI* eye discs stained with a DNA-binding dye to measure DNA content. Flow analysis indicates that cells expressing both $CycB^{FUCCI}$ and $E2f^{FUCCI}$ have 4C DNA content, indicative of cells in G2 (Fig. 1F). We also analyzed a line containing a GFP protein trap insertion into the endogenous *Cyc B* locus (Buszczak et al., 2007). CycB-GFP expression in eye discs from this line mirrors the endogenous CycB expression pattern

(compare Fig. 1C to Fig. S1A-A"). In addition, CycB-GFP expressing cells have 4C DNA content based on flow analysis (Fig. S1B) and enter mitosis following *hs-stg* expression (Fig. S1C-F"), consistent with cells arrested in G2. We conclude that a G2 cell population posterior to the MF exists in eye discs at an abundance of approximately one G2 cell per ommatidium, confirming and extending the previous observations of Baker and Yu (2001).

We hypothesized that these G2 cells arise from undifferentiated cells that enter S phase of the SMW but do not undergo mitosis during larval development. We tested this hypothesis by eliminating the SMW through *GMR*-driven expression of the human CDK inhibitor, p21 (de Nooij and Hariharan, 1995). EdU labeling revealed that the SMW is completely ablated in *GMR-p21* eye discs while S phases anterior to the MF are not affected (Fig. 1G,G'). In addition, no $E2f^{FUCCI}$/$CycB^{FUCCI}$ double-positive G2 cells are observed posterior to the MF in *GMR>FUCCI, GMR-p21* eye discs (Fig. 1G,G'), confirming these G2 cells arise from the SMW. We predicted that G2 arrest after the SMW was due to lack of Stg expression. We therefore drove ectopic *UAS-stg* expression with *GMR-Gal4* to determine whether we could bypass the G2 arrest. Consistent with our prediction, *GMR>stg* eye discs have very few G2-arrested cells posterior to the MF (Fig. 1H,I,I'), suggesting that all cells have undergone mitosis. Since photoreceptors and other differentiated retinal cell types arrest in G1 (Buttitta et al., 2007), we hypothesized that G2-arrested cells are undifferentiated. We therefore stained *GMR>FUCCI* discs with a marker for undifferentiated cells (Yan) and a marker for photoreceptors (ELAV), the primary differentiated cell type in larval discs. All the G2-arrested cells express Yan (Fig. 1J-J") but not ELAV (Fig. 1K,K'), indicating that they are undifferentiated. We conclude

that a small population of cells remain arrested in G2 after S phase of the SMW and that these G2-arrested cells remain undifferentiated throughout larval development.

G2 cells express markers of SOPs and divide during pupation to produce interommatidial mechanosensory bristles

We hypothesized that these G2-arrested eye precursor cells adopt a specific fate(s). We therefore performed a series of experiments to follow these G2-arrested cells through pupal development and determine whether they contribute to the adult eye. During the first ~12 hours after puparium formation (APF), the MF and SMW continue traversing the disc. When the MF reaches the anterior of the disc and the SMW concludes, a subset of undifferentiated cells across the disc epithelium re-enter the cell cycle and divide (Cagan and Ready, 1989). These cell divisions begin centrally in the disc and radiate outwards, continuing for the next 12 hours of development. Cagan and Ready (1989) previously showed that proliferating cells, which incorporate BrdU injected during pupal development, all become part of the interommatidial mechanosensory bristles, which are positioned at three vertices of each ommatidium and cover the adult eye (see Fig. 4A,B). These bristles are composed of a group of four cells: a neuron, a glial cell, a socket cell, and a shaft cell. Each bristle group is derived from a single precursor cell called a sensory organ precursor (SOP) (Fig. 2A). By 24 hours APF, the bristle group divisions have concluded, and the vast majority of retinal cells arrest in G1 based on flow cytometry (Buttitta et al., 2007) and expression of FUCCI transgenes (Fig. S2A-F'). The absence of G2 cells is not a result of apoptosis, a common phenomenon during pupal retinal development (Cagan and Ready, 1989), as retinas expressing the p35 caspase inhibitor also contain very few cells expressing $CycB^{FUCCI}$ at 24hrs APF (Fig. S2G,G'; see Fig. S2H

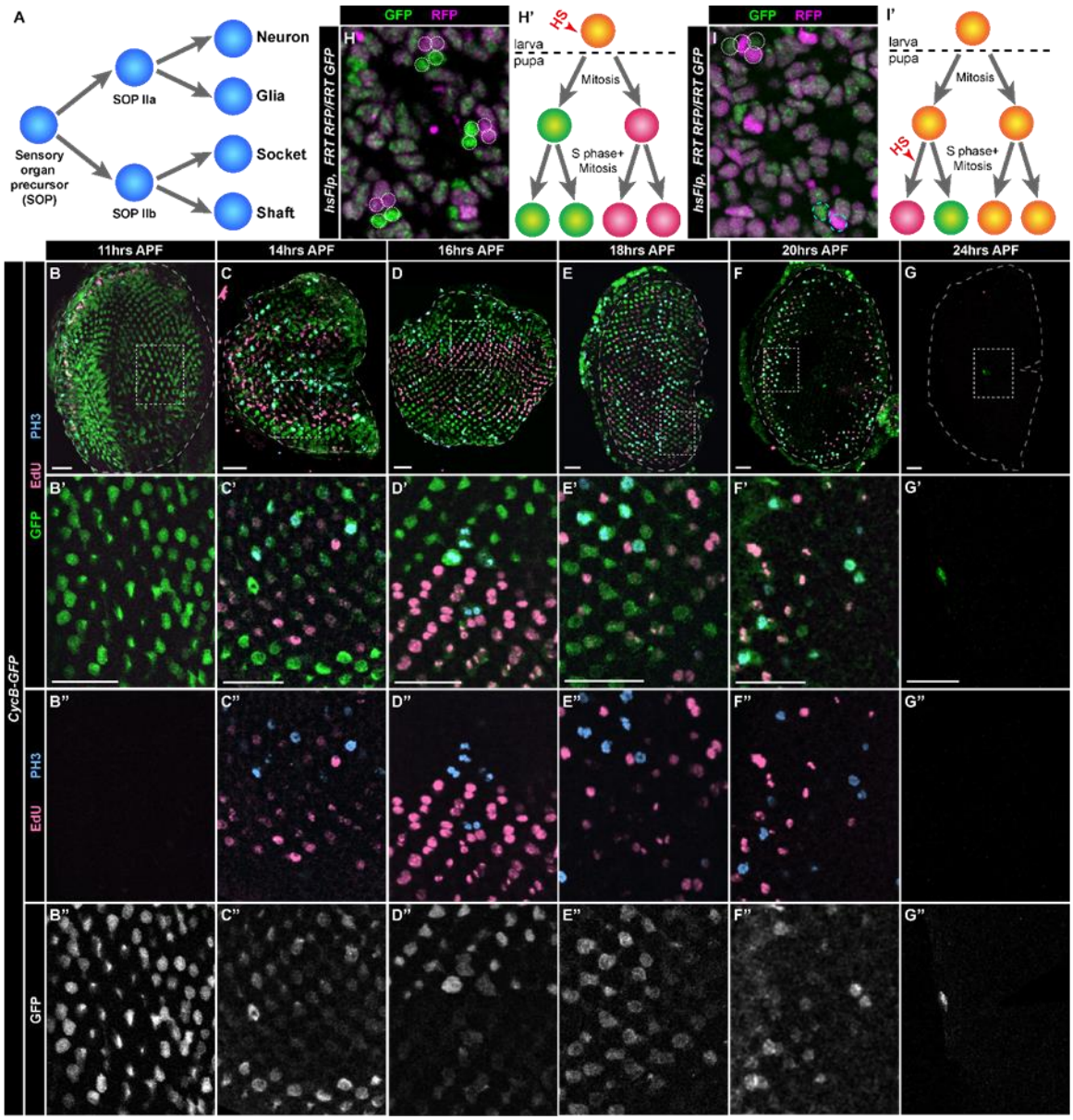

Fig. 2. Cells arrested in G2 in larval eye discs divide during pupation. (A) Diagram of SOP divisions and bristle group lineage in the pupal retina. (B-G") *CycB-GFP* retinas dissected at various times after pupal formation (APF) and stained with EdU (pink, S-phase) and anti-PH3 (blue, mitosis). Cells in G2/M express GFP (B-G', green; B"-G", grey). (H,H') *hs-Flp, FRT19A Ubi-mRFP.nls/FRT19A His2Av-GFP* retina at 24hrs APF in which mitotic recombination was induced at the 3rd instar larval stage to produce GFP expressing (green) and RFP expressing (magenta) clones in the posterior. Dotted circles indicate clones with two cells expressing GFP and two cells expressing RFP. Such four cell-clones indicate mitotic recombination in a precursor cell that subsequently underwent two divisions (H'). (I,I') Clones as in panel H resulting from mitotic recombination induced at 19hrs APF and analyzed at 29hrs APF. Two cell-clones (dashed circles) with one cell expressing GFP (green) and one cell expressing RFP (magenta) result from mitotic recombination in a precursor cell that subsequently underwent one division (I'). Four cell-clones as in panel H are also apparent (dotted circles). Scale bars = 20μM.

for retina at 48hrs APF where p35 expression results in excess numbers of cells that would normally be cleared by apoptosis).

Previous models for mechanosensory bristle development have presumed the SOP is arrested in G1 and undergoes two cycles of S phase and cell division to provide the four cells for each bristle group (Cagan and Ready, 1989). Instead, we hypothesized that retinal SOPs are arrested in G2 and first enter mitosis, followed by one round of S phase and mitosis to make the four cell bristle groups. Therefore, we predicted these G2-arrested cells undergo mitosis during the first 24 hours of pupal development when SOP divisions occurs. By 12hrs APF, we observed S phase and mitosis throughout the disc, beginning interiorly and radiating outward over the next 12 hours (Fig. 2B-G''). By 24hrs APF, the majority of divisions have ceased (Fig. 2G-G''). Cells in G2, marked by CycB-GFP (Fig. 2B-G'') or $CycB^{FUCCI}$ expression (Fig. S2A-F'), also progressively disappear between 12 and 24hrs APF. To determine whether the G2-arrested cells themselves undergo mitosis and S-phase, we used the FRT/Flp system (Xu and Rubin, 1993) to generate cell clones by mitotic recombination, which occurs between homologous chromosomes in G2 after DNA replication. Thus, when the FLP recombinase is induced by heat shock in third instar larval eye discs, recombination will only occur within the posterior of the disc in cells arrested in G2. The products of recombination will only be observed if these G2-arrested cells divide and segregate genetically marked homologous chromosomes (in this experiment with His2Av-GFP and Ubi-mRFP.nls) into different daughter cells. When larvae were heat shocked and pupal retinas were dissected at 24hrs APF, in the posterior of the retina we observed four-cell clones in which two cells express GFP and two cells express RFP (Fig. 2H). These data indicate cells in G2 larval discs can divide twice during pupation (Fig. 2H'). When we heat shocked pupae at 19hrs APF and dissected retinas 10

hours later, in addition to four cell clones we observed two cell clones containing one cell expressing GFP and one cell expressing RFP (Fig. 2I). This result is consistent with cell division of the SOPs occurring asynchronously, such that at the time of heat shock mitotic recombination was induced in an SOP daughter that divided once, generating the two-cell clone (Fig. 2I'). These data indicate that G2-arrested cells are not eliminated from the developing retina and undergo two rounds of mitosis during the first 24 hours of pupal development.

Based on their morphological location and composition, we hypothesized that these clones were derived from SOP cells and comprise the bristle group lineage. To test this hypothesis, we induced clones and stained retinas with antibodies recognizing Cut, which is expressed in all cells of the bristle group at 24hrs APF (Frankfort et al., 2004). We found that every cell within all clones located in the posterior of the retina expressed Cut (Fig. 3A-A"). In contrast, clones in the anterior marked all cell lineages as they arose in asynchronously proliferating precursor cells anterior to the MF that have the potential to contribute to every retinal cell type (Fig. S3A-C). Although all posteriorly located clones were Cut+, not all Cut+ bristle group cells were part of a marked clone. This result could indicate either that some bristle groups are derived from cells in G1 or that mitotic recombination was not induced in all G2 cells, which is likely because the FLP recombinase is not 100% efficient. We therefore analyzed younger pupal retinas to determine if cells in G2 expressed markers of SOPs. By 6hrs APF, SOPs express Sens (Frankfort et al., 2004). We found using the *CycB-GFP* line that the vast majority of cells in G2 express Sens (Fig. 3B-C). The majority of cells that are in G1 and express Sens are likely R8 photoreceptors, which have been previously shown to express Sens (Frankfort et al., 2004), since there is a similar number of G1 arrested, Sens-expressing cells and

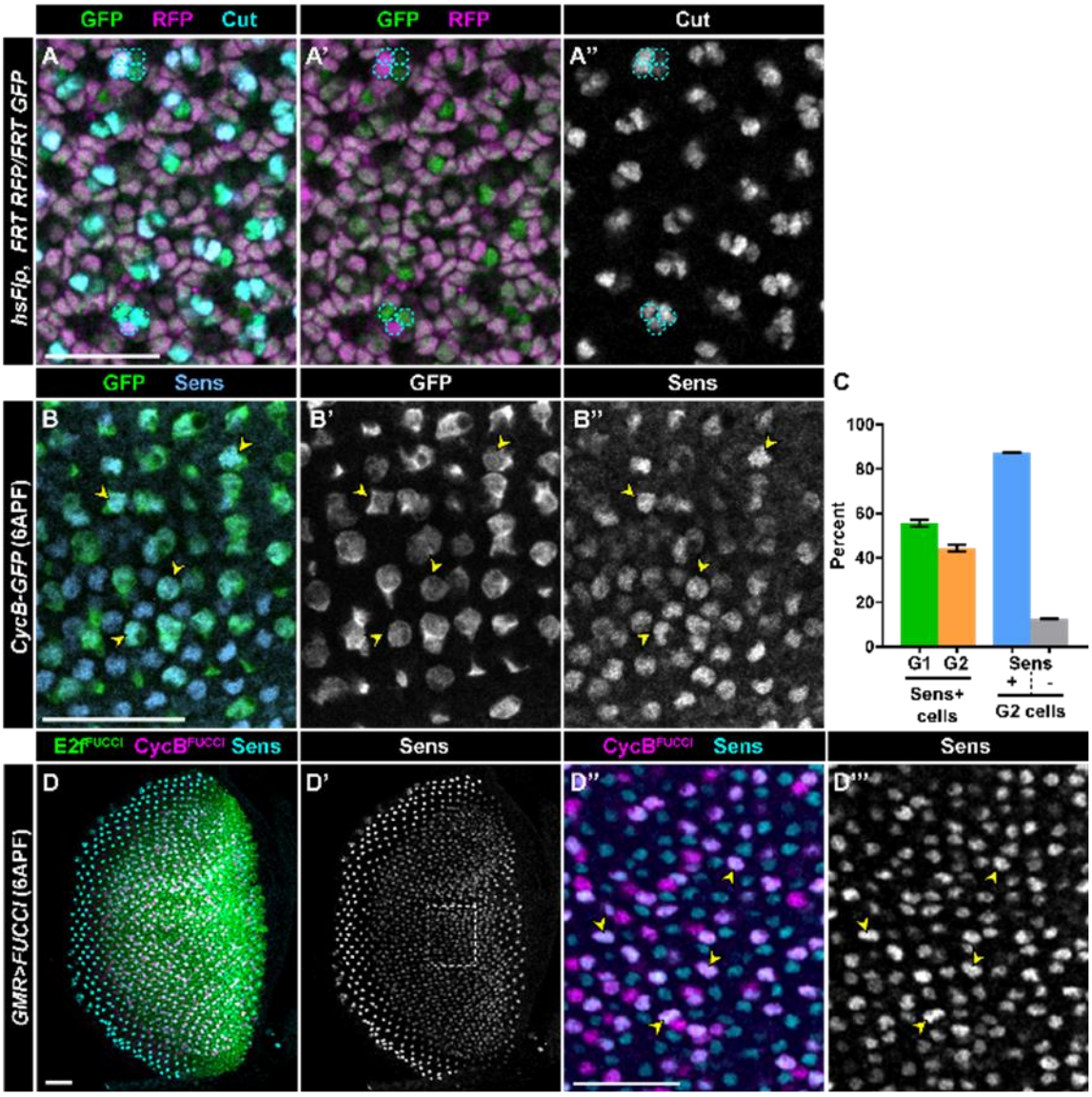

Fig. 3: G2 arrested cells express SOP markers and divide to become the bristle groups. (A-A'') *hs-Flp, FRT19A Ubi-mRFP.nls/FRT19A His2Av-GFP* retina at 24 hrs APF stained with antibodies recognizing Cut (cyan) in which mitotic recombination was induced at the 3rd instar larval stage to produce GFP expressing (green) and RFP expressing (magenta) clones in the posterior. Four cell clones (dashed circles) are Cut+. Some of the clones, including the three cells marked in the lower section of the panel, appear to have three cells because the fourth cell is out of the focal plane. (B-B'') *CycB-GFP* retinas at 8hrs APF stained with antibodies recognizing Senseless/Sens (B, blue; B'', grey); most cells expressing GFP (B, green; B', grey) also express Sens (arrowheads; quantified in C). Scale bars = 20μM.

ommatidia in our quantification (Fig. 3C). These data indicate that G2-arrested cells are selected as SOPs and divide twice to become the bristle group.

Disruption of G2 arrest disrupts bristle development

Our observations thus far raise two new questions regarding development of mechanosensory bristles: 1) is G2 arrest of SOPs necessary for bristle formation? And 2) are the cell divisions of the SOP and its daughters necessary for bristle formation? Although asymmetric divisions are important for many neuronal lineages (Sousa-Nunes and Somers, 2013; Paridaen and Huttner, 2014) and have demonstrated to be important for bristle development as well (Bellaïche et al., 2001), the bristle cells are the only cells in the retina that are clonally derived. All other cells in an ommatidium (for example, the four cone cells and eight photoreceptors) are derived independently (Ready et al., 1976). To test whether cell division in the pupal retina is required for bristle development, we blocked S phase entry by expressing p21. In *GMR-p21* flies in which the SMW and bristle divisions are ablated, retinas are missing bristles at 48hrs APF (Fig. S4A; compare to control Fig. 4A,B) and adult eyes display only 13% of the normal number of bristles (Fig. S4A') (de Nooij and Hariharan, 1995). The great reduction of bristles in this genotype has previously been attributed to a reduction in precursor cell number resulting from loss of the SMW as other non-bristle cell types are also missing (de Nooij and Hariharan, 1995). Indeed, *GMR-p21* retinas are disorganized and appear to be missing several cell types (Fig. S4A). However, we hypothesized that bristle defects observed in *GMR-p21* retinas are due to disruption of SOP divisions and not merely a consequence of reduction of precursor cell number. To test this prediction, we expressed *UAS-p21* under control of *GMR-Gal4* (*GMR>p21*) rather than expressing p21 directly from the *GMR* promoter. *GMR>p21* eye discs retain the SMW, likely due to delayed accumulation of p21 in this genotype (Fig. S4C,C'). Therefore, *GMR>p21* is predicted to disrupt divisions of the SOP lineage during pupation without reducing precursor cell number (Fig. S4D,D'). Retinas

from *GMR>p21* pupae at 48hrs APF appear morphologically normal, but the majority of bristle groups are missing (Fig. S4B). Consequently, adults lack most interommatidial bristles (Fig. S4B'). Therefore, SOP divisions during pupation are required for the full complement of bristles in the adult eye.

We next investigated whether G2 arrest preceding SOP selection is required for bristle development. We explored this question by expressing *UAS-stg* under control of *GMR-Gal4* (*GMR>stg*), which precociously drives G2-arrested cells into mitosis following the SMW. Although *GMR>FUCCI, stg* larvae lack a G2-arrested cell population (Fig. 1I,I'), adults of this genotype have qualitatively normal interommatidial bristles compared to control flies (Fig. 4B',C'). However, we observe bristle placement defects in *GMR>stg* retinas at 48hr APF (Fig. 4C). Normally, bristle groups appear at alternating vertices of the ommatidia, with tertiary pigment cells occupying the other vertices (Fig. 4A,B). In *GMR>stg* retinas, we often observe bristle groups at neighboring vertices, missing from an ommatidium, or occurring between two vertices (Fig. 4C). These results suggest that while G2 arrest is not essential for bristle development, cells arrested in G2 may provide positional information to ensure proper bristle patterning in the retina.

We predicted that cell division of the SOP and its daughters occur in *GMR>stg* retinas prior to bristle development. To monitor this process in *GMR>stg* retinas, we assessed cell cycle progression and the appearance of SOP markers at various time points during the first 24hrs of pupal development (Fig. 4D-I'). Although almost all cells post-SMW arrest in G1 in *GMR>FUCCI, stg* larval eye discs, a subset of these cells re-enter the cell cycle during early pupal development. By ~3hrs APF, a small number of $CycB^{FUCCI}$+ cells appear in the posterior region of the eye disc (Fig. 4E,E'). $CycB^{FUCCI}$+ cells increase in number as pupal development continues, and by 12hrs APF, widespread mitoses and S

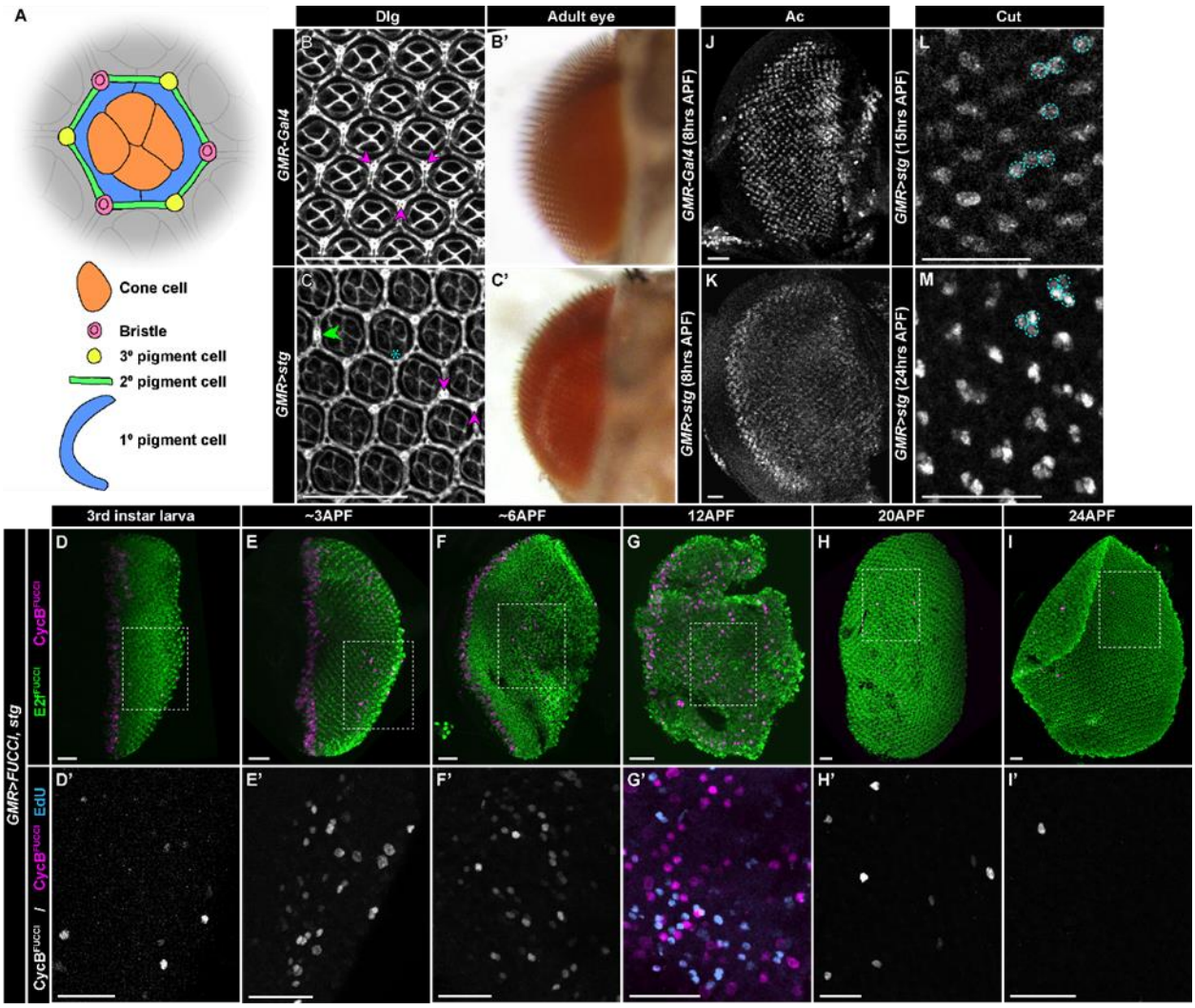

Fig. 4: Stg expression disrupts but does not block bristle development. (A) Diagram of cell types in an ommatidium visible in apical sections of the retina at 48hrs APF. The morphological organization of the ommatidium allows identification of each cell type using membrane staining. (B,B') Retinas from control (*GMR-Gal4*) flies. (B) Retina at 48hrs APF stained with antibodies recognizing Dlg, which marks cells membranes. Bristles (purple arrows) are normally located at alternating vertices of the hexagonal ommatidia, generating a regular pattern in the adult eye (B'). (C,C') Retinas from *GMR>stg* flies. (C) In a retina stained with anti-Dlg at 48hrs APF, bristles are misplaced. Examples include bristles located at neighboring vertices (purple arrows), absent bristles (blue asterisk), and bristles located in between two vertices (green double arrow). Bristles are visible in adult eyes (C'). (D-I') *GMR>FUCCI, stg* retinas expressing $E2f^{FUCCI}$ (green) and $CycB^{FUCCI}$ (D-I,G', magenta; D'-F',H',I' grey) analyzed at the indicated times after pupal formation (APF). (G') Retina at 12APF stained with EdU (blue). Dotted boxes indicate areas of magnification in D'-I'. (J,K) Retinas at 8hrs APF expressing with anti-Achaete/Ac antibodies in (J) control and (K) *GMR>stg*. (L,M) *GMR>stg* retinas at 15hrs APF (L) or 24hrs APF (M) stained with antibodies recognizing Cut. Groups of cells expressing Cut (circled at present). (M) At 24hrs APF, four cells groups are present; groups that appear to have less than four cells, like the three circled cells, have additional cells outside the plane. Scale bars = 20μM.

phases are observed throughout the retina (Fig. 4G,G'; compare to Fig. 2D). These data suggest that cells can re-enter the cell cycle during pupation in the absence of a preceding G2 arrest, though this cell cycle re-entry in *GMR>stg* retinas occurs earlier than in wild type. SOP selection genes are also activated in *GMR>stg* retinas. By 8hrs APF, the proneural gene Achaete (Ac) is observed throughout the retina (Fig. 4K), although expression appears somewhat lower than in control (Fig. 4J). Cells expressing Cut appear at 15hrs APF (Fig. 4L) and 24hrs APF (Fig. 4M). Therefore, G2 arrest preceding SOP selection is not absolutely essential, but contributes to the normal pattern of bristle location in the eye.

Compensatory proliferating cells contribute to the bristle lineage.

Our interest in characterizing the G2-arrested cell population in the eye is part of our broader interest in determining whether there is a functional relationship between cell cycle progression and cell fate. Therefore, as an extension of this study we investigated another cell population posterior to the MF that has a unique cell cycle program. When tissue damage is genetically induced posterior to the MF by expression of the pro-apoptotic protein, Hid, under control of *GMR*, undifferentiated cells that are normally quiescent re-enter the cell cycle and divide to replenish the pool of precursor cells depleted by apoptosis (Fan and Bergmann, 2008; Meserve and Duronio, 2015). This process is called compensatory proliferation (CP). We hypothesized that the subset of cells capable of re-entering the cell cycle during CP represents an uncharacterized subset of lineage restricted cells. In *GMR-hid* eye discs, a wave of CP S phase precedes mitosis (Fig. 5A,A'), suggesting that the cells enter the cell cycle from G1. In addition, the pattern

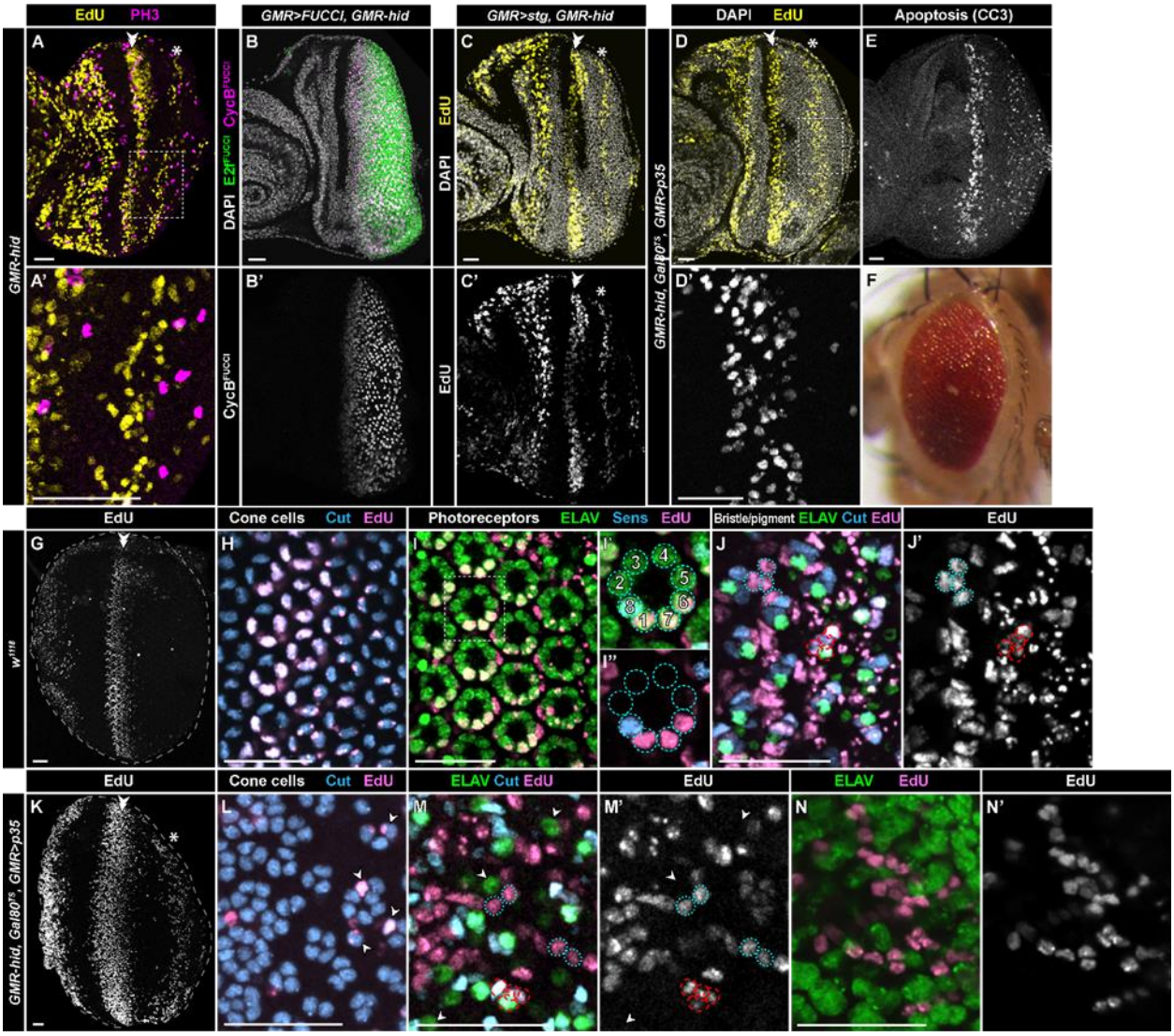

Fig. 5: Compensatory proliferating cells can differentiate into bristle cells without arresting in G2. (A,A') *GMR-hid* larval eye disc stained with EdU (yellow) and PH3 (magenta). In this and subsequent panels, the double arrowhead indicates the SMW and the asterisk indicates the CP wave. Dotted box indicates area of magnification in A'. (B,B') *GMR>FUCCI, GMR-hid* larval eye disc expressing CycB^{FUCCI} (B, magenta; B', grey) and E2F^{FUCCI} (green) and stained with DAPI (B, gray) (compare to control Fig. 1D). (C,C') *GMR>stg, GMR-hid* larval eye disc labeled with EdU (C, yellow; C', grey) and DAPI (grey). (D,D') *GMR-hid, Gal80^{TS}, GMR>p35* larval eye discs labeled with EdU (D, yellow; D', grey) and DAPI (grey). Dotted box indicates area of magnification D'. (E') *GMR-hid, Gal80^{TS}, GMR>p35* larval eye disc stained with antibodies recognizing cleaved-caspase 3 (CC3). (F) *GMR-hid, Gal80^{TS}, GMR>p35* adult eye. (G-J') *w^{1118}* control retina at 24hrs APF labeled with EdU (G,J', gray; H-J, pink) derived from 3rd instar larvae fed with EdU for 10 hours. Posterior of the retina is oriented to the right, and SMW-derived EdU+ cells are indicated with a double arrowhead. EdU+ cells within the SMW label (H) Cut-expressing cone cells (blue); (I-I") ELAV-expressing photoreceptors R1, R7, and R6 (green), identified based on orientation to Sens-expressing R8 (blue); *(cont next page)*

(cont) (J,J') Cut-expressing basal bristle groups (red dashed circles; Cut, blue; neurons express ELAV (green)); and pigment cells (blue dotted circles; Cut/ELAV-). (K-M') *GMR-hid, Gal80^{TS}, GMR>p35* retina at 24hrs APF labeled with EdU (K,M', gray; L,M, pink) derived from 3rd instar larvae fed with EdU for 10 hours. The SMW (double arrowhead) and CP (asterisk) are visible. (L,M') Magnification of apical section of CP displays (L) Cut expressing cone cells (blue) that are EdU+. (M,M') Magnification of basal section of CP displays Cut-expressing bristle groups (red dashed circles; Cut, blue; neurons express ELAV (green)) and pigment cells (blue dotted circles; Cut/ELAV-) that are EdU+ (pink). ELAV expressing photoreceptors (Cut-) are EdU- (arrowheads). (N,N') *GMR-hid, Gal80^{TS}, GMR>p35* retina at ~8hrs APF derived from 3rd instar larvae fed with EdU for 10 hours. ELAV expressing photoreceptors (green) are not labeled with EdU (N, pink; N', grey). Scale bars = 20μM.

of G2-arrested cells is not greatly disrupted by *hid* expression (Fig. 5B,B') and *stg* expression in a *GMR-hid* background does not disrupt CP (Fig. 5C,C'). These data suggest that cells undergoing CP are not the same population of G2-arrested cells that we describe above. Since inhibition of CP exacerbates the rough eye phenotype caused by *GMR-hid* (Meserve and Duronio, 2015), cells resulting from CP likely contribute to the adult eye.

Based on the location of the CP wave within the disc, cell cycle re-entry during CP occurs after photoreceptors have differentiated (Fan and Bergmann, 2008), suggesting that cells resulting from CP contribute to non-neuronal cell types of the adult eye. To determine whether cells resulting from CP are lineage restricted or are competent to become any retinal cell type, we performed lineage tracing experiments. Our strategy was to feed third instar larvae EdU in order to label cells in S phase as they undergo CP, followed by detection of EdU-positive cells in pupal retinas at a stage when cell differentiation is complete. First, we developed an EdU-labeling protocol in which third instar wild type larvae are fed EdU for 10 hours followed by dissecting pupal retinas at 24hrs APF. Using this protocol we found EdU+ cells in the anterior portion of the retina and within the SMW (Fig. 5G-J'). All accessory cells (e.g. cone and pigment cells) derived from the SMW were labeled with EdU (Fig. 5H,J,J'). In contrast, only photoreceptors derived from the SMW were EdU+ (i.e. R1, R7, and R6), while photoreceptors that began

to differentiate within the MF and never entered S phase of the SMW were EdU- (i.e. R8, R5, R4, R3, and R2) (Fig. 5I-I").

We next applied this EdU-labeling strategy to *GMR-hid* discs to determine the retinal cell types resulting from CP. Because *GMR-hid* adult eyes are drastically reduced in size as a result of continued apoptosis during pupal development (Grether et al., 1995), we attenuated Hid activity by expressing *UAS-p35* under control of *GMR-Gal4*. Expression of p35 alone inhibits both apoptosis and CP (Fan and Bergmann, 2008); therefore, we attempted to modulate the amount of p35 expression using *UAS-Gal80^{TS}* (an inhibitor of Gal4) such that CP was not affected. At 25^{0}C, apoptosis and CP are present in the posterior eye disc of *GMR-hid, Gal80^{TS}, GMR>p35* larvae (Fig. 5D-E), and the resulting adult eyes are rough but relatively normal in size (Fig. 5F). Under these conditions, EdU feeding of *GMR-hid, GMR>p35, tub-Gal80^{TS}* larvae resulted in robust labeling of retinal cells derived from the SMW as well as CP at 24hrs APF (Fig. 5K). Within the population of cells derived from CP, we observe EdU+ cone cells (Fig. 5L), bristle group cells, and pigment cells (Fig. 5M,M'). At 24hrs APF, many photoreceptors are missing due to the continual expression of *hid*, but those present are all EdU- (Fig. 5M,M'). To determine whether CP cells differentiate into photoreceptors that are subsequently eliminated before 24hrs APF, we assayed earlier time points of retinal development. At ~8hrs APF, the majority of photoreceptors are still present, but we did not detect any EdU+ photoreceptors in cells resulting from CP (Fig. 5N,N'). These data suggest that cells resulting from CP do not differentiate into photoreceptors but can differentiate into any accessory cell type.

DISCUSSION

The complex interactions between cell cycle control and differentiation programs are still not fully understood, particularly when considering *in vivo* systems. Here, we report results characterizing differentiation of two populations of cells with different cell cycle properties in the developing *Drosophila* retina.

G2 arrest refines SOP selection

Although G1 arrest often precedes terminal differentiation during development, arrest in G2 phase allows cells to "pause" without committing to a specific lineage. In some cases, this "pause" preceding mitosis is required for normal cell movement during morphogenesis. For example, cells in the *Drosophila* embryo temporarily arrest in G2 during mesoderm invagination, and precocious entry into mitosis disrupts their movements (Edgar and O'Farrell, 1989; Grosshans and Wieschaus, 2000; Mata et al., 2000; Seher and Leptin, 2000). Similarly, horizontal cell progenitors arrest in G2 as they migrate through the developing chick retina (Boije et al., 2009). G2 arrest may also synchronize cell division with developmental signals to properly coordinate cell cycle exit and differentiation. Our data show that during bristle development in the *Drosophila* retina, a subset of cells from the SMW arrest in G2 and become selected as SOPs during pupation. While precocious entry of G2-arrested cells into mitosis does not eliminate bristles in the eye, it does disrupt their organization. These results are similar to previous results in the developing *Drosophila* wing, where a subset of cells in the larval wing disc arrest in G2 and are subsequently selected as SOPs, which undergo divisions during pupal development and become bristles of the adult wing (Phillips and Whittle, 1993; Johnston and Edgar, 1998). Ectopic expression of Stg in the developing wing causes G2-arrested

SOPs to prematurely enter mitosis, resulting in adult flies with bristles that are reduced in number, disorganized, and shorter than in wildtype (Nègre et al., 2003). Similar phenotypes occur in bristles of the thorax when progenitors precociously undergo mitosis (Ayeni et al., 2016). These results suggest arrest in G2 is not absolutely required for bristle development but likely helps refine the differentiation program.

What regulates G2 arrest during development? A major regulator of the G2/M transition in *Drosophila* is Stg. The *stg* locus has a very large a0nd complex collection of *cis*-regulatory modules that are acted upon by many transcription factors (Lehman et al., 1999; Lopes and Casares, 2015), and the Stg protein is relatively unstable (Edgar and Datar, 1996; Bernardi et al., 2000). Thus, during *Drosophila* development, transcriptional regulation of *stg* typically determines whether cells arrest in G2, and when they subsequently enter mitosis. For instance, G2 arrest in presumptive SOPs of the wing depends on expression of the transcription factors Ac and Sc, which is controlled by Wg signaling (Johnston and Edgar, 1998). In the eye disc, Ac is not expressed at the time in which cells arrest in G2 ((Garcia-Alonso et al., 1995) and data not shown), and Wg signaling inhibits bristle development (Cadigan et al., 2002). Instead, Baker and Yu (2001) showed that the EGF receptor signaling is required for G2→M progression following the SMW. EGF signaling depends on differentiation of the photoreceptor preclusters, which are thought to secrete the EGF ligand Spitz. Cells that receive Spitz upregulate Stg, allowing entry into mitosis. As Spitz is a short range signal, the authors hypothesized that cells not directly in contact with preclusters do not receive a signal to transcribe *stg* and subsequently remain arrested in G2. This hypothesis is supported by the observation that roughly 1-2 cells per ommatidium do not contact the precluster, which is similar to the number of cells arrested in G2 (Baker and Yu, 2001). This spatially

constrained mechanism may ensure the proper number of cells at the appropriate positions arrest in G2. Our data support this hypothesis as inhibition of EGF signaling results in increased numbers of G2 cells in *GMR>FUCCI* eye discs and G2 cells in the posterior of eye discs lack *stg* mRNA (data not shown). Other mechanisms likely also contribute to G2 arrest. For example, mutations in *roughex*, a Cyclin/CDK inhibitor, result in inappropriate mitoses within the posterior eye disc, including in photoreceptors (Ruggiero et al., 2012). The Cyclin/CDK inhibitor Dacapo is also required for proper cell cycle arrest following the SMW; *dacapo* mutants in a *GMR>p35* background have drastically increased numbers of interommatidial bristles (Sukhanova and Du, 2008). These processes likely coordinate to arrest the majority of cells in G1 following the SMW, while allowing a subset to arrest in G2 and subsequently proliferate during pupation.

How does G2 arrest inform the developmental program of sensory organs? We hypothesize G2 arrest may provide a cell an advantage in being selected as an SOP. A recent model proposed by Troost et al (2015) suggests SOP selection in the developing notum depends on differential expression of Extramacrochaetae (Emc) throughout the tissue. Emc inhibits Ac and Sc, such that cells with lower levels of Emc are more likely to be selected as SOPs. Notch activity further refines SOP selection. However, Emc levels and Notch signaling alone cannot explain how an SOP is selected, and the authors suggest an unknown, "pre-selecting mechanism" drives SOP selection. Our results suggest that G2 arrest may drive this pre-selection, ensuring properly selected SOPs, as abolishing G2 arrest results in improperly selected SOPs, which we infer from misplaced bristles. G2 arrest may affect this selection directly, through interaction of cell cycle machinery with proneural gene pathways, or indirectly, due to lack of EGF signaling. In this model, Emc levels and Notch signaling may be sufficient for SOP selection in a field of cells in which

no cells are arrested in G2 (as in the *GMR>stg* retinas), although final bristle placement will not be precise. Further research is required to investigate this model and what factors may predispose G2-arrested cells to adopt an SOP fate.

G2 arrest likely also ensures the proper number of cell divisions of the SOP lineage. In both the thorax (Ayeni et al., 2016) and the eye (Fig. 4G), driving G2-arrested cells precociously through mitosis results in premature pupal divisions. Additionally, SOPs in the thorax that prematurely enter mitosis also undergo more divisions than in wildtype (Ayeni et al., 2016). G2 arrest may ensure that SOP selection and mitotic entry are coordinated. To induce cell cycle re-entry in *Drosophila*, Stg and Cyclin E are upregulated by developmental signals to control the G2/M and G1/S transitions, respectively (Swanhart et al., 2005). SOPs in the notum transition rapidly from mitosis into S phase without an intervening G1 phase due to high levels of accumulated Cyclin E (Audibert et al., 2005). In the absence of G2 arrest, high levels of Cyclin E may drive selected SOPs prematurely into S phase, as in our *GMR>stg* experiments. G2-arrested cells may be induced to enter mitosis at a specific point in development by coupling Stg expression with levels of the hormone ecdysone. In abdominal histoblasts, a pulse of ecdysone during pupation induces *stg* transcription and subsequent entry into mitosis (Ninov et al, 2009). Therefore, developmental signals like ecdysone likely trigger upregulation of Cyclin E and Stg in SOPs.

Compensatory proliferating cells differentiate into retinal accessory cells

Our data suggest cell cycle position can influence cell cycle fate. Could G1-arrested cells that are competent to re-enter the cell cycle following tissue damage be lineage restricted? A critical aspect of repairing tissue damage is the replacement of cells that have

died via compensatory proliferation, which restores a normal number of cells that differentiate into the proper cell types. In damaged tissues, cell cycle re-entry of quiescent precursor cells can promote regeneration (Heber-Katz et al., 2013). In the developing *Drosophila* larval eye disc, this is precisely what happens following genetically induced tissue damage using *GMR-hid* (Meserve and Duronio, 2015). However, although both photoreceptors and accessory cells undergo apoptosis in *GMR-hid* discs (Fan and Bergmann, 2014), we found that compensatory proliferating cells contribute only to accessory cells lineages and not photoreceptors. What might explain this result? Photoreceptor differentiation occurs in a stereotyped and stepwise manner beginning with R8, which is required for further photoreceptor recruitment (Kumar, 2012), and by the point in development when CP occurs, photoreceptor development has already been completed. In contrast, accessory cell differentiation has yet to occur. Although R8 photoreceptors are resistant to Hid induced apoptosis (Fan and Bergmann, 2014), they are likely not reactivated to drive photoreceptor differentiation following damage. Therefore, compensatory proliferating cells contribute to an undifferentiated cell population that can subsequently differentiate into each type of retinal accessory cell. These results stress that without re-activation of developmental programs driving differentiation, cells in a regenerating tissues will not be faithfully replaced.

MATERIALS AND METHODS

Drosophila culture conditions and stocks

All experiments were carried out at 25^0 C, except heat shocks, which were carried out at 37^0 C. For experiments with staged pupae, white prepupae were marked (counted as 0hr APF) and aged for the appropriate number of hours. Due to the length of the white

prepupal stage (Bainbridge and Bownes, 1981), pupal ages listed may be +20 minutes. Stocks used are as follows (Bloomington Stock numbers are listed where applicable): ***w^{1118}***, ***GMR-Gal4*** [*w*;P{GAL4-ninaE.GMR}12*] #1104 , ***UAS-E2f^{FUCCI}/ UAS-CycB^{FUCCI}*** [*w^{1118};P{UASp-GFP.E2f1.1-230}64, P{UASp-mRFP1.NLS.CycB.1-266}5*] #55111, ***GMR-p21*** [*y^{1} w^{1118}; P{GMR-p21.Ex}3*] #8414, ***UAS-stg*** [*w^{1118}; P{UAS-stg.N}4*] #4778, ***CycB-GFP*** [*y^{1} w*; P{PTT-GC}CycB^{CC01846}*] #51568, ***hs-stg***, (Edgar and O'Farrell, 1990), ***UAS-p35*** [*w*; P{UAS-p35.H}BH2*] #5073, ***hs-Flp, FRT19A Ubi-mRFP.nls*** [*P{Ubi-mRFP.nls}1, w*, P{hsFLP}12 P{neoFRT}19A*] #31418**,** ***FRT19A His2Av-GFP*** [*y^{1} w* P{His2Av$^{T:Avic\GFP-S65T}$}1 P{hsFLP}12 P{neoFRT}19A/FM7a*] #32045, ***UAS-p21*** (I. Hariharan), ***GMR-hid*** [*P{GMR-hid}G1*] #5771, ***tub-Gal80^{TS}*** [*w*; P{tubP-GAL80ts}7/TM6B*] #7018.. Genotypes listed in figures as *GMR-p21*, *GMR>p21*, or *GMR>stg* (except Fig. 1H) also have *UAS-FUCCI*. Transgenic genotypes described in all experiments are heterozygous, with the exception of *GMR>FUCCI* alone (as in Fig. 1E) and *CycB-GFP* alone (as in Fig. S1A).

EdU feeding experiments

For EdU-containing food, 0.6 g of crushed Carolina Formula 4-24 Instant Drosophila Medium was placed in a narrow culture vial and mixed with 3.4 mL of 0.2mM EdU (5-Ethynyl-2′-deoxyuridine, Santa Cruz) and 25 mg/mL amaranth (Sigma) in H_2O. Early third instar larvae were placed on EdU-containing media for 10 hours. Larvae that had eaten food (confirmed by presence of amaranth dye in the gut) were transferred to unlabeled food and cultured until they were selected for dissection.

Immunostaining

Immunostaining of larval and pupal retinas was performed using standard protocols (Klein, 2008). CC3 staining and EdU staining were performed as previously described (Meserve and Duronio, 2015). Primary antibodies: 1/1000 rabbit α-PH3 (Millipore 06-570), 1/50 mouse α-CycB (Developmental Studies Hybridoma Bank (DSHB) F2F4), 1/1000 mouse α-GFP (Abcam ab1218), 1/1000 rabbit α-RFP (Clontech 632496), 1/500 mouse α-Yan (DSHB 8B12H9), 1/100 rat α-ELAV (DSHB 9F8A9), 1/100 mouse α-Cut (DSHB 2B10), 1/200 guinea pig α-Sens (H. Bellen), 1/50 mouse α-Ac (DSHB anti-achaete), 1/1000 rabbit α-Dlg (DSHB 4F3), 1/100 rabbit α-CC3 (Cell Signaling 9661). Secondary antibodies (all 1/1000): Oregon Green 488-conjugated goat α-mouse (Invitrogen O6380), Cy3-conjugated goat α-mouse (Jackson ImmunoResearch 115-165-003), Cy5-conjugated goat α-mouse (Jackson ImmunoResearch 115-175-146), Alexa 488-conjugated goat anti-rabbit (Jackson ImmunoResearch 111-545-144), Rhodamine Red-conjugated goat α-rabbit (ThermoFisher Scientific R6394), Cy5-conjugated goat α-rabbit (Abcam ab6564), Cy2-conjugated goat α-rat (Jackson ImmunoResearch 112-225-143), Cy3-conjugated goat α-rat (Jackson ImmunoResearch 112-165-143), Cy5-conjugated goat anti-rat (Jackson ImmunoResearch 712-175-153), Cy5-conjugated donkey α-guinea pig (Jackson ImmunoResearch 706-175-148).

Flow cytometry

Eye discs were prepared for flow analysis as previously described (de la Cruz and Edgar, 2008). Briefly, eye discs from 15-20 larvae were dissected in Grace's media, rinsed with 1x PBS, and dissociated in a trypsin/Hoescht solution for ~3 hrs. GFP expression and

DNA content (Hoescht) were measured using a Becton Dickinson LSR II flow cytometer. Histograms were made using FlowJo software.

SUPPLEMENTARY FIGURES

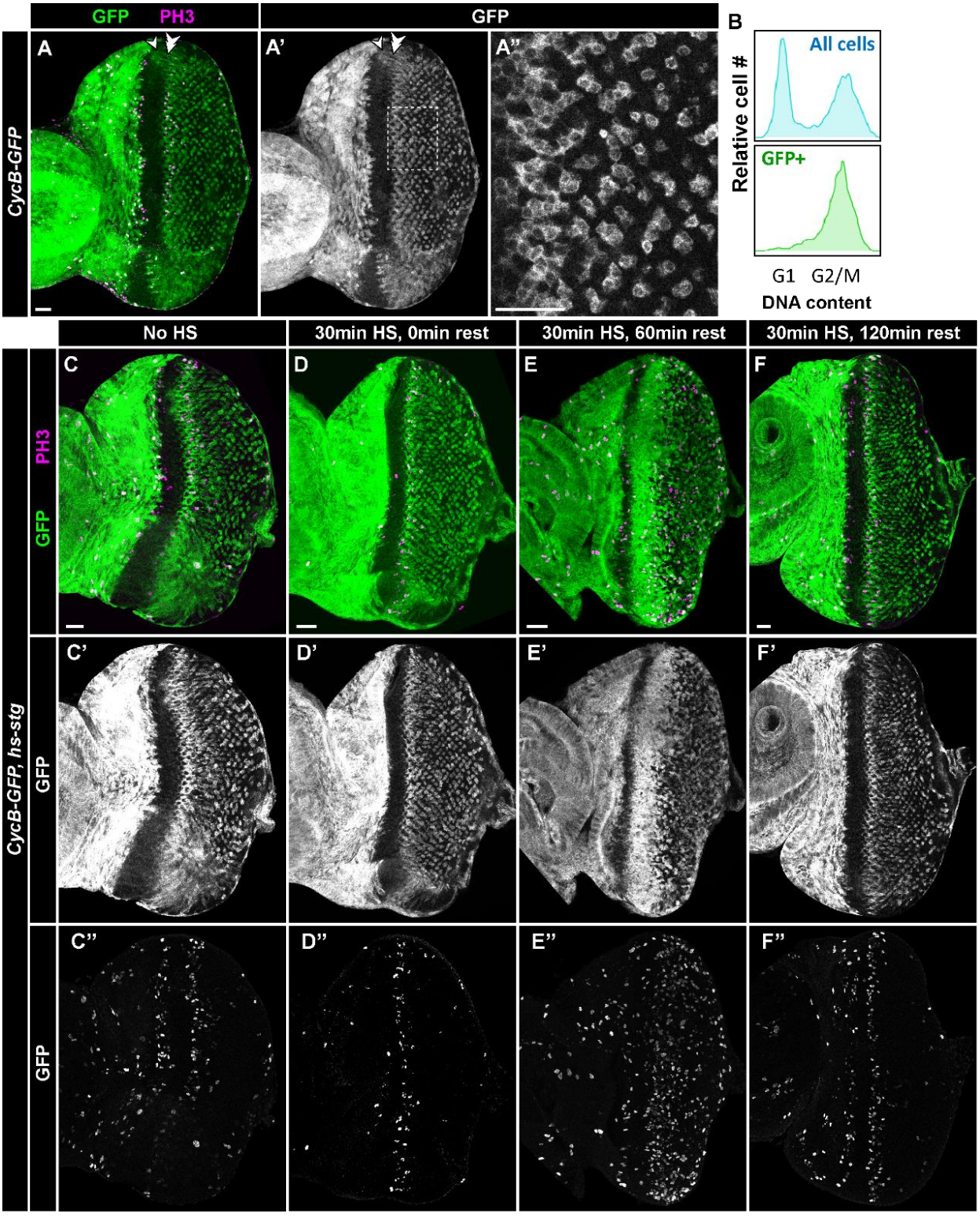

Fig. S1. Cell expressing CycB-GFP are arrested in G2 and undergo mitosis following Stg expression.
(A-A") CycB-GFP (A, green; A',A", grey) expression in a larval eye disc from a protein trap transgene inserted into the *Cyc B* locus. Dotted box indicates magnification in A".
(B) Flow cytometry histogram of relative cell number versus DNA content for dissociated *CycB-GFP* eye discs. Cell cycle phase peaks (G1 and G2/M) are based on measurements from all cells (top panel, blue). Cells expressing GFP have G2 DNA content.
(C-F") *CycB-GFP, hsp70-stg* eye discs fixed and stained with anti-PH3 (C-F, magenta; C"-F", grey) at 0, 30, and 60 min following a 30-min 37^{0}C heat shock. (E-E") 60 min after heat shock, cells expressing GFP (E, green; E', grey) enter mitosis.
Scale bars = 20μM.

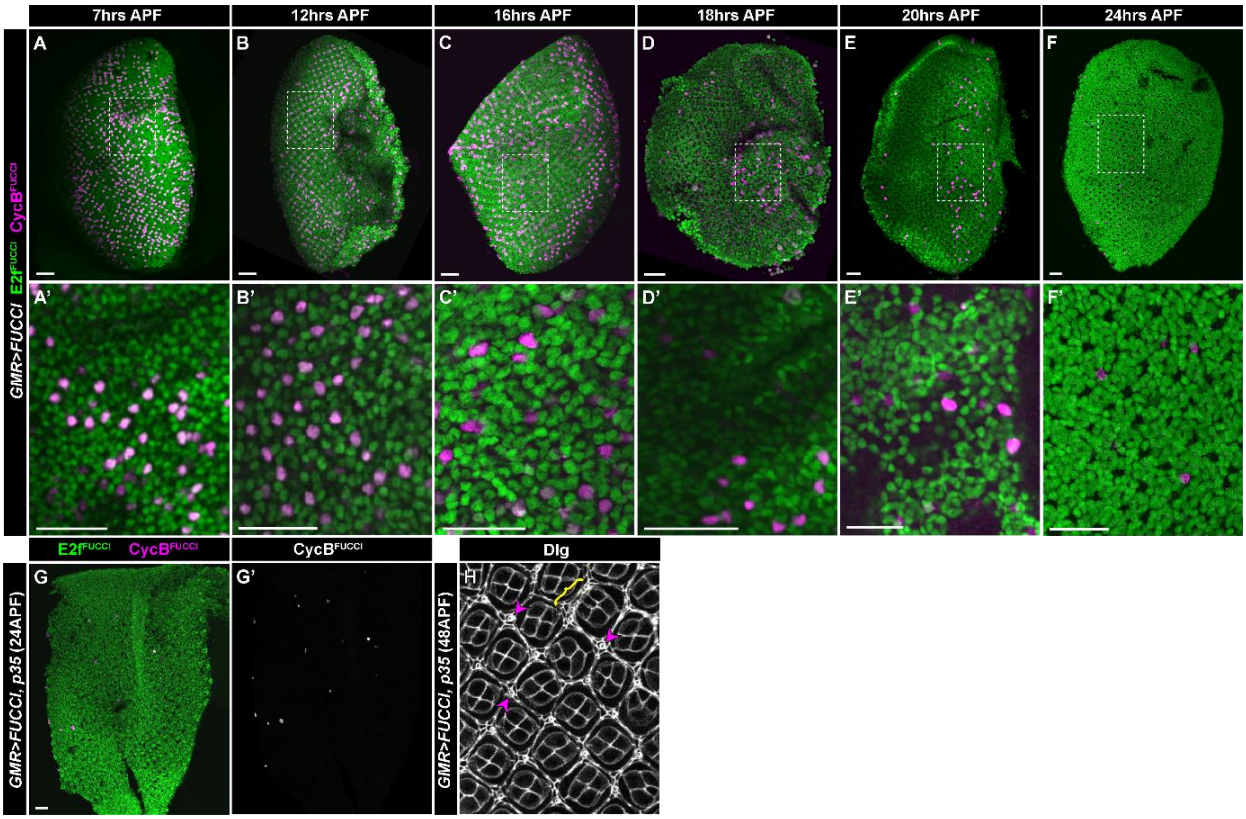

Fig. S2. G2-arrested cells do not undergo apoptosis during the first 24 hours of pupal development.

(A-F') *GMR>FUCCI* retinas expressing E2f^{FUCCI} (green) and CycB^{FUCCI} (magenta) analyzed at the indicated times after pupal formation (APF). Dotted boxes indicate areas of magnification in A'-F'. By 24hrs APF, very few CycB^{FUCCI} expressing G2 cells are present.

(G,G') *GMR>FUCCI, p35* retina at 24hrs APF expressing E2f^{FUCCI} (green) and CycB^{FUCCI} (G, magenta; G', grey).

(H) *GMR>FUCCI, p35* retina at 48hrs APF stained with antibodies recognizing Dlg, a cell membrane marker. Purple arrows indicate bristles and yellow bracket indicates excess accessory cells in the pupal retina (compare to Fig. 4A,B for control).

Scale bars = 20μM.

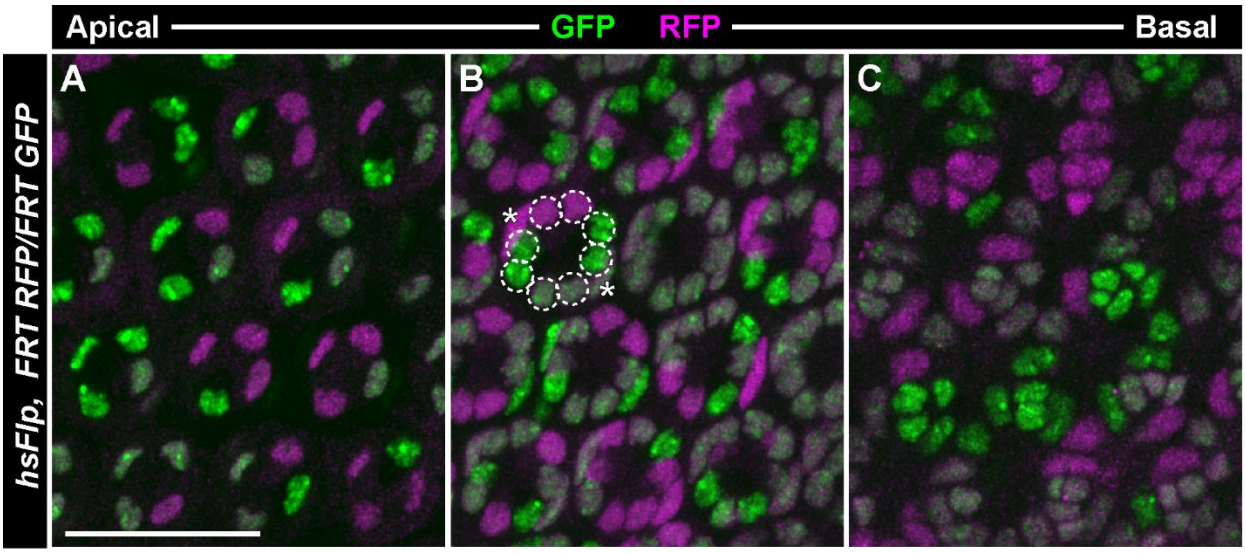

Fig. S3: Pre-MF clones are not bristle restricted
(A-C) *hs-Flp, FRT19A Ubi-mRFP.nls/FRT19A His2Av-GFP* retina at 24 hrs APF in which mitotic recombination was induced at the 3rd instar larval stage to produce GFP expressing (green) and RFP expressing (magenta) clones in the anterior. Clones induced before the MF progresses develop into all retinal lineages: (A) apical cone cells, (B) photoreceptors (circles) and primary pigment cells (asterisks), and (C) basal bristle groups and secondary/tertiary pigment cells.
Scale bar = 20μM.

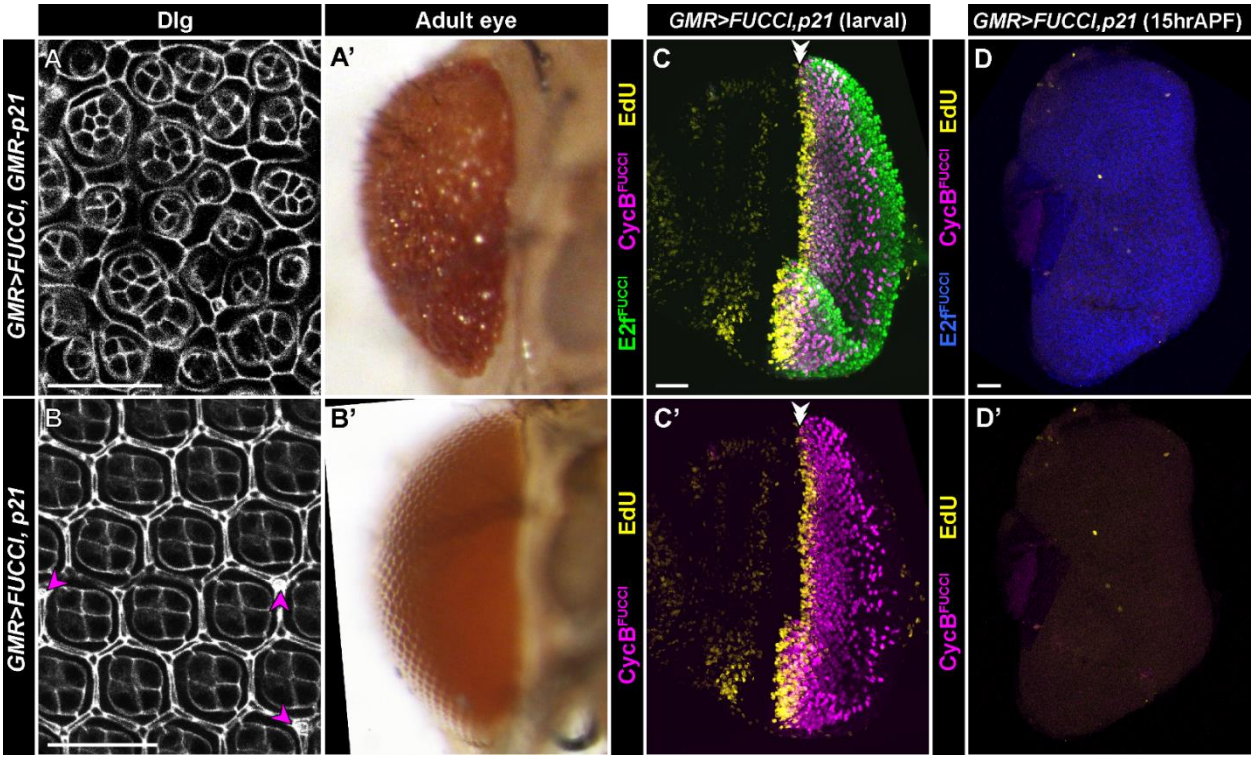

Figure S4: p21 expression blocks SOP divisions and bristle development.
(A,A') *GMR>FUCCI, GMR-p21* retinas, which develop from eye discs that lack the SMW. (A) Retina at 48hrs APF stained with antibodies recognizing Dlg, a cell membrane marker (control Fig. 4A,B). Bristles are not easily identified in the grossly disorganized pupal retina and are mostly lacking in the adult eye (A').
(B,B') *GMR>FUCCI, p21* retinas, which develop from eye discs with a normal SMW (see panel C). Bristles are largely but not entirely (purple arrows) absent in the (B) pupal retina and (B') adult eye.
(C,C') *GMR>FUCCI, p21* larval eye disc labeled with EdU (yellow) and expressing CycB^{FUCCI} (magenta) and E2f^{FUCCI} (green) (compare to control Fig. 1D). The double arrowhead indicates the SMW.
(D,D') *GMR>FUCCI, p21* retina at 15hrs APF expressing CycB^{FUCCI} (magenta) and E2f^{FUCCI} (blue) and labeled with EdU (yellow). Note the lack of cells in S-phase (yellow) or G2 (magenta).
Scale bars = 20μM.

REFERENCES

Anatskaya, O. V., Vinogradov, A. E. and Kudryavtsev, B. N. (1994). Hepatocyte polyploidy and metabolism/life-history traits: hypotheses testing. J. Theor. Biol. 168, 191-199.

Audibert, A., Simon, F. and Gho, M. (2005). Cell cycle diversity involves differential regulation of Cyclin E activity in the Drosophila bristle cell lineage. Development 132, 2287-2297.

Ayeni, J. O., Audibert, A., Fichelson, P., Srayko, M., Gho, M. and Campbell, S. D. (2016). G2 phase arrest prevents bristle progenitor self-renewal and synchronizes cell division with cell fate differentiation. Development 143, 1160-1169.

Bainbridge, S. P. and Bownes, M. (1981). Staging the metamorphosis of Drosophila melanogaster.. J Embryol. Exp. Morphol. 66, 57-80.

Baker, N. E. and Yu, S. Y. (2001). The EGF receptor defines domains of cell cycle progression and survival to regulate cell number in the developing Drosophila eye. Cell 104, 699-708.

Bellaïche, Y., Gho, M., Kaltschmidt, J. A., Brand, A. H. and Schweisguth, F. (2001). Frizzled regulates localization of cell-fate determinants and mitotic spindle rotation during asymmetric cell division. Nat. Cell Biol. 3, 50-57.

Bernardi, R., Liebermann, D. A. and Hoffman, B. (2000). Cdc25A stability is controlled by the ubiquitin-proteasome pathway during cell cycle progression and terminal differentiation. Oncogene 19, 2447-2454.

Boije, H., Edqvist, P. H. and Hallbook, F. (2009). Horizontal cell progenitors arrest in G2-phase and undergo terminal mitosis on the vitreal side of the chick retina. Dev. Biol. 330, 105-113.

Buszczak, M., Paterno, S., Lighthouse, D., Bachman, J., Planck, J., Owen, S., Skora, A. D., Nystul, T. G., Ohlstein, B., Allen, A. et al. (2007). The carnegie protein trap library: a versatile tool for Drosophila developmental studies. Genetics 175, 1505-1531.

Buttitta, L. A., Katzaroff, A. J., Perez, C. L., de la Cruz, A. and Edgar, B. A. (2007). A double-assurance mechanism controls cell cycle exit upon terminal differentiation in Drosophila. Dev. Cell 12, 631-643.

Cadigan, K. M., Jou, A. D. and Nusse, R. (2002). Wingless blocks bristle formation and morphogenetic furrow progression in the eye through repression of Daughterless. Development 129, 3393-3402.

Cagan, R. L. and Ready, D. F. (1989). The emergence of order in the Drosophila pupal retina. Dev. Biol. 136, 346-362.

de la Cruz, A. F. and Edgar, B. A. (2008). Flow cytometric analysis of Drosophila cells. Methods Mol. Biol. 420, 373-389.

de Nooij, J. C. and Hariharan, I. K. (1995). Uncoupling cell fate determination from patterned cell-division in the Drosophila eye. Science 270, 983-985.

Di Giorgio, E., Gagliostro, E., Clocchiatti, A. and Brancolini, C. (2015). The control operated by the cell cycle machinery on MEF2 stability contributes to the downregulation of CDKN1A and entry into S phase. Mol. Cell Biol. 35, 1633-1647.

Edgar, B. A. and Datar, S. A. (1996). Zygotic degradation of two maternal Cdc25 mRNAs terminates Drosophilas early cell cycle program. Genes Dev. 10, 1966-1977.

Edgar, B. A. and OFarrell, P. H. (1989). Genetic control of cell division patterns in the Drosophila embryo. Cell 57, 177-187.

Edgar, B. A. and OFarrell, P. H. (1990). The three postblastoderm cell cycles of Drosophila embryogenesis are regulated in G2 by string. Cell 62, 469-480.

Fan, Y. and Bergmann, A. (2008). Distinct mechanisms of apoptosis-induced compensatory proliferation in proliferating and differentiating tissues in the Drosophila eye. Dev. Cell 14, 399-410.

Fan, Y. and Bergmann, A. (2014). Multiple mechanisms modulate distinct cellular susceptibilities toward apoptosis in the developing Drosophila eye. Dev. Cell 30, 48-60.

Frankfort, B. J., Pepple, K. L., Mamlouk, M., Rose, M. F. and Mardon, G. (2004). Senseless is required for pupal retinal development in Drosophila. Genesis 38, 182-194.

Garcia-Alonso, L., VanBerkum, M. F., Grenningloh, G., Schuster, C. and Goodman, C. S. (1995). Fasciclin II controls proneural gene expression in Drosophila. Proc. Natl. Acad. Sci. U. S. A. 92, 10501-10505.

Gentric, G., Celton-Morizur, S. and Desdouets, C. (2012). Polyploidy and liver proliferation. Clin. Res. Hepatol. Gastroenterol. 36, 29-34.

Grether, M. E., Abrams, J. M., Agapite, J., White, K. and Steller, H. (1995). The head involution defective gene of Drosophila melanogaster functions in programmed cell death. Genes Dev. 9, 1694-1708.

Grosshans, J. and Wieschaus, E. (2000). A genetic link between morphogenesis and cell division during formation of the ventral furrow in Drosophila. Cell, 523-531.

Hay, B. A., Wolff, T. and Rubin, G. M. (1994). Expression of baculovirus P35 prevents cell death in Drosophila. Development 120, 2121-2129.

Heber-Katz, E., Zhang, Y., Bedelbaeva, K., Song, F., Chen, X. and Stocum, D. L. (2013). Cell cycle regulation and regeneration. Curr. Top. Microbiol. Immunol. 367, 253-276.

Johnston, L. A. and Edgar, B. A. (1998). Wingless and Notch regulate cell-cycle arrest in the developing Drosophila wing. Nature 394, 82-84.

Klein, T. (2008). Immunolabeling of imaginal discs. Methods Mol. Biol. 420, 253-263.

Korzelius, J., The, I., Ruijtenberg, S., Prinsen, M. B., Portegijs, V., Middelkoop, T. C., Groot Koerkamp, M. J., Holstege, F. C., Boxem, M. and van den Heuvel, S. (2011). Caenorhabditis elegans cyclin D/CDK4 and cyclin E/CDK2 induce distinct cell cycle re-entry programs in differentiated muscle cells. PLoS Genet. 7, e1002362.

Kumar, J. P. (2012). Building an ommatidium one cell at a time. Dev. Dyn. 241, 136-149.

Lehman, D. A., Patterson, B., Johnston, L. A., Balzer, T., Britton, J. S., Saint, R. and Edgar, B. A. (1999). Cis-regulatory elements of the mitotic regulator, string/Cdc25. Development 126, 1793-1803.

Lopes, C. S. and Casares, F. (2015). Eye selector logic for a coordinated cell cycle exit. PLoS Genet. 11, e1004981.

Ma, Y., Kanakousaki, K. and Buttitta, L. (2015). How the cell cycle impacts chromatin architecture and influences cell fate. Front. Genet. 6, 19.

Mata, J., Curado, S., Ephrussi, A. and Rorth, P. (2000). Tribbles coordinates mitosis and morphogenesis in Drosophila by regulating string/CDC25 proteolysis. Cell 101, 511-522.

Meserve, J. H. and Duronio, R. J. (2015). Scalloped and Yorkie are required for cell cycle re-entry of quiescent cells after tissue damage. Development 142, 2740-2751.

Nègre, Nicolas, Ghysen, Alain and Martinez, Anne-Marie (2003). Mitotic G2-arrest is required for neural cell fate determination in Drosophila. Mech. Dev. 120, 253-265.

Paridaen, J. T. and Huttner, W. B. (2014). Neurogenesis during development of the vertebrate central nervous system. EMBO Rep. 15, 351-364.

Pauklin, S. and Vallier, L. (2013). The cell-cycle state of stem cells determines cell fate propensity. Cell 155, 135-147.

Phillips, R. G. and Whittle, J. R. (1993). wingless expression mediates determination of peripheral nervous system elements in late stages of Drosophila wing disc development. Development 118, 427-438.

Ready, D. F., Hanson, T. E. and Benzer, S. (1976). Development of the Drosophila retina, a neurocrystalline lattice. Dev. Biol. 53, 217-240.

Reiner, J. M. (1983). Differentiation, ageing, and terminal differentiation: a semantic analysis. J. Theor. Biol. 105, 545-552.

Remaud, S., Audibert, A. and Gho, M. (2008). S-phase favours notch cell responsiveness in the Drosophila bristle lineage. PLoS One 3, e3646.

Ruggiero, R., Kale, A., Thomas, B. and Baker, N. E. (2012). Mitosis in neurons: Roughex and APC/C maintain cell cycle exit to prevent cytokinetic and axonal defects in Drosophila photoreceptor neurons. PLoS Genet. 8, e1003049.

Ruijtenberg, S. and van den Heuvel, S. (2016). Coordinating cell proliferation and differentiation: Antagonism between cell cycle regulators and cell type-specific gene expression. Cell Cycle 15, 196-212.

Seher, T. C. and Leptin, M (2000). Tribbles, a cell-cycle brake that coordinates proliferation and morphogenesis during Drosophila gastrulation. Curr. Biol. 10, 623-629.

Sousa-Nunes, R. and Somers, W. G. (2013). Mechanisms of asymmetric progenitor divisions in the Drosophila central nervous system. Adv. Exp. Med. Biol. 786, 79-102.

Sukhanova, M. J. and Du, W. (2008). Control of cell cycle entry and exiting from the second mitotic wave in the Drosophila developing eye, BMC Dev Biol 8: 7.

Swanhart, L., Kupsco, J. and Duronio, R. J. (2005). Developmental control of growth and cell cycle progression in Drosophila. Methods Mol. Biol. 296, 69-94.

Thomas, D. M., Carty, S. A., Piscopo, D. M., Lee, J. S., Wang, W. F., Forrester, W. C. and Hinds, P. W. (2001). The retinoblastoma protein acts as a transcriptional coactivator required for osteogenic differentiation. Mol. Cell 8, 303-316.

Tintignac, L. A., Leibovitch, M. P., Kitzmann, M., Fernandez, A., Ducommun, B., Meijer, L. and Leibovitch, S. A. (2000). Cyclin E-cdk2 phosphorylation promotes late G1-phase degradation of MyoD in muscle cells. Exp. Cell Res. 259, 300-307.

Wolff, T. and Ready, D. F. (1991). The beginning of pattern formation in the Drosophila compound eye: the morphogenetic furrow and the second mitotic wave. Development 113, 841-850.

Xu, T. and Rubin, G. M. (1993). Analysis of genetic mosaics in developing and adult Drosophila tissues. Development 117, 1223-1237.

Zielke, N., Korzelius, J., van Straaten, M., Bender, K., Schuhknecht, G. F., Dutta, D., Xiang, J. and Edgar, B. A. (2014). Fly-FUCCI: A versatile tool for studying cell proliferation in complex tissues. Cell Rep. 7, 588-598.

CHAPTER 4: DISCUSSION

The results from my studies have contributed to our understanding cell cycle regulation during development and how this regulation may influence cell fate. These experiments have been performed using the developing *Drosophila* retina, where cell cycle regulation and differentiation are tightly controlled and contribute to precise patterning of the adult eye. While a great deal of research has investigated cell cycle regulation in the eye, there remains a number of open questions. The questions I have focused on are: 1) what induces quiescent cells to re-enter the cell cycle in response to damage, and does this affect the fate of these cells, and 2) does a G2-arrested cell population contribute to a specific retinal lineage, and is G2 arrest required for eye development? I first investigated cell cycle re-entry following tissue damage in the eye. I found that apoptotic cells induce tension-dependent activation of the transcription factor Sd and its binding partner Yki, resulting in CycE upregulation and subsequent S phase entry (Chapter 2). These results demonstrate an essential role for apoptotic cells in inducing quiescent cells to re-enter the cell cycle. Interestingly, a recent study in zebrafish demonstrated that fin regeneration also relies on activation of the vertebrate Yki homolog, Yap, in an F-actin-dependent mechanism (Mateus et al., 2015), suggesting this may be a conserved regenerative process. I subsequently discovered that the G1-arrested, undifferentiated cells that are competent to re-enter the cell cycle are not restricted to a specific retinal lineage, though they do not differentiate into photoreceptors (Chapter 3). This suggests undifferentiated cells have an equivalent threshold for cell cycle re-entry at this stage in development, and the photoreceptor differentiation program is not re-activated during CP. Accordingly, in considering therapies to induce regeneration in damaged tissue, one must consider mechanisms to induce both proliferation and differentiation into the

appropriate cell types. Additionally, my work has identified a separate population of undifferentiated cells that are arrested in G2. I demonstrated that these G2-arrested cells are selected as SOPs and become interommatidial bristles (Chapter 3). Additionally, I have shown that G2 arrest is important for appropriate selection of SOPs as disrupting G2 arrest disrupts bristle patterning. This newly defined population of G2-arrested cells will serve as an excellent *in vivo* model to dissect the relationship between cell cycle phase and cell fate. The conservation of cell cycle proteins and developmental pathways across species suggest these findings are likely applicable to organisms in addition to *Drosophila*.

INVESTIGATING ADDITIONAL SCREEN CANDIDATES FOR CP REGULATION

My screen for transcription factors that regulate compensatory proliferation in the eye identified multiple candidates, of which I only characterized one. Other candidates from my screen may be worthy of further investigation, particularly *fork head* (*fkh*) and *knirps* (*kni*), whose RNAi lines displayed complete inhibition of compensatory proliferation, and *lilliputian* (*lilli*), whose RNAi strongly suppressed the small adult eye phenotype in the *GMR-hid* background. Fkh has primarily been studied for its role in salivary gland development in *Drosophila* (Myat and Andrew, 2000), where Fkh blocks hormone-induced transcriptional activation of cell death genes (Lehmann, 2014). Fkh has not been demonstrated to have a role in eye development or in CP in other *Drosophila* tissues. Preliminary results suggest that apoptosis is not disrupted in *GhG, fkh RNAi* eye discs compared with *GMR-hid* eye discs (data not shown), so it is unlikely the lack of CP in this genotype is due to suppression of apoptosis. Additionally, a second *fkh* RNAi line with a different target sequence did not suppress CP in the *GhG* background (data not shown), so it is unclear how robust this phenotype is. There are no predicted off-target sequences for the initial *fkh* RNAi line based on the UP-TORR (Updated Targets of RNAi Reagents) online tool (Hu et al., 2013). Kni has previously been shown to repress expression of S phase genes in the developing embryonic gut (Fuss et al., 2001), which does not explain how inhibition of *kni* would inhibit S

phase entry during CP. Apoptosis is also not noticeably disrupted in *GhG, kni RNAi* eye discs, based on preliminary experiments, so it remains unclear what role *kni* may play in regulating CP. Surprisingly, I do not observe an obvious decrease in apoptosis in *GhG, lilli RNAi* eye discs (not shown) or a clear increase in CP (see Chapter 2, Fig. S4) even though these flies display suppression of the *GMR-hid* adult eye phenotype (see Chapter 2, Fig. 2E). Lilli promotes proneural expression in the developing eye (Distefano et al., 2012), and *lilli* mutant clones in the eye display reduced size of photoreceptors, though cell proliferation does not appear to be disrupted (Distefano et al., 2012). Perhaps inhibition of *lilli* suppresses differentiation in the developing eye, allowing continued compensatory proliferation following *GMR-hid*-induced tissue damage; this hypothesis remains to be tested.

TRANSCRIPTIONAL PROFILE OF COMPENSATORY PROLIFERATING CELLS

As a related question to transcription factors that regulate CP, what are the transcriptional targets of these transcription factors? In addition to unidentified transcription factors that may be activated during CP, the Sd/Yki transcriptional complex and the Hedgehog transcription factor Ci likely activate genes in addition to *CycE* to promote cell cycle re-entry. Previous work investigating anterior versus posterior gene expression in the eye utilized microdissection techniques to separate regions of the disc by essentially cutting at the furrow and comparing expression differences anterior and posterior to the furrow using microarrays (Baig et al., 2010). While this technique is straightforward and would allow comparisons of gene expression between wild type and *GMR-hid* posterior tissues, the majority of cells in the posterior do not undergo CP, and changes specifically within these cells could be drowned out in the analysis. Other techniques allow isolation of RNA from discrete cells populations, either by isolating specific cells, then extracting RNA from these cells, or by uniquely labeling mRNA within these cells such that it can be isolated from whole-disc RNA samples. Specific cells can be isolated from a larger cell population using fluorescence activated cell sorting (FACS). While FACS works well in dissociated

Drosophila imaginal discs, cells must be sorted live and cannot be fixed and stained with antibody preparations (de la Cruz and Edgar, 2008). Instead, a fluorescent transgene that is expressed in a specific cell type is often employed to uniquely mark a cell population. Ideally, there would be a protein that expresses only in cells that undergo compensatory proliferation, but there are no known proteins that fit this description. Another possibility is to isolate cells posterior to the SMW that are undergoing S phase, which will only be compensatory proliferating cells. Although this approach might miss transcriptional changes that occur prior to S phase entry, there will likely still be gene expression changes compared to other cells undergoing S phase. One difficulty in this approach is that there is not a well-defined transgenic line that expresses posterior to the SMW in a robust manner. Even in screening through lines generated by the Janelia FlyLight Project, in which expression patterns of thousands of different enhancer fragments were analyzed (Jenett et al., 2012), none of the 343 lines with posterior MF expression in the eye disc (based on the FlyLight search tool at http://flweb.janelia.org/cgi-bin/flew.cgi) displayed appropriate expression. However, I did generate a line for the gene *dachshund* (*dac*), which was previously shown to have enhancer activity (using a *lacZ* transgene) posterior to the SMW (Pappu et al., 2005). My *dac-GFP* line displays similar expression. *dac-GFP* is first expressed around the same time that CP occurs and consequently may not express in all compensatory proliferating cells; further investigation is required to determine whether *dac-GFP* is an appropriate marker. Isolating cells in S phase from the *dac-GFP* population could be accomplished by sorting based on DNA content, by expression of the S phase marker *PCNA-RFP*, or a combination of these two methods. In the absence of a post-SMW marker, it is still possible to isolate cells in S phase from the posterior of the eye disc, which would likely include SMW S phase cells, by using a combination of a posterior marker (such as *GMR-Gal4* or *yan-Gal4* driving GFP expression in all posterior cells or undifferentiated posterior cells, respectively) and an S phase marker (DNA content and/or *PCNA-RFP*).

Although disc dissociation works relatively well, a significant portion of cells are lost during the cell sorting process. To avoid loss of sample, it is also possible to specifically label mRNA in these cells. mRNA can be specifically marked by incorporation of unique nucleotides; for example, the *Toxoplasma gondii* nucleotide salvage enzyme uracil phosphoribosyltransferase (UPRT), which can be transgenically expressed, will use the synthetic molecule 4-thiouracil as a substrate for production of 4-thiouridine monophosphate, which is incorporated into RNA (Cleary et al., 2005). Thio-RNA can be coupled to biotin and subsequently isolated from a whole RNA population using streptavidin (Miller et al., 2009). 4-thiouracil can be injected into or fed to larvae but will not be incorporated into RNA unless UPRT, which can be expressed with a tissue-specific promoter, is present (Miller et al., 2009). I have attempted using this technique to isolate mRNA from *GMR-Gal4, UAS-UPRT* eye discs. Although I did observe expression of UPRT specifically in the posterior of the eye discs based on in situs, the assay did not generate cleanly labeled samples. This issue was likely due to recently discovered endogenous UPRT activity in *Drosophila* (Ghosh et al., 2015). An alternative approach is to express a tagged version of an mRNA binding protein, such as poly(A)-binding protein (PABP) (Yang et al., 2005) or the ribosomal protein RpL10A (Thomas et al., 2012), so that tagged-protein/mRNA complexes can be purified from a larger population of RNAs. This approach using PABP has been used successfully to isolate mRNA from adult *Drosophila* retinas and therefore may be a viable option for isolation of larval mRNA as well, although *GMR-Gal4* driving PABP was shown to be lethal at later pupal stages (Yang et al., 2005). Ultimately, a protocol that can faithfully isolate RNA from compensatory proliferating cells would be invaluable for providing a transcriptional profile of these cells.

CHARACTERIZING THE TRANSCRIPTIONAL PROFILE OF G2-ARRESTED CELLS

Another open question based on my work is why G2-arrested cells are biased towards becoming SOPs. My results suggest that G2 arrest is not strictly required for SOP development

but is important for patterning SOP selection. G2-arrested cells are likely predisposed in some unknown way to respond to signals inducing SOP commitment. It is unclear whether this predisposition is directly related to cell cycle phase or is a consequence relating to the mechanism, possibly EGF signaling, driving G2 arrest. Transcriptional profiling of G2-arrested cells may offer some insight into activated pathways that could drive SOP selection. The methods described above could be utilized to collect RNA from G2-arrested cells, with the FUCCI system providing an excellent fluorescent marker for cells in G2. Once potential gene expression changes are identified in G2-arrested versus G1-arrested cells, further experiments utilizing RNAi or previously characterized cell cycle/developmental mutants could be performed to further elucidate the path to SOP selection.

IDENTIFYING CHROMATIN DIFFERENCES BETWEEN G2-ARRESTED AND G1-ARRESTED CELLS

In addition to isolating RNA from G2-arrested cells, genomic DNA could be isolated to investigate potential chromatin changes. As described in Chapter 1, chromatin changes are associated with different cell cycle phases and may make a cell more receptive to certain developmental signals. Perhaps arrest in G2 predisposes cells to SOP selection because genes associated with this process are more open in G2 than in G1. Researchers have previously used techniques including ATAC-seq, FAIRE-seq, and DNaseI-seq to identify open chromatin and enhancers in *Drosophila* eye discs (Davie et al., 2015). These methods provide a general view of open chromatin across the genome and can identify whether enhancers in genes controlling SOP selection are differentially open in G2-arrested versus G1-arrested cells.

In addition to assaying open chromatin in G2-arrested cells, specific chromatin marks could be investigated for a role in SOP selection and development. Histone modifications have been demonstrated to play a role regulating proliferation and quiescence. For example, quiescent fibroblasts display increased methylation of histone 4 on lysine 20 (H4K20me) when compared to proliferating fibroblasts (Evertts et al., 2013). As H4K20me is associated with chromatin

compaction and is cell cycle regulated, with newly deposited histones only being methylated at H4K20 during mitosis (Nishioka et al., 2002), cells in G2 may have lower levels of H4K20me and subsequently more open chromatin at SOP loci. Our lab has designed a system for generating histone mutants in *Drosophila*, including H4K20 (McKay et al., 2015), so the potential role of various histone marks can be tested directly in our system. There are also many well characterized mutants for histone modifying enzymes and chromatin associated proteins that could be investigated. I predict that mutations that lead to less compact chromatin in G1-arrested cells or more compact chromatin in G2-arrested cells will disrupt bristle patterning.

CONCLUSION

The relationship between cell cycle progression and differentiation is complex and highly dynamic during development and regeneration. The results presented in this thesis suggest that the developing *Drosophila* retina remains a powerful system to probe cell cycle regulation during development, despite being studied for decades. New techniques designed to track cell cycle progression, such as the FUCCI transgenes, or probe transcriptional and chromatin profiles of small populations of cells have opened the door for researchers to finely dissect biological processes *in vivo*. Furthermore, increasing collaboration within the scientific community and new methods for whole genome sequencing and editing provide researchers an unprecedented opportunity to test predictive hypotheses from genetic models like *Drosophila* in vertebrate and mammalian models. The combination of genetic studies in *Drosophila* and other *in vivo* systems, experiments in cell culture, and genomic data from a variety of systems, including humans, will provide a comprehensive understanding of cell cycle regulation and its role during development, regeneration, and disease.

REFERENCES

Baig, J., Chanut, F., Kornberg, T. B. and Klebes, A. (2010). The chromatin-remodeling protein Osa interacts with CyclinE in Drosophila eye imaginal discs. Genetics 184, 731-744.

Cleary, M. D., Meiering, C. D., Jan, E., Guymon, R. and Boothroyd, J. C. (2005). Biosynthetic labeling of RNA with uracil phosphoribosyltransferase allows cell-specific microarray analysis of mRNA synthesis and decay. Nat. Biotechnol. 23, 232-237.

Davie, K., Jacobs, J., Atkins, M., Potier, D., Christiaens, V., Halder, G. and Aerts, S. (2015). Discovery of transcription factors and regulatory regions driving in vivo tumor development by ATAC-seq and FAIRE-seq open chromatin profiling. PLoS Genet 11, e1004994.

de la Cruz, A. F. and Edgar, B. A. (2008). Flow cytometric analysis of Drosophila cells. Methods Mol. Biol. 420, 373-389.

Distefano, G. M., Gangemi, A. J., Khandelwal, P. J., Saunders, A. J. and Marenda, D. R. (2012). Drosophila lilliputian is required for proneural gene expression in retinal development. Dev. Dyn. 241, 553-562.

Evertts, A. G., Manning, A. L., Wang, X., Dyson, N. J., Garcia, B. A. and Coller, H. A. (2013). H4K20 methylation regulates quiescence and chromatin compaction. Mol. Biol. Cell 24, 3025-3037.

Fuss, B., Meissner, T., Bauer, R., Lehmann, C., Eckardt, F. and Hoch, M. (2001). Control of endoreduplication domains in the Drosophila gut by the knirps and knirps-related genes. Mech. Dev. 100, 15-23.

Ghosh, A. C., Shimell, M., Leof, E. R., Haley, M. J. and O'Connor, M. B. (2015). UPRT, a suicide-gene therapy candidate in higher eukaryotes, is required for Drosophila larval growth and normal adult lifespan. Sci Rep 5, 13176.

Hu, Y., Roesel, C., Flockhart, I., Perkins, L., Perrimon, N. and Mohr, S. E. (2013). UP-TORR: online tool for accurate and Up-to-Date annotation of RNAi Reagents. Genetics 195, 37-45.

Jenett, A., Rubin, G. M., Ngo, T. T., Shepherd, D., Murphy, C., Dionne, H., Pfeiffer, B. D., Cavallaro, A., Hall, D., Jeter, J. et al. (2012). A GAL4-driver line resource for Drosophila neurobiology. Cell Rep 2, 991-1001.

Lehmann, Michael (2014). Roles of the FOXA transcription factor Fork head in autophagic developmental cell death. Autophagy 4, 713-714.

Mateus, R., Lourenco, R., Fang, Y., Brito, G., Farinho, A., Valerio, F. and Jacinto, A. (2015). Control of tissue growth by Yap relies on cell density and F-actin in zebrafish fin regeneration. Development 142, 2752-2763.

McKay, D. J., Klusza, S., Penke, T. J., Meers, M. P., Curry, K. P., McDaniel, S. L., Malek, P. Y., Cooper, S. W., Tatomer, D. C., Lieb, J. D. et al. (2015). Interrogating the function of metazoan histones using engineered gene clusters. Dev. Cell 32, 373-386.

Miller, M. R., Robinson, K. J., Cleary, M. D. and Doe, C. Q. (2009). TU-tagging: cell type-specific RNA isolation from intact complex tissues. Nat. Meth. 6, 439-U457.

Myat, M. M. and Andrew, D. J. (2000). Fork head prevents apoptosis and promotes cell shape change during formation of the Drosophila salivary glands. Development 127, 4217-4226.

Nishioka, K., Rice, J. C., Sarma, K., Erdjument-Bromage, H., Werner, J., Wang, Y., Chuikov, S., Valenzuela, P., Tempst, P., Steward, R. et al. (2002). PR-Set7 Is a Nucleosome-Specific Methyltransferase that Modifies Lysine 20 of Histone H4 and Is Associated with Silent Chromatin. Mol. Cell 9, 1201-1213.

Pappu, K. S., Ostrin, E. J., Middlebrooks, B. W., Sili, B. T., Chen, R., Atkins, M. R., Gibbs, R. and Mardon, G. (2005). Dual regulation and redundant function of two eye-specific enhancers of the Drosophila retinal determination gene dachshund. Development 132, 2895-2905.

Thomas, A., Lee, P. J., Dalton, J. E., Nomie, K. J., Stoica, L., Costa-Mattioli, M., Chang, P., Nuzhdin, S., Arbeitman, M. N. and Dierick, H. A. (2012). A versatile method for cell-specific profiling of translated mRNAs in Drosophila. PLoS One 7, e40276.

Yang, Z., Edenberg, H. J. and Davis, R. L. (2005). Isolation of mRNA from specific tissues of Drosophila by mRNA tagging. Nucleic Acids Res. 33, e148.